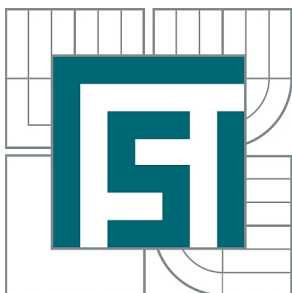


VYSOKÉ UČENÍ TECHNICKÉ V BRNĚ

BRNO UNIVERSITY OF TECHNOLOGY



FAKULTA STROJNÍHO INŽENÝRSTVÍ
ÚSTAV AUTOMOBILNÍHO A DOPRAVNÍHO
INŽENÝRSTVÍ

FACULTY OF MECHANICAL ENGINEERING
INSTITUTE OF AUTOMOTIVE ENGINEERING

FRONT AXLE OF A HIGH-PERFORMANCE SPORTS CAR

PŘEDNÍ NÁPRAVA VYSOKOVÝKONNÉHO SPORTOVNÍHO VOZU

DIPLOMOVÁ PRÁCE

MASTER'S THESIS

AUTOR PRÁCE

AUTHOR

Bc. JAN HRUDÍK

VEDOUcí PRÁCE

SUPERVISOR

Ing. LUBOMÍR DRÁPAL

BRNO 2011



Vysoké učení technické v Brně, Fakulta strojního inženýrství

Ústav automobilního a dopravního inženýrství

Akademický rok: 2010/2011

ZADÁNÍ DIPLOMOVÉ PRÁCE

student(ka): Bc. Jan Hrudík

který/která studuje v **magisterském navazujícím studijním programu**

obor: **Automobilní a dopravní inženýrství (2301T038)**

Ředitel ústavu Vám v souladu se zákonem č.111/1998 o vysokých školách a se Studijním a zkušebním řádem VUT v Brně určuje následující téma diplomové práce:

Přední náprava vysokovýkonného sportovního vozu

v anglickém jazyce:

Front Axle of a High-performance Sports Car

Stručná charakteristika problematiky úkolu:

Popište vůz, jehož přední náprava je předmětem práce. Uveďte výchozí teorii pro kinematiku zavěšení kol a řízení. Analyzujte a vyhodnoťte stávající řešení. Navrhněte novou geometrii zavěšení kola a řízení a jeho uchycení na nosnou strukturu karoserie. Proved'te zástavbovou studii. V závěru vše kriticky zhodnoťte.

Cíle diplomové práce:

Výpočtově-konstrukční práce, zaměřená na zavěšení kol a řízení přední hnané nápravy vysokovýkonného sportovního vozu.

Seznam odborné literatury:

- [1] GILLESPIE, T. Fundamentals of Vehicle Dynamics. Society of Automotive Engineers, Inc., First edition, Warrendale, PA, USA, 1992. 519 p. ISBN 1 1-56091-199-9.
- [2] MILLIKEN, W., MILLIKEN, D. Race car vehicle dynamics. Society of Automotive Engineers, Inc., First edition, Warrendale, PA, USA, 1995. 890 p. ISBN 1-56091-526-9.
- [3] VLK, F. Dynamika motorových vozidel. Prof. Ing. František Vlk, DrSc., nakladatelství a vydavatelství, Druhé vydání, Brno, 2003. 464 s. ISBN 80-239-0024-2.
- [4] VLK, F. Podvozky motorových vozidel. Prof. Ing. František Vlk, DrSc., nakladatelství a vydavatelství, Třetí vydání, Brno, 2006. 432 s. ISBN 80-239-6464-X.

Vedoucí diplomové práce: Ing. Lubomír Drápal

Termín odevzdání diplomové práce je stanoven časovým plánem akademického roku 2010/2011.

V Brně, dne 24.11.2010

L.S.

prof. Ing. Václav Pištěk, DrSc.
Ředitel ústavu

prof. RNDr. Miroslav Doupovec, CSc.
Děkan fakulty

ABSTRACT

This master's thesis has been conducted during author's *ERASMUS Student Mobility for Placement* at the premises of **a.d. Tramontana**, company placed in Palau de Santa Eulàlia, España. This student internship has been carried out from December 2010 to May 2011.

Design of suspension system of any vehicle requires technical knowledge in several disciplines. This thesis covers mainly two of those disciplines – **suspension** and **steering** kinematics.

In the first chapters both suspension and steering theory is taken apart, allowing dealing with praxis thereafter.

A great effort was made to cover all the main topics in understandable and illustrative way without omitting anything important. Where desired the mathematical expressions in the form of equations are used. Many visual images are matter-of-course. That is why this thesis can be treated like a manual/layout for suspension design.

The practical part of this thesis is focused on application of steering and suspension theory into real life. The main purpose of this is to deal with Ackermann Steering geometry and Bump Steer in real vehicle suspension system.

The final chapters give some examples of day-to-day tasks in small-series vehicle production, such as overall front suspension kinematics resulting in swept volume and wishbones manufacturing process, including design of their attachments to the chassis.

KEYWORDS

A.d.Tramontana, MBS, CAD, Suspension, Un/Sprung Mass, Spring, Damper, Pull-rod, Push-rod, Steering, Kingpin Axis, Steering Ratio, Instillation Ratio, Ackermann, Oversteer, Understeer, Bump Steer, Hartmann-Bobilier, Wishbone, Jig, Bushing, Swept Volume.

ABSTRAKT

Tato diplomová práce byla psána při studentské zahraniční stáži, pod záštitou Evropské Unie – program „*ERASMUS Student Mobility for Placement*“. Stáž byla absolvována mezi prosincem 2010 a květnem 2011 ve společnosti a.d.Tramontana, mající sídlo v Palau de Santa Eulàlia, Španělsko.

Pro kompletní návrh podvozku a odpružení jakéhokoli vozidla je nezbytná znalost mnoha technických disciplín. Tato diplomová práce se zabývá dvěma z nich – odpružení a řízení.

Nejprve je rozebrána teorie, na kterou se může navázat v praktické části práce.

Velká pozornost byla věnována srozumitelnosti textu a názornosti obrázků, bez zbytečných detailů, avšak bez vynechání důležitého. Tuto práci je tedy možné užít jako prvního kroku před návrhem podvozku.

V další části je popsáno, jak byla probraná teorie využita při návrhu řízení u skutečného vozu, přičemž největší pozornost je věnována Ackermannově teorii řízení a geometrii zabráňující samořízení při propružení.

V závěrečných částech je pozornost věnována ukázce některých z každodenních činností v malosériové výrobě automobilů – jde o zjištění maximálně možného pohybu kola při propružení a proces výroby příčných trojúhelníkových ramen včetně návrhu jejich připevnění k šasi.

KLÍČOVÁ SLOVA

A.d.Tramontana, MBS, CAD, odpružení, odpružená hmota, neodpružená hmota, pružina, tlumič, přepákování tlačné, přepákování tažné, řízení, rejdová osa, poměr řízení, poměr sil, Ackermann, přetáčivost, nedotáčivost, samořízení vlivem propružení, Hartmann-Bobilier, příčné trojúhelníkové rameno, sestavovací zařízení, pouzdro zavěšení, obálka pohybu.

LITERATURE REFERENCE

According to ČSN ISO 960

HRUDÍK, Jan. *Front Axle of a High-performance Sports Car*. Brno: Vysoké učení technické v Brně, Fakulta strojního inženýrství, 2011. 119 s. Vedoucí diplomové práce Ing. Lubomír Drápal.



STATEMENT

With this statement I claim, that this thesis is genuine my own work, which was created under the leadership of my master's thesis supervisor Ing. Lubomír Drápal and with usage of mentioned bibliography references.

Roses, España, 27th May 2011

.....
Jan Hrudík



ACKNOWLEDGEMENTS

There are a few persons to whom I would like to express my gratitude.

First of all these would be some people from a.d. Tramontana.

Special thanks goes to

señor **Josep Ferrer Nieto**, technical manager at a.d.Tramontana, outstanding engineer with spectacular technical knowledge, who gave me a lot of information and hints about technical stuff, all in very friendly atmosphere;

Ms. **Lara Oliveras Valls**, marketing and communication manager, for her overall warm approach;

Mr. Albert Foncillas;

Mr. Jordi Manyer;

Mechanics **David, Daniel, José Luis, Neto** and **Pere**.

It would be hard to find a more helpful and understanding company for this internship placement.

I would like to take the opportunity to acknowledge the help and overall cooperation of **Ing. Lubomír Drápal**, my master's thesis supervisor.

I am also indebted to my family who has supported my studies. These would be mainly my mother **Ing. Irena Hrudíková** and my father **Ing. Jiří Hrudík**.

I am also grateful to two of my personal abilities - patience and encouragement – which don't allow me neither to stop in steady state nor to go backwards, but push me forwards.

Last but not least, I would like to thank to all my life loves, both human beings and inanimate objects.

All the support was much appreciated.

Roses, España, 27th May 2011

.....
Jan Hrudík





TABLE OF CONTENTS

Introduction	17
1 Introducing a.d.Tramontana	19
2 Suspension Characteristics	21
2.1 Definition of Suspension	21
2.1.1 Unsprung Mass	22
2.1.2 Sprung Mass	22
2.2 Technical Terminology	23
2.2.1 SAE Vehicle Axis System	23
2.2.2 Ride Height	23
2.2.3 Wheel Base	23
2.2.4 Track	24
2.2.5 Centre Of Gravity (CG)	24
2.2.6 Kingpin Axis	25
2.2.7 Miscellaneous	25
2.3 Suspension System Varieties	26
2.3.1 Beam Type Axle Suspension	26
2.3.2 Independent Suspension	30
2.4 Spring/Damper Operation	39
2.4.1 Suspension Vertical Movements Definition	41
2.4.2 Directly Operated Suspension System	41
2.4.3 Rocker Operated Suspension System	41
2.4.4 Relative Ratios	43
2.4.5 Anti-roll Bar (ARB)	50
2.4.6 Unispring – Monoshock Suspension System	51
2.5 Definition of Suspension Geometrical Characteristics	52
2.5.1 Front View Suspension Geometry	53
2.5.2 Top View Suspension Geometry	55
3 Steering Characteristics	57
3.1 Definition of Steering	57
3.2 Technical Terminology	58
3.2.1 SAE Tire Force and Moment Axis System	58
3.2.2 Wheel Centre Line	59
3.2.3 Kingpin Axis	59
3.2.4 Steering Ratio	59
3.2.5 Tire Properties	60



3.3	Steering System Varieties	62
3.3.1	Rack-and-pinion.....	62
3.3.2	Steering Gearbox.....	64
3.3.3	Truck Steering System	66
3.4	Definition of Steering Geometrical Characteristics	66
3.4.1	Front View Steering Geometry	67
3.4.2	Side View Steering Geometry.....	70
3.5	Ackermann Steering Geometry	72
3.5.1	Positive Ackermann	74
3.5.2	Negative Ackermann.....	75
3.5.3	Parallel Non-Ackermann Steering	76
3.6	Cornering Equations.....	77
3.6.1	Low Speed Turning.....	77
3.6.2	High Speed Cornering.....	78
3.7	Ride Steer (Bump Steer).....	81
3.7.1	Geometry error	82
4	Real Steering Clevis.....	85
4.1	Preface	85
4.1.1	Work Process Layout	86
4.1.2	Software Description.....	86
4.1.3	Definition of Main Points	87
4.2	Design According to Bump Steer.....	90
4.2.1	CAD Software	90
4.3	Design According to Ackermann	96
4.3.1	CAD Software	97
4.4	Outer Steering Point Conclusion.....	97
4.4.1	MBS	97
4.4.2	Result vs. Starting Point.....	101
4.4.3	Conclusion:	102
4.4.4	Steering Clevis Design.....	102
5	Wishbones' Assembly.....	103
5.1	Wishbones' Manufacturing	103
5.1.1	Work Process Layout	103
5.2	Wishbone's Bushings	106
5.2.1	Old Bushings' Design	106
5.2.2	New Improved Design	106



5.2.3	Conclusion	107
6	Swept Volume	108
6.1	Work Process Layout.....	108
6.1.1	Simulation Assembly.....	108
6.1.2	DMU Kinematics Simulation	110
6.2	Conclusion	111
	Conclusion.....	112
	Bibliography References	113
	List of Symbols.....	114
	List of Figures.....	116
	List of Appendixes	119

There is a driving force that is more powerful than steam, electricity or atomic energy

THE WILL

“Anonymous”





INTRODUCTION

The author has shown a great effort to get some student internship placement abroad, which finally resulted with placement at Catalan small-series high-power sports car manufacturer - a.d. Tramontana.

One of the supposed main advantages of this thesis is the fact that it is dealing with real problem for a company, resulted in manufacturing a real piece which is used in real life. Furthermore many of foreign literature sources, which varied in attitude to the topic and number of details given from basics to ones targeted on experts in this field, were used. There was a wonder that some literature source is missing something important what can be found in another and vice-versa. The author has taken this chance to collect all important facts into one piece – this thesis.

This thesis doesn't aim to be scientific or ground-breaking work. It is supposed to give the reader a reasonable view inside suspension and steering knowledge, and also a view into a real-life small-series car production process, shown by mean of some examples of work performed at front-axle of a real car.

In order to keep some overall order and achieve clarity in the text at the first sight, some font style was used in the whole work: links to figures are in dark blue italics as well as the title under each figure; equations are in dark red colour; links to another parts are in black italics, links to appendixes are in brown colour. Where necessary the equations are added to intensify the knowledge. Many visual images are used to simplify the understanding process.

Clarity in communication is vital to problem solving. Over the years, appropriate terminology for automotive engineering has been defined to facilitate communication [1]. Therefore this terminology is used in the whole thesis; some meanings are explained in a Technical Terminology part in the chapter 2 and 3 and also in *List of Symbols* in the very end of this work, letting the reader become familiar with this terminology.

The first chapter briefly describes the a.d.Tramontana car – to let the reader know the vehicle for which the work was performed.

The main aim of *second* and *third* chapter is to give general overview of suspension and steering design knowledge, which has to be taken into account while designing suspension system of any vehicle. The layout is systematically ordered, the work contains all the necessary kinematics and geometrical characteristic of suspension and steering systems.

In the second chapter, part 2.5 there are described all the main **suspension** geometrical characteristics in front and top view planes, e.g. camber, toe angle, IC, RC. All the main suspension design varieties are mentioned in part 2.3, both solid axle and independent suspension, each accompanied by their main advantages and disadvantages. Anti-roll bar and rocker operated suspension are not overlooked even (refer to part 2.4). Both linear and non-



linear installation ratios are also explained and calculated. Technical terminology doesn't miss in this chapter – part 2.2.

Steering geometrical characteristics in two plane view, such as Kingpin axis inclination and castor, are explained in chapter 3, part 3.4, including some most commonly used steering system varieties accompanied by steering ratio equations in part 3.3. Some pages of this chapter are dedicated to Ackermann steering in part 3.5, whose fundamentals are broaden in part 3.6, which is dealing with steering geometry in both low and high speed cornering situation. Finally the part 3.7 deals with Ride steer behaviour, aiming to achieve zero toe-angle change during bump/rebound wheel travel. Technical terminology doesn't miss in this chapter – part 3.2, e.g. reverse efficiency and steering axis are described here.

To fully cover suspension design topic there should be also chapters dealing with issues about dynamics (load transfer, rollover etc.), elastic elements (spring properties), vibration and tire properties and behaviour. Anyway, as far this should cross the stated borders and tasks of this thesis work, they are not included. Hopefully some another thesis will deal with them.

Following chapters are transferring the theory into praxis.

In the **chapter 4** the steering geometry of high-power sports car front axle was designed and constructed. Main intention was to achieve Bump steer as close to zero as possible, furthermore some good Ackermann was desired to be achieved. The work process started with CAD design according to theory (Hartmann's construction of Bobilier Line and Ackermann geometry). Thereafter the results were transferred to MBS software where appropriate simulations were run to prove their sufficiency and/or to final adjustment. Some comparison between desired and achieved steering values is shown there. This process finishes with real steering clevis design, which was manufactured and nowadays is mounted at the car and used.

Chapter 5 concentrates at wishbone manufacturing process, where some engineering work is also necessary before the worker can start manufacturing, including the design of some tool to make the assembly as precise as possible and achieve as nice final look as possible. Furthermore connection pieces between wishbones and chassis were designed and manufactured.

A demand from designing company gave rise to **Chapter 6**, which represents the way how to find out the total area, in which the wishbone-wheel assembly can move in bump/rebound travel, with wheel steered straight ahead, full right and full left.



1 INTRODUCING A.D. TRAMONTANA

In the automotive history, there has never been car which reminds Formula 1 design so much as the Tramontana does.

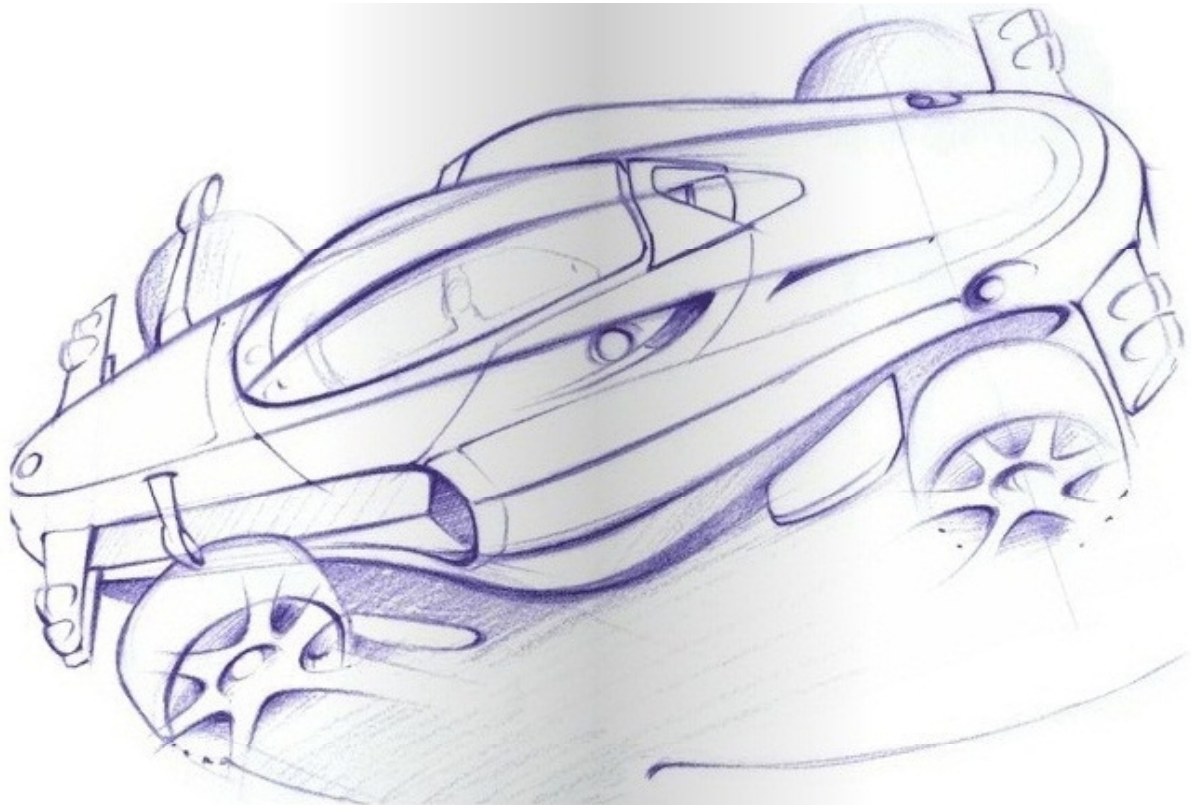


Fig. 1 A.d.Tramontana [9]

A.d. Tramontana is a European company established in 2005 with its headquarter situated in Costa Brava, Spain.

It shares the same passion of luxury and competition as many famous Spanish car producers in the history like Hispano Suiza and Pegaso, both were desponding very advanced technology in their time as well as Tramontana nowadays. The idea to develop an exclusive tailor-made super sport car, a combination of a Formula 1 racing car and a jet fighter was achieved and now it is a reality.



The production is limited to few units per year, thus each on is unique.

The deep influence of Formula 1 design results in one piece chassis represented by carbon fibre monocoque, working hand in hand with its suspension system – matchless at the market, consisting of great-length double wishbones on each wheel, pushrod operated with anti-roll bar stabilisation.

The exceptional conception of two seats, placed one behind another - in one row - adds another portion to the total vehicle rareness.

With innovative carbon fibre technology and other cutting edge engineering Tramontana has set the benchmark for super exotic cars some years ago, while many of the competitors are starting to use similar technology and ideas just nowadays.

It will never be forgotten by anyone lucky enough to have driven it, or even seen and heard it at full charge.

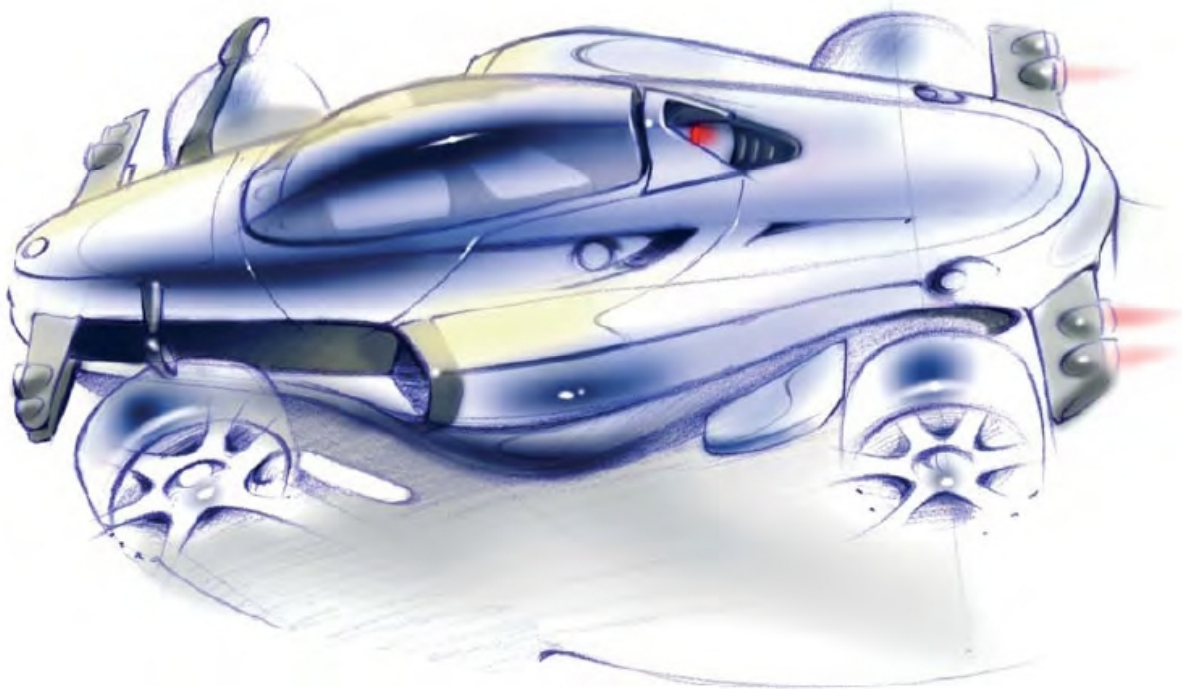


Fig. 2 A.d.Tramontana 2 [9]

Detailed technical specifications are listed in [App. 1.](#) [6]

More real photos of a.d.Tramontana are shown in [App.2.](#) [9]



2 SUSPENSION CHARACTERISTICS

In the beginning of this chapter there are described the main reasons of using suspension system in every road, race and also transport vehicle. For better understanding the explanation of the difference between sprung and unsprung mass is given in part 2.1.

As each field of knowledge, also in automotive industry there is some specific common-known technical terminology, which is necessary for being able to communicate in international collective, some of the expressions already became familiar in foreign languages. Part 2.2 focuses at this terminology.

All the main suspension design varieties are mentioned in part no. 2.3, from solid axles (based at dependence of one wheel to another) over semi-independent up to fully independent ones. For obvious reasons and simplicity each type of independent suspension contains list of its **advantages** and **disadvantages**. As this thesis deals about the front axle of a high-performance sports car the main concern is focused on Double Wishbone Suspension System, which can be operated directly or via a movement transmitter – so called “rocker”.

This type of indirect operated suspension system is described in detail in part 2.4, as well as directly operated suspension system. Some mathematical equations dealing with movement relative ratios are not missing in this part. Some is also focused at important suspension element – Anti-roll Bar.

Finally, after getting general overview of this topic there is the part 2.5 where the main suspension geometrical characteristics are described, logical ordered by view from front and top of the vehicle. The knowledge of fundamentals and understanding of their advantages and disadvantages are crucial for any suspension design.

2.1 DEFINITION OF SUSPENSION

The purpose of the suspension is to make the job easier for the tires and give a predictable behaviour so that the driver will have control of the car. Good suspension design also helps keeping the tires in constant contact with the ground thus increasing their efficiency and letting them being used to the limit of their capacity.

The primary functions of a suspension system are:

- Provide the vertical compliance, so the wheel can follow the uneven road
- Isolating the chassis (and passengers) from roughness in the road
- Maintain the wheels in proper steer and camber attitudes to the road surface
- React to the control forces produced by the tires
 - longitudinal forces (acceleration, braking)
 - Lateral forces (cornering)
 - braking and driving torques
- Resist roll of the chassis

[1]

In simple way, as “suspension” can be considered everything what is connecting the unsprung and sprung mass of a vehicle.

2.1.1 UNSPRUNG MASS

By an unsprung mass are meant all those parts of the vehicle which are not supported by suspension springs – represented e.g. by upright, connection parts (according to concrete suspension design), wheels (rims, tires), brake callipers, brake discs etc. It is undesirable since it compromises handling.

All the unsprung weight must be accelerated vertically (by tire stiffness in bump or suspension spring in rebound). [4]

TIRES

The tires also fall into unsprung mass category, furthermore while they are not rigid they also play the role of some kind of separate suspension unit.

As the tires are the part of the race car having the biggest dynamic influence and the whole driving behaviour is starting with them, lot of work should be carried out while choosing appropriate ones. There are many sizes, brands, rubber compounds at the market. It would be a waste of time to lead the design of chassis and suspension to the perfection and, then, choose inappropriate tires.

Only the tire manufacturer can control those many factors allowing the tire to have good grip, while the suspension design can control the angles in which the tires are presented to the road.

Unlucky, the tires' topic is so demanding, that it could discuss in the whole thesis. Hopefully some of the future thesis will deal with it.

Thereafter, for simplicity reasons, the compliance in the tire will be ignored in this thesis and for assumption reasons the tire will be treated as rigid body.

2.1.2 SPRUNG MASS

Sprung mass is represented by all the other vehicle components which are not unsprung (mass of the car constituted by the chassis, engine, gearbox etc.).

Graphic expression of both sprung and unsprung mass can be seen in [Fig. 3](#).

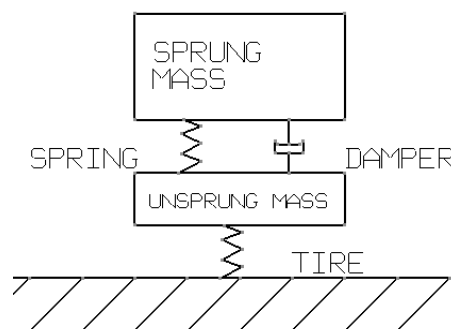


Fig. 3 Sprung/Unsprung mass general layout



2.2 TECHNICAL TERMINOLOGY

2.2.1 SAE VEHICLE AXIS SYSTEM

SAE (Society of Automotive Engineers) has selected a convention by which to describe the forces on a vehicle. The coordinate system has its beginning in CG; the forces are measured at the CG.

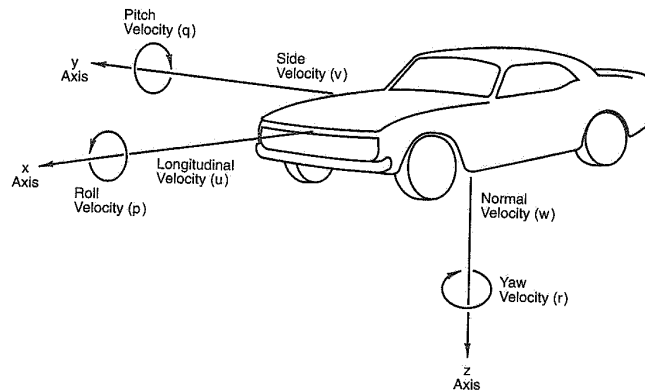


Fig. 4 SAE vehicle axis system [2]

2.2.2 RIDE HEIGHT

Ride height is the amount of space between the base of an automobile tire and the underside of the chassis; in the meaning of the shortest distance between a flat bottom surface (e.g. road) and any part of a vehicle other than those parts designed to contact the ground (e.g. tires) tracks, skis, etc.). It is measured with standard vehicle equipment without any passengers.

2.2.3 WHEEL BASE

The wheelbase, L [m], is the distance between the centre of the front axle and the centre of the Rear axle. The wheelbase has a big influence on the axle load distribution.

A long wheelbase will give less load transfers between the front and rear axles than a shorter wheelbase during acceleration and braking, thus softer springs can be used at long-wheelbase vehicles, increasing the level of comfort for the passengers.

On the other hand a shorter wheelbase has the advantages of smaller turning radius for the same steering input. [7]

It is always same for both sides.



Fig. 5 Wheel base [5]

2.2.4 TRACK

Track width is a distance between the centre of left and right wheels.

The track width is of major importance when designing a vehicle. It has influence on the vehicle cornering behaviour and tendency to roll. A larger track width has the disadvantage that more lateral movement of the vehicle is needed to avoid obstacles, but by contrast it brings smaller lateral load transfer.

The value can be different at front and rear axle.

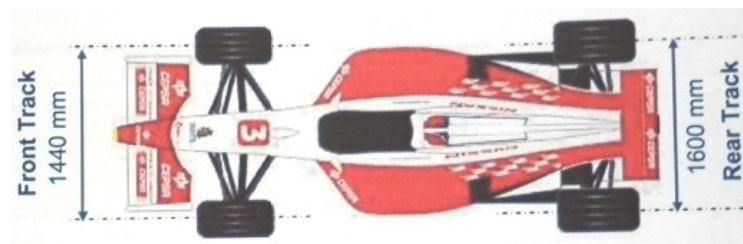


Fig. 6 Track width [5]

2.2.5 CENTRE OF GRAVITY (CG)

Centre of Gravity represents the location of all mass of a vehicle into one place.

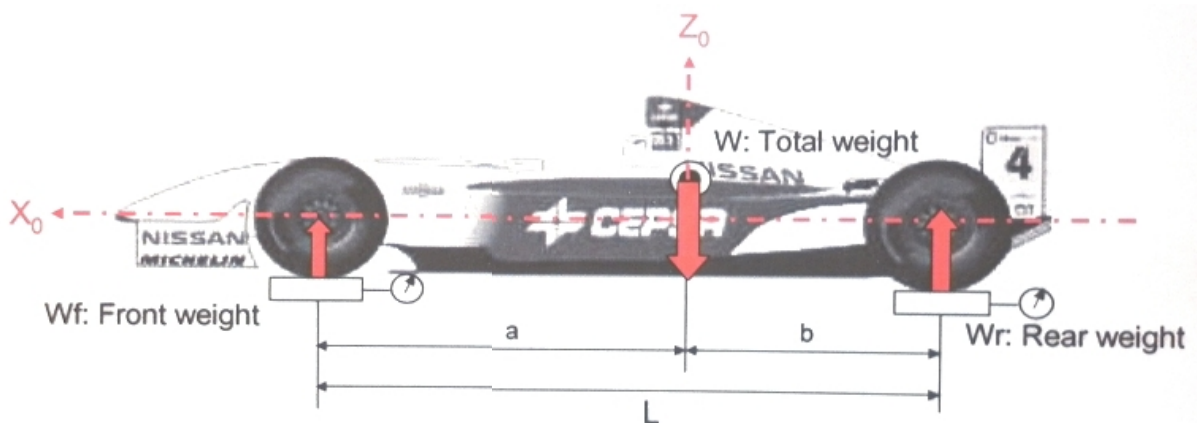


Fig. 7 Centre of Gravity - side view [5]

If the tires front and rear are of the same size and CG placed exactly in the geometrically centre of the tire footprints, the car is neutral steering.

Otherwise some good way how to get the CG position is to use scale weights under each wheel to get know each wheel load; supplemented with wheelbase and track width dimensions the appropriate equations can be used.

Normally at real sports car, the heaviest part – engine - is placed in the rear behind the driver, we often find the CG is more rearward from this geometric centre, which causes oversteer. This is often balanced by using wider rear tyres which restores neutrality of steering. [4]



2.2.6 KINGPIN AXIS

In general, kingpin axis (sometimes also called “steer rotation axis”, which reminds its function) influences more steering than suspension characteristics, that is why it is deeply described in 3.2.3

2.2.7 MISCELLANEOUS

To help achieve clarity of the following text some technical terms are in order to explain.

UPRIGHT

Rigid part which connects the suspension linkages and wheel, all in moveable was using ball-bearings and ball-joints. Its shape and design rules the geometry characteristics of suspension system.

BUSHINGS

It is some kind of joint (rotary, spherical) by which the suspension linkages are attached to the chassis.

OVERSTEER

The car is oversteered, when it delivers smaller turning radius than the driver demanded. The certain radius of corner is less that in the neutral steering case (when driver gets the steering he asked for). In other words, the rear of the car goes ahead of the front. (see more in 3.6)

UNDERSTEER

The car is understeered, when it delivers larger turning radius than the driver demanded. The certain radius of corner is more that in the neutral steering case (when driver gets the steering he asked for). In other words, the car is not able to go through the turn and remains in more straight way. (see more in 3.6)

LIVE AXLE

This axle of a vehicle is propelled by engine. It can be also called “driving”.

DEAD AXLE

This axle of a vehicle is not propelled by engine. It can be also called “driven”.

2.3 SUSPENSION SYSTEM VARIETIES

For understanding the suspension properties that affect ride and directional response it is appropriate to examine the various types of suspension used on modern passenger cars.

Main characteristics which for choosing the most appropriate suspension design are (in consequence order):

- Purpose of vehicle
- Cost
- Weight
- Package space
- Manufacturability
- Mounting conditions

[1]

Suspension system can be generally divided into two groups according to the difference in its functionality:

- 2.3.1 Beam Type Axle Suspension
- 2.3.2 Independent Suspension

2.3.1 BEAM TYPE AXLE SUSPENSION

Beam Type Axle Suspension (sometimes also called Solid Axle) has two wheels tied together (by a tube, beam or other rigid structure), thus motion of one affects the movement and/or camber change of the other.

The wheels have two different motions relative to the chassis (2 DOF). They can go either up and down together (parallel bump motion) or they can move in opposite directions one up and second down (roll). [2]

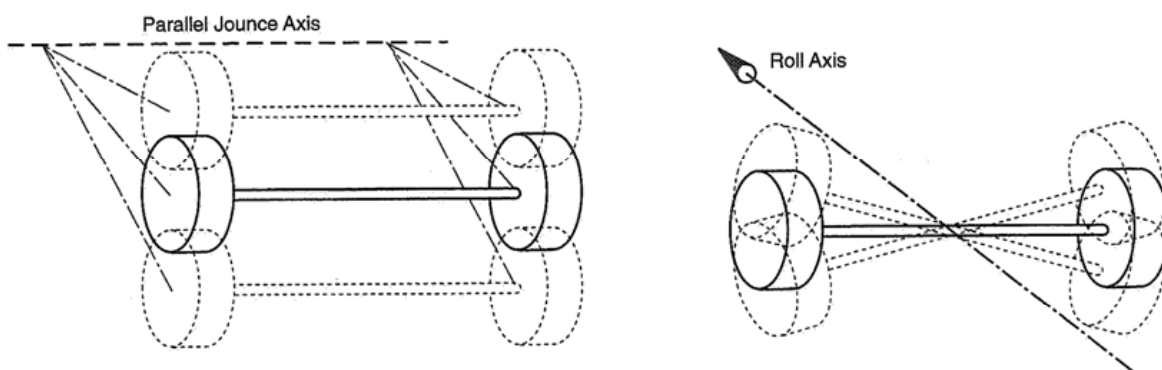


Fig. 8 Parallel and roll motion of Solid axle suspension [2]

This type of suspension used to be widely used in the past, because it its quite simple design with very good strength. Some of the disadvantages can be high unsprung weight (2.1.1) and high demands on package space.



Since the wheels are rigidly connected it seems to be good choice while it meets the desire to avoid camber change in a corner or while body rolls. This might seem like a good thing, but some suspension (e.g. double wishbone design, *see further on in this chapter*) are able to gain positives from this, while they are compensate the body roll with camber change when cornering. Furthermore, when one wheel goes over a bump, the other experience the camber change, causing loss of its grip. [4]

In great amount it was used before World War II (1939-1945) even for passenger cars.

Nowadays usage

Since the solid axle is not able to change the camber, it is not used for high-power sports car or car for racing purposes. Anyway they are still used at some passenger, high-load and 4WD vehicles where the weight doesn't play the major role or in order to push the production cost lower.

The usage is mainly at rear axle with propulsion task (so called "Live Axle") or (very occasionally) at front axle without propulsion (so called "Dead Axle").

The most common examples of Solid Axle Suspension are:

- Hotchkiss Axle
- De Dion Axle
- Twist Beam Axle

HOTCHKISS AXLE

One axle with a pair of longitudinal leaf springs, which doesn't perform only springing function, but also reacts lateral and longitudinal forces and also torque from the central drive shaft.

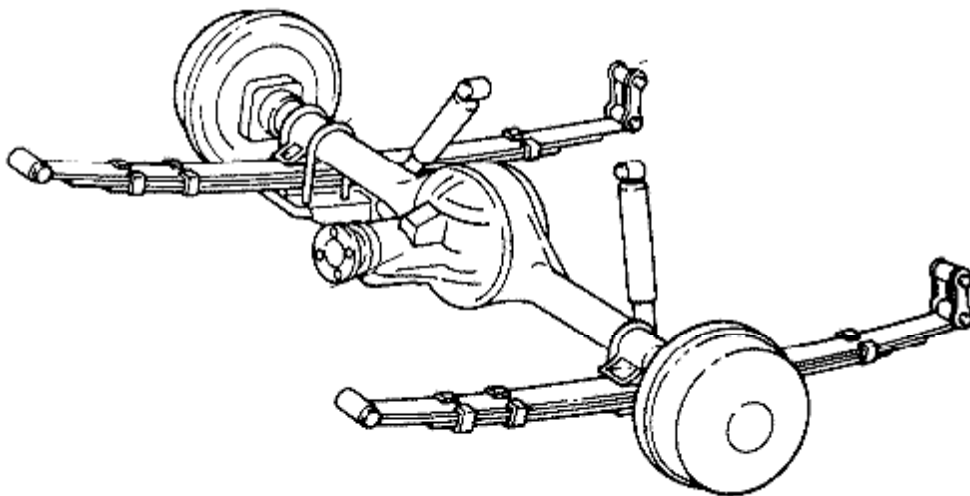


Fig. 9 Hotchkiss Solid axle suspension [1]



DE DION AXLE

Some improvement from Hotchkiss Axle can be seen at De Dion Axle. Here, the two wheels are tied together by a stiff beam bended around the differential, which is mounted to the chassis and uses two half-shafts to proper the wheels. There is no drive torque reaction requirement. Further the weight is much lower comparing to the Hotchkiss Axle, thus less unsprung mass.



Fig. 10 De Dion axle suspension, with coil springs [12]

TWIST BEAM AXLE

This design can be called semi-solid. The two trailing arms are connected with a torsion bar, which twists around its axis while the car goes to roll. Nowadays this is commonly used design, only for FWD vehicles. It is quite cheap comparing to the other designs, low demands on package space (allowing placing e.g. fuel tank between) is another advantage.

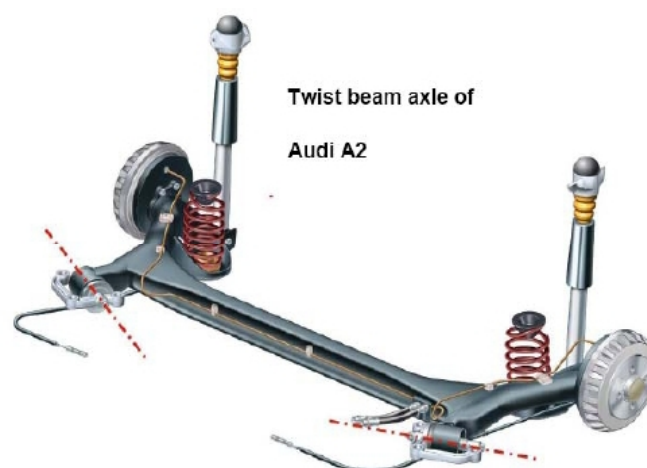


Fig. 11 Twist beam axle suspension Audi A2 [11]



LATERAL RESTRAINT

As said before since the suspension type of Solid Axle has two degrees of freedom, for keeping it requires some lateral restriction unit.

As the axle moves up and down relative to the body it is desirable that it moves on a straight vertical path. [2]

There are several designs of mechanism which can be used in order to achieve this:

- Panhard Bar
- Watt's Linkage
- Cam Follower-in-track

Panhard Bar

It is a link of finite length and therefore its end travels on a curved arc relative to its opposite end. The longer the bar the closer it approximates linear motion. [2]

It is an example of design which doesn't fully behave according to the desired movement on a straight vertical path, which is some disadvantage.

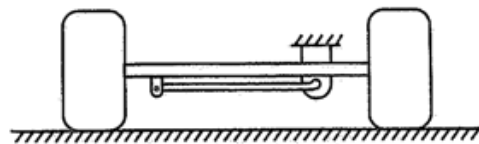


Fig. 12 Panhard bar lateral restriction [2]

Watt's Linkage

This clever solution was invented by Scott James Watt (1736-1819).

This design fully behaves according to the desired movement on a straight vertical path.

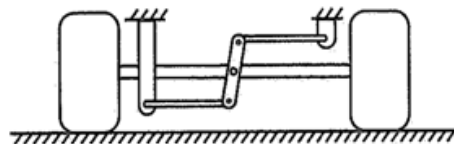


Fig. 13 Watt's linkage lateral restriction [2]

Cam Follower-in-track

It is represented by a sliding pin. It is not so common used due to suffering from lateral free-play and/or friction. [2]

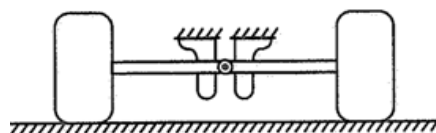


Fig. 14 Cam follower-in-track lateral restriction [2]



2.3.2 INDEPENDENT SUSPENSION

General: Independent suspension allows one wheel to move without affecting the other.

In this type of suspension system the position and layout of the control arms are intended to control the wheel motion relative to the chassis in a single prescribed path, ruled by the geometry. [2]

While considering the chassis and all the suspension components fully rigid it can be stated, that there is one fixed path relationship between suspension movement and each geometry parameter. By these parameters they are mainly meant camber gain/loss, caster change, toe angle change.

The most common examples of Independent Suspension are:

- Swing Axle
- Pure-trailing Arm
- Semi-trailing Arm
- Double Wishbone
- McPherson
- Multi-link

Nowadays the most common front axle suspension design are McPherson, and Double Wishbone. The other types suffer from either high bending loads, poor geometry, high friction, or a combination of these problems. [2]

SWING AXLE

The swing axle represents the first attempt at solving the problems of solid axle design. The good example of this configuration can be seen at VW Beetle rear axle.

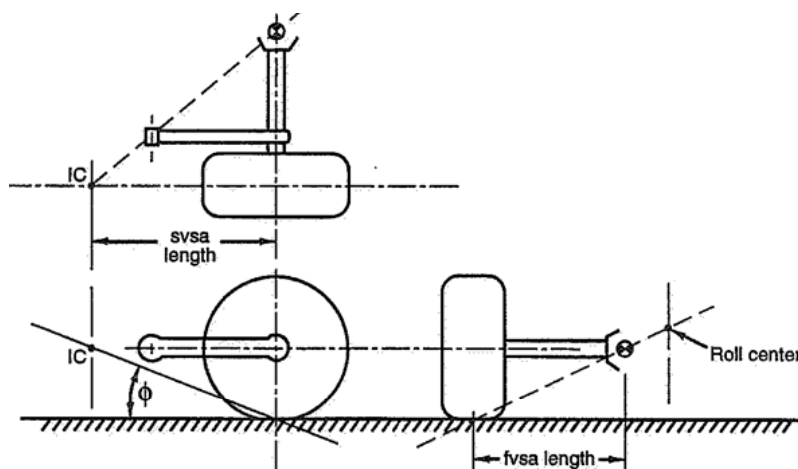


Fig. 15 Swing axle suspension – 3 plane view geometry [2]



Advantage

As the motion axis in top view passes through the inner pivot joint of the half shaft, the half shaft doesn't need to be changeable in length, furthermore there is no need to use another U-joint, thus reduction of costs.

Disadvantages

The roll centre is situated very high which leads inevitably to jacking. While body rolls the wheels gain a lot of camber, which results into grip losing and thereafter in oversteer behaviour.

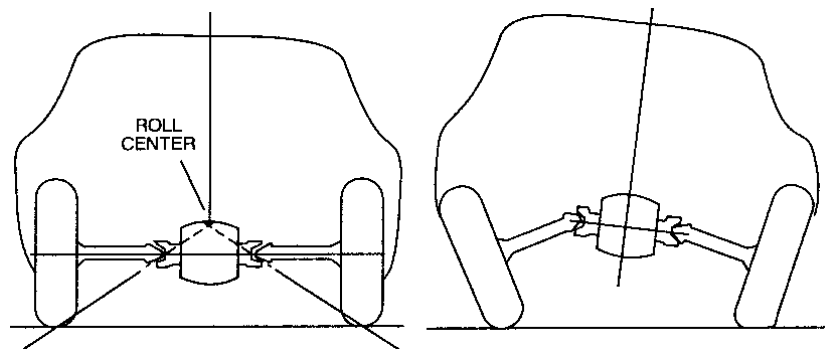


Fig. 16 Swing axle suspension - roll behaviour [1]

PURE-TRAILING ARM

Pure-trailing arm represents one of the most simple and economical design of independent suspension. It consists of very simple hinge mechanism - either of **one trailing arm** (mainly used at rear axle [Fig. 17](#), e.g. Chevrolet Corvette [Fig. 18](#)) or **two parallel**, equal-length trailing arms (mainly used at front suspension, e.g. VW Beetle, [Fig. 19](#)). Connection to the chassis is done by bushings, whose axis are perpendicular to the centreline of the vehicle and parallel to the ground.

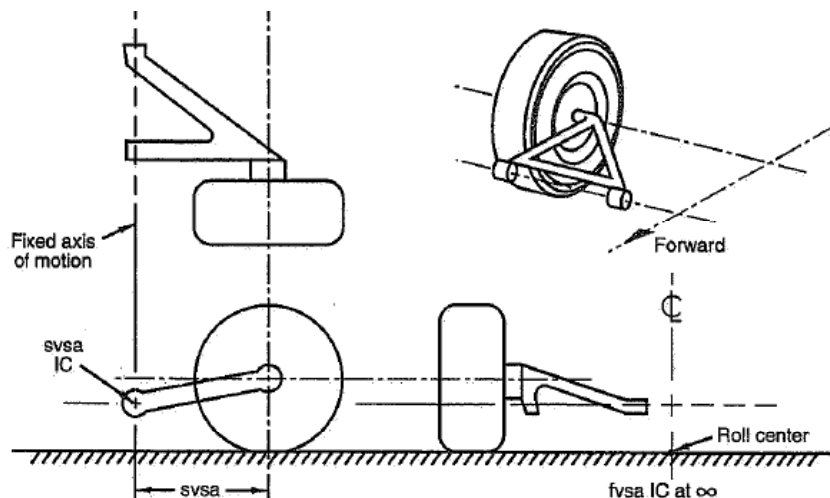


Fig. 17 Pure-trailing arm suspension – 3 plane view geometry [2]



Advantages

Since the wheel is **trailed** over the terrain, bump negotiation is good thereafter. Very low package space demand is another advantage.

Disadvantages

This configuration offers no camber and toe change during bump/rebound movement. This brings very undesirable result - while the body rolls the outer wheel experiences camber gain in reference to the ground (camber values are going to positive mean), causing jacking. Furthermore this reduces the cornering power of this outside loaded tire resulting in oversteer effect.

In addition, while used at rear live axle, since the wheel doesn't move in an arc about some inboard fixed point, the half shaft has to be able to accommodate some extension/compression.

There are heavy structural requirements at the connection arms which must be strong in all three directions.

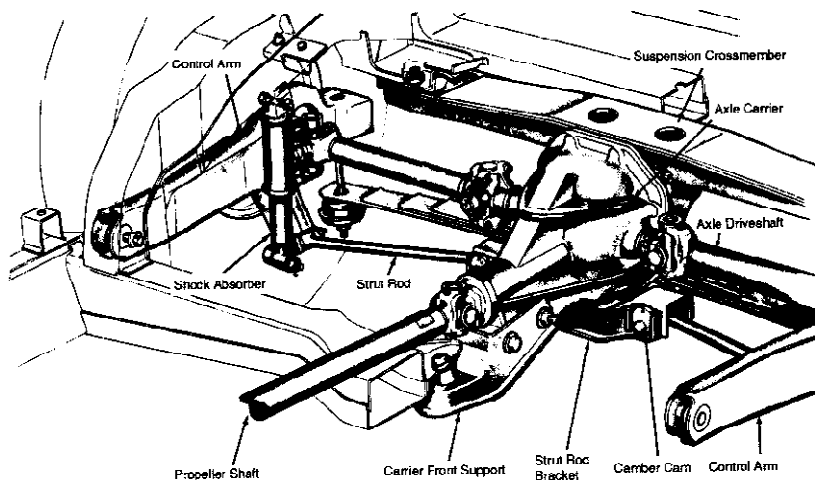


Fig. 18 Pure trailing arm suspension – Chevrolet Corvette rear axle [1]

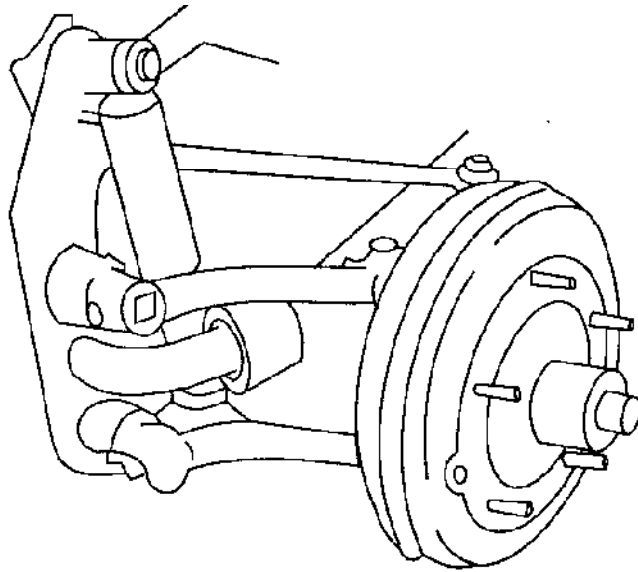


Fig. 19 Pure-trailing arm suspension – VW Beetle front axle [1]

SEMI-TRAILING ARM

As further development of swing axle and pure-trailing arm is considered the semi-trailing arm system. In this configuration the bushings' axis are inclined in all three planes view. The outside wheel can experience camber loss under body roll, which is desirable for ride stability.

This type of suspension was so much popularized by BMW, who gain its sportive reputation mainly because of it.

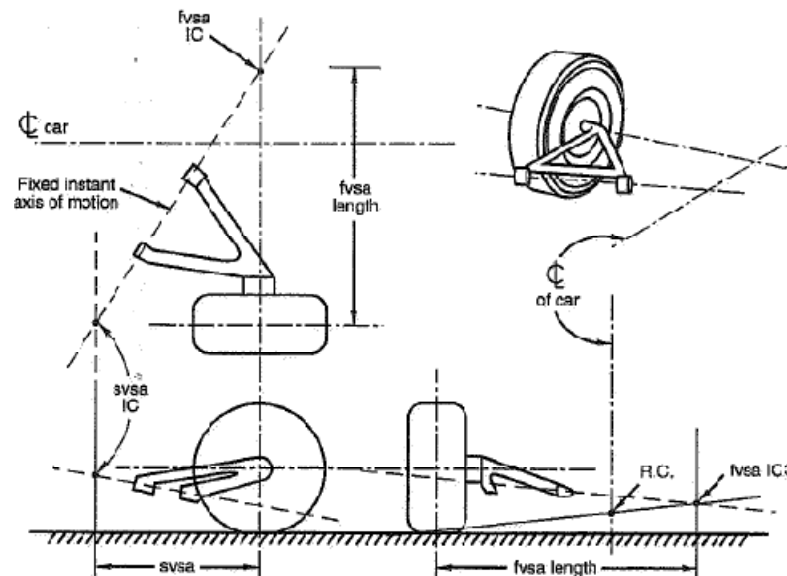


Fig. 20 Semi-trailing arm suspension – 3 plane view geometry [2]



Advantages

This design is very simple and the arms need small packing space. It is mainly used at the rear axle. This benefit is used e.g. at VW Transporter rear axle, allowing wide and low-level cargo space between wheels, furthermore supplemented with four-wheel drive possibility (*Fig. 21*).

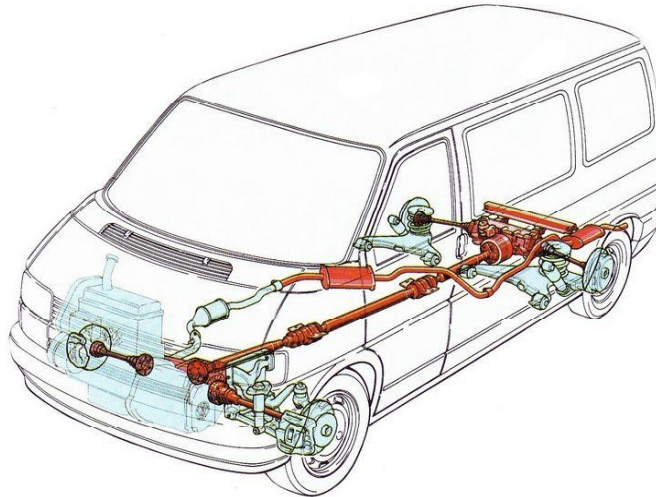


Fig. 21 VW Transporter suspension [11]

Disadvantages

Like a pure-trailing arm, also this configuration is exposed to bending when the car corners and to be rigid enough not to bend significantly the arms must be heavy.

According to geometrical terms this design acts in exactly opposite way than the good suspension should.

Here, toe change is progressive - moving along a curved line, and furthermore the rate of camber loss is constant along a straight line. Both stated characteristics are not suitable choice for racing purposes nowadays.

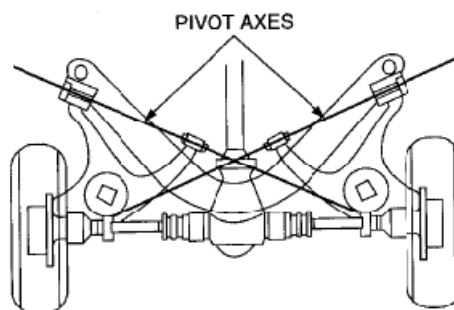


Fig. 22 Semi-trailing axle – rear axle [1]



DOUBLE WISHBONE

(In USA known as SLA - Short-long Arm)

Acronym “SLA” stands for Short-Long Arm and refers to the different length of the upper and lower control arms. These arms are sometimes (mainly in the USA) called “A-arms”

This A-arm design can be considered as two straight links with their outer ends coming together at the outer ball-joint.

A-Arm = 2 Links



Fig. 23 A-Arm general layout [2]

This suspension system consists of two lateral control arms. Is generally regarded as the most flexible in achieving desired overall geometric parameters with the least amount of compromise. [2]

There always have to be some additional link in order to:

- keep the desired **toe angle** and **straight direction**
(represented by tie rod at rear axle, attached to the chassis *Fig. 24a*), or one of the wishbone, *Fig. 24b*))
or
- allow **steering manoeuvres**
(steering tie rod at front axle attached to the steering unit)

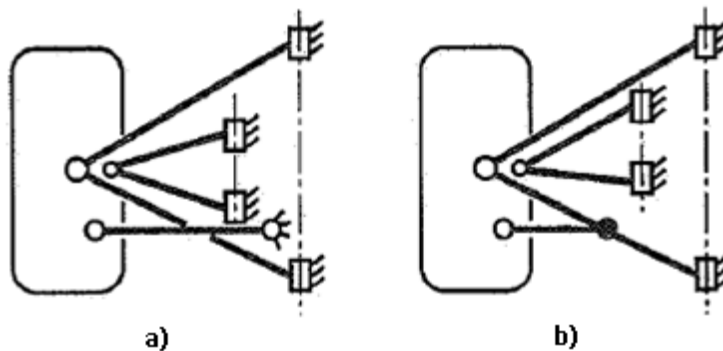


Fig. 24 Tie rod link at rear suspension connected a) to the chassis; b) to the wishbone [2]

This type of suspension can be used at the front axle as well as at the rear axle. To give roll understeer the difference between front and rear geometrical characteristic has to be considered:

Use exactly opposite geometric toe consideration for front and rear axle at the same side. In other words, use e.g. left front side components as the right rear side components and vice-versa.



Advantages

- The roll centre can be easily controlled and setup
- The camber can be controlled and setup
- Toe can be easily controlled and setup
- Easy to make spring rate progressive, many possibilities of spring/damper operation (*see 2.4*)
- Very low unsprung mass

Disadvantages

Difficult to package at the front axle of a FWD car (this is mostly not relevant to racing purposes since there is the engine mainly at the rear).

In spite of advantage of improving the camber at the outside wheel by counteracting camber due to body roll, here can be stated that this usually carries less favourable camber at the inside wheel. While the outside wheel is always higher loaded than the inside this can be stated as minor disadvantage.

Because of all above mentioned reasons the Double Wishbone Suspension design seems to be the best option for racing purposes.

McPHERSON STRUT

This configuration represents the most popular choice of front suspension of road cars.

In McPherson suspension design there can be seen the similarity with Double Wishbone Suspension design.

The upper wishbone is replaced by a telescopic member - a strut (which is kinematically a slider mechanism which is equal to an A-arm that is infinitely long at right angles to the slider travel. [2])

MacPherson Strut = 2 Links;
Slider = A-Arm of Infinite Length



Fig. 25 McPherson strut general layout [2]

Advantages

The main advantage is a great package space it offers (in lateral meaning), mainly for FWD transverse-engine cars. Along with acceptable driving performance this established success of McPherson.



Disadvantages

As the strut axis is due to limited construction possibilities not aligned with the kingpin axis, the strut suffers from overturning moment, which causes its bending and friction. Thereafter it is obvious that usage of wide tires is limited, while it would cause even bigger difference between these axes bringing even more friction.

This can be more or less counteracted with the spring position. Its axis is inclined with respect to strut axis, starting in the upper mount point and finishing very close to the centre of the contact patch. If this axis intersects ground in the same point as the wheel centre axis, there will be no bending loads in the strut.

There is always some minimum height of this configuration, which doesn't allow making the front of the car under some limit.

As the strut is a telescopic member, camber control is poor, in fact there is rather camber gain than caber loss. Body roll is transferred to the outside wheel and it is not possible to arrange for the geometry to overcome the undesirable camber gain.

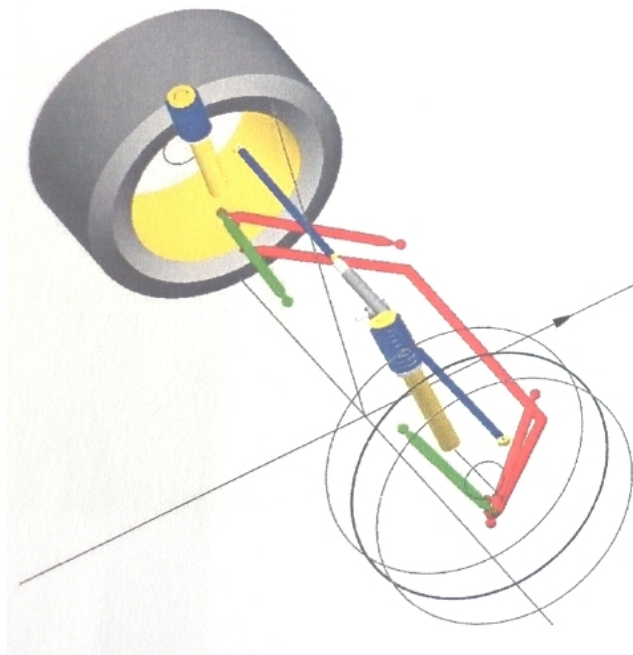


Fig. 26 McPherson suspension [13]

McPherson Strut at rear axle

This configuration is also used at rear axles with many design options exist because large steer angles and specific kingpin axis properties are not absolutely required for proper function.

One of the representatives of several variations is Tri-link strut (*Fig. 28*, e.g. Mazda 323F 1994-1998 in *Fig. 27*). It consists of three individual tension-compression links and McPherson strut.

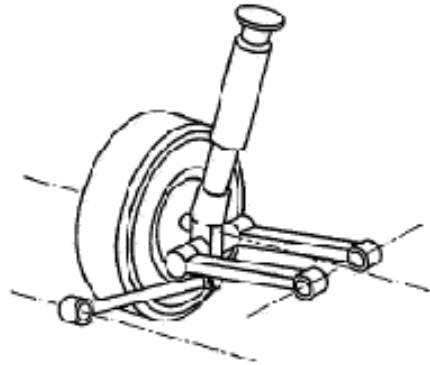


Fig. 28 McPherson suspension – rear axle Tri link configuration [2]



Fig. 27 McPherson suspension – rear axle Tri link configuration at Mazda 323F, 1996

MULTI-LINK

One of the latest suspension designs is called Multi-link created by a set of unequal length linkages. It is characterized by ball-joint connections at the ends of the linkages so they do not experience any bending moments. As there is a need to restraint 5 DOF (Degree of Freedom), five pieces of these tension-compression links has to be used. This type of is commonly called as **5 Links Suspension**.

Most common usage is at the rear axles, both live and dead.

Advantages

This configuration provides the highest flexibility for the designers to achieve the wheel motion desired. [1]

It is possible to get wanted front view kinematics (**2.5.1**) without compromising the side view geometry. [2]



Disadvantages

This configuration has high package space demands. Another disadvantage can be more difficult and time-demanding geometry characteristics setting process.

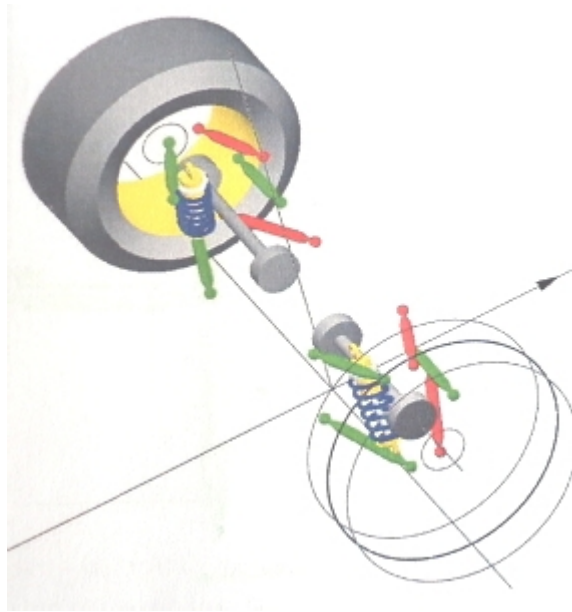


Fig. 29 Multilink suspension [13]

2.4 SPRING/DAMPER OPERATION

Examples and explanations in this chapter are built on double wishbone system – the one with many possibilities of suspension operation.

Spring and damper (both in many design varieties) are two indivisible parts of any suspension system. There cannot be just either spring or damper. Thereafter the expression “spring/damper unit” can be used.

SPRING DEFINITION

A spring is an elastic object used to store mechanical energy.

The amount of suspension travel is a function of spring stiffness, weight transfer and installation ratio.

There are two main type of spring design:

- coil spring (*Fig. 30*)
- leaf spring (*Fig. 31*)



Fig. 30 Coil spring [11]



Fig. 31 Leaf spring [11]

DAMPER DEFINITION

The main aim of damper unit is to transfer the mechanical energy into the heat energy, thus damping the movement of suspension system, not allowing it to oscillate. This is done by hydraulic resistance while transferring the liquid place inside the damper body. The liquid is commonly represented by high-quality hydraulic oil. More sophisticated dampers are equipped with two types of liquid channels, each with separate setting possibility, thus two-way adjustment is provided: compression and rebound damping adjustment.

This is possible by using two types of liquid channels, each with separate setting possibility.

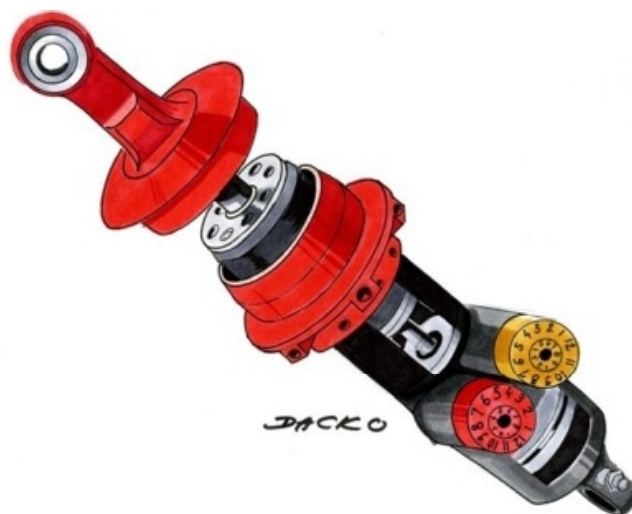


Fig. 32 Suspension damper with two-way adjustment [12]



2.4.1 SUSPENSION VERTICAL MOVEMENTS DEFINITION

We describe two main type of wheel vertical movement:

- **Bump**
- **Rebound**

BUMP (JOUNCE)

As **bump** (sometimes called "Jounce") is meant the upward movement of the wheel according to the chassis, while the chassis is moving closer to the road surface. The spring length is becoming shorter furthermore.

REBOUND (DROOP)

As **rebound** (sometimes called "Droop") is meant the downward movement of the wheel according to the chassis, while the chassis is moving further from the road surface. The spring is becoming longer until to its full (uncompressed) length.

2.4.2 DIRECTLY OPERATED SUSPENSION SYSTEM

Many of mass-production vehicles are Spring/Damper Directly Operated.

This construction is represented by placement of these two units directly to the moving rigid suspension linkages. This is mainly done at the bottom link (bottom A-arm) because higher forces act here.

Examples can be seen in all suspension design varieties listed in chapter 2.3

2.4.3 ROCKER OPERATED SUSPENSION SYSTEM

This type of suspension can be also named **Spring/Damper Indirectly Operated**.

The main advantage comparing to directly operated suspension system are:

- less unsprung mass
- better aerodynamics
- more design varieties
- more setting varieties

The great usage of this construction can be seen in competition field; at high performance sports cars; low-series production or special individual production range. Here the benefits (described further) are above the difficulties which it also brings (as package space, higher cost and more difficult design).

There is a **rocker**, the main part, which transmits the movement provided by some rigid connection rod to the damper/spring unit. This connection rod is connected to the moving rigid suspension linkages at its other end.



There are two main types of connecting rods depending at load conditions they are working at:

- **PUSH-ROD** - compression load
- **PULL-ROD** - tension load

PUSH-ROD SYSTEM

As stated before, the configuration of this layout results into **compression load** of the rigid connection rod. This brings **higher** demands on its stiffness according to refrain from buckling stability of a rod. Furthermore as all the following suspension parts (rocker, spring, damper, anti-roll bar) are placed at the **top** of the vehicle, the CG is moved higher.

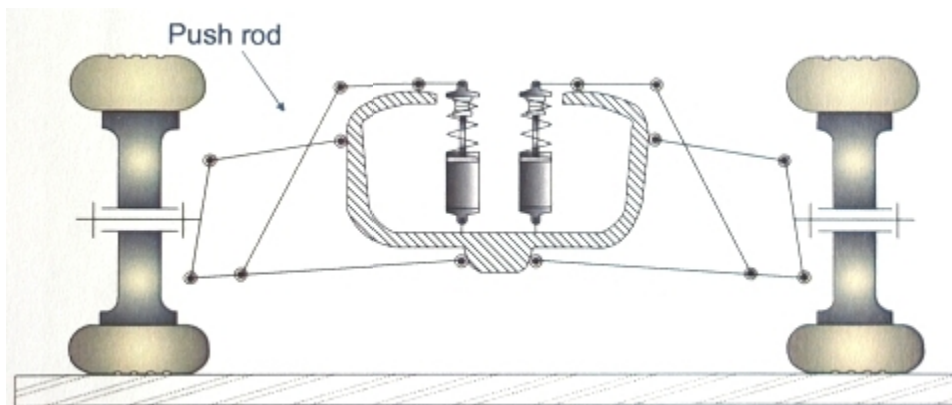


Fig. 33 Push-rod actuated suspension [5]

PULL-ROD SYSTEM

As stated before, the configuration of this layout results in **tension load** of the rigid connection rod. This brings **lower** demands on its stiffness according to refrain from buckling stability of a rod. Moreover as all the following suspension parts (rocker, spring, damper, anti-roll bar) are placed at the **bottom** of the vehicle, the CG is moved lower.

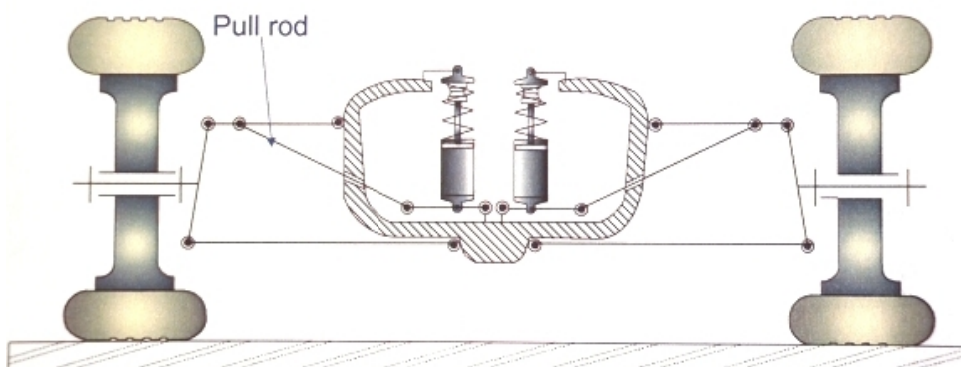


Fig. 34 Pull-rod actuated suspension [5]



2.4.4 RELATIVE RATIOS

As the spring/damper unit is not connected directly to the wheel centre, some **relative ratio** has to be used to know the relationship between travel of wheel and spring/damper unit.

Note: In following part there is an assumption that the whole assembly rim-tire (called 'wheel') is totally rigid, no tire rate is considered at all.

WHEEL RATE

(k_{wheel}); [N/mm]

Wheel Rate is defined as vertical force applied to the wheel over its vertical displacement.

$$k_{\text{wheel}} = \frac{F_{\text{wheel}}}{\Delta_{\text{wheel}}} \quad (1)$$

where:

F_{wheel} [N] Vertical force applied to the wheel

Δ_{wheel} [mm] Displacement of the wheel (measured relative to the chassis)

SPRING RATE

(k_{spring}); [N/mm]

Spring Rate is defined as force applied at the suspension spring over its axial displacement.

$$k_{\text{spring}} = \frac{F_{\text{spring}}}{\Delta_{\text{spring}}} \quad (2)$$

where:

F_{spring} [N] Force applied at the spring, acting directly along spring axis

Δ_{spring} [mm] Displacement of the spring (measured axially along the centreline)

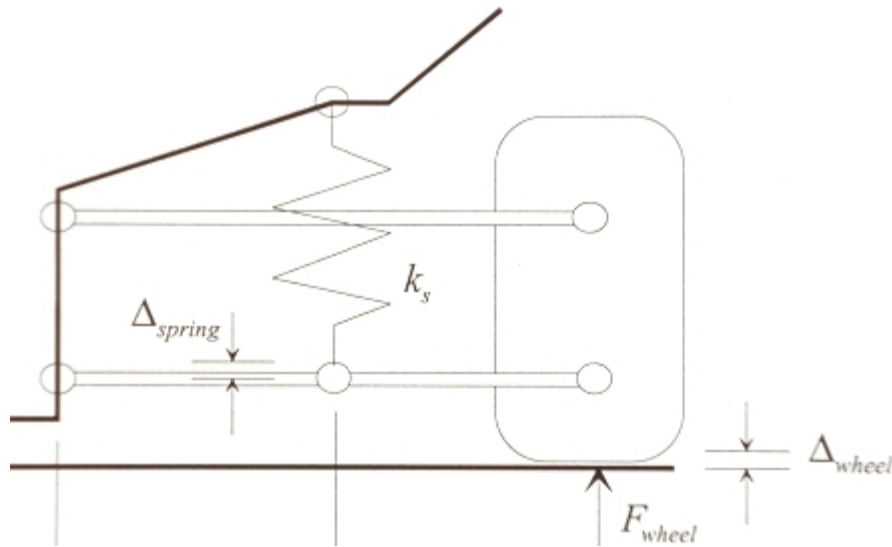


Fig. 35 Wheel and spring rate [4]

INSTALLATION RATIO – LINEAR

(IR); [-]

For explanation of **Linear Installation Ratio** the simple example of Directly Operated Suspension System is used.

Note: the assumptions for further definitions include:

- The Installation Ratio remains constant during the wheel travel
- The displacement is small
- Spring/damper unit is connected perpendicularly to the suspension link, stays perpendicular all the time.
- Force acts still straight at the wheel contact patch with no inclination angle (no camber change)
- All mentioned suspension points are assumed to lie in one plane (2D problem); if not a layout is required to determine IR

All further definitions refers to [Fig. 35](#), [4]

The equation for **Installation Ratio** is defined as the rate of change of spring compression with wheel movement:

$$IR = \frac{\Delta_{spring}}{\Delta_{wheel}} \quad (3)$$

The **IR** is usually lower than 1, in other words the vertical wheel travel is usually larger than the corresponding displacement of the spring.



In force meaning it can be defined also as stated in equation (4)

$$IR = \frac{F_{\text{wheel}}}{F_{\text{spring}}} \quad (4)$$

Having in mind the value of **IR** is still the same for some instant example, this means that the force which acts at the spring is in opposite rate than the travel is. That is why sometimes the **Force Ratio (FR)**, [-] is stated, defined as inverse value of **IR**:

$$FR = \frac{1}{IR} \quad (5)$$

$$FR = \frac{F_{\text{spring}}}{F_{\text{wheel}}} \quad (6)$$

INSTALLATION RATIO – NON-LINEAR

(IR); [-]

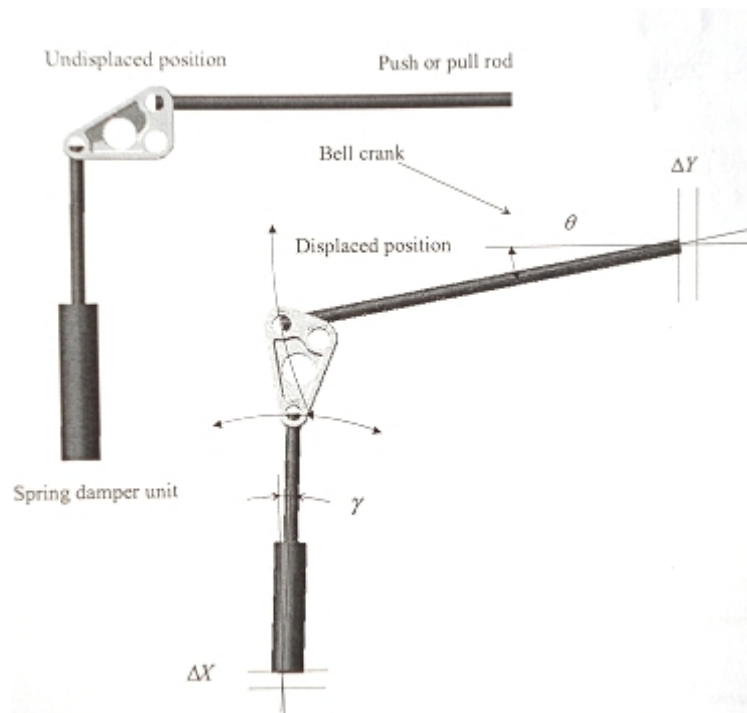


Fig. 36 Non-linear Installation Ratio [4]

The approximation of Linear Installation Ratio is usually sufficiently accurate for race cars, while they use spring with high stiffness. Normally, according to truth, the shape of slope representing IR is neither horizontal, nor linear. The reason is shown at rocker actuated suspension system with significant change of γ and θ angle in *Fig. 36*. The suspension becomes either progressive (raising rate) or digressive; e.g. **IR** decreases as bump increases (*Fig. 37* - digressive curve), the suspension is becoming harder with more wheel bump travel.

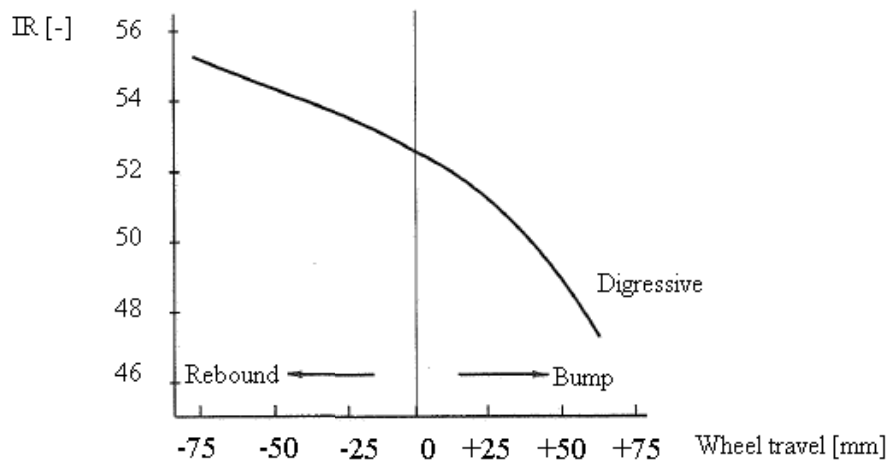


Fig. 37 Non-linear Installation Ratio graph [2]

Despite this, some good way how to obtain an appropriate estimation of **non-linear-IR** curve is shown below at some example of rocker operated suspension system, push-rod actuated.

All further definitions refers to Fig. 38.

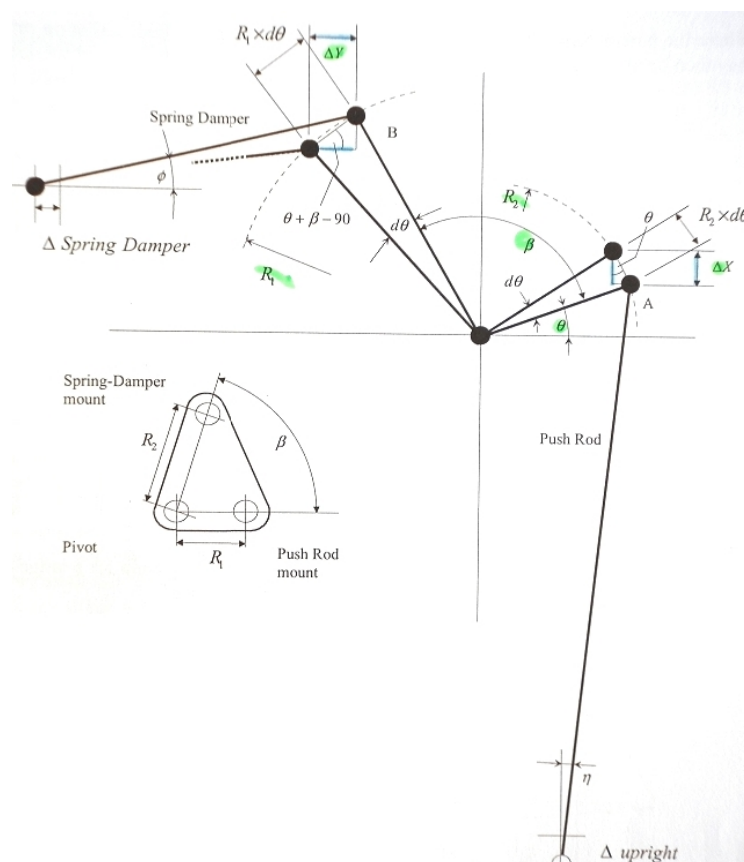


Fig. 38 Non-linear Installation ratio – calculations [4]



Note: the assumptions for further definitions include:

Non-linear Installation ratio - calculations

- All mentioned suspension points are assumed to lie in one plane (2D problem); if not a layout is required to determine IR
- Force acts still straight at the wheel contact patch with no inclination angle (no camber change)
- Spring/damper unit is connected parallel to the suspension link at the beginning, otherwise another geometrical calculations has to be added
- Force acting at the wheel is acting parallel to the suspension link at the beginning, otherwise another geometrical calculations has to be added

Small Angles Approximations:

$$\eta \approx 0 \quad \Rightarrow \quad \Delta_{\text{upright}} \approx \Delta X$$

$$\Phi \approx 0 \quad \Rightarrow \quad \Delta_{\text{springdamper}} \approx \Delta Y$$

where:

η	[deg]	angular change of pushrod relative to vertical axis
Φ	[deg]	angular change of spring/damper unit relative to horizontal axis
Δ_{upright}	[mm]	vertical pushrod displacement
$\Delta_{\text{springdamper}}$	[mm]	horizontal displacement of spring/damper unit
ΔX	[mm]	vertical displacement of one rocker side
ΔY	[mm]	horizontal displacement of other rocker side

Rocker actuated from push-rod:

$$R_2 \cdot d\theta \cdot \cos \theta = \Delta X \quad (7)$$

$$d\theta = \frac{\Delta X}{R_2 \cdot \cos \theta} \quad (8)$$

where

R_2	[mm]	length between rocker axis and second pivot
θ	[deg]	rocker axis angular change
ΔX	[mm]	spring/damper displacement change



Rocker actuating the spring:

$$R_1 \cdot d\theta \cdot \cos(\theta + \beta - 90) = \Delta Y \quad (9)$$



$$d\theta = \frac{\Delta Y}{R_1 \cdot \cos(\theta + \beta - 90)} \quad (10)$$

where

R_1 [mm] length between rocker axis and first pivot

β [deg] rocker specific angle

ΔY [mm] upright displacement change

Resume:



$$\frac{\Delta X}{R_2 \cdot \cos \theta} = \frac{\Delta Y}{\cos(\theta + \beta - 90)} \quad (11)$$



$$\frac{\Delta Y}{\Delta X} = \frac{R_1}{R_2} \cdot \frac{\cos(\theta + \beta - 90)}{\cos \theta} \quad (12)$$

Comparing this result with (3), this derivation shows that the Installation Ratio is given by formula:

$$IR = \frac{R_1}{R_2} \cdot \frac{\cos(\theta + \beta - 90)}{\cos \theta} \quad (13)$$

The **Non-linear Installation Ratio** for some instant example can be graphed as shown in [Fig. 37](#).

Some good example of suspension design which needs to be treated according to non-linear approximation rules is shown in [Fig. 39](#).

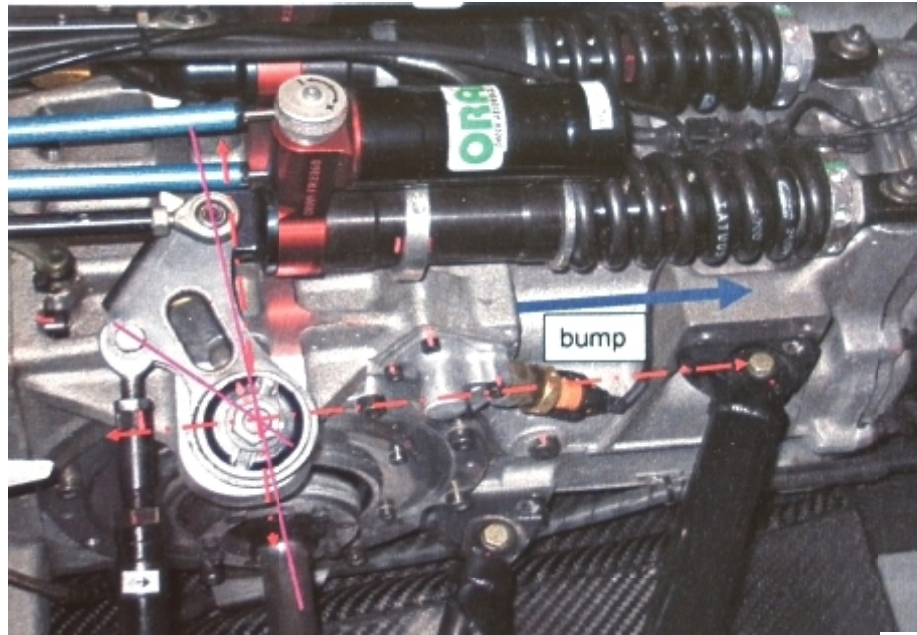


Fig. 39 Non-linear Installation Ratio suspension construction [5]

WHEEL RATE TO SPRING RATE RATIO

(IR^2); [-]

The final equation is got from following process:

$$\Delta_{spring} = IR \cdot \Delta_{wheel} \quad (14)$$

$$F_{spring} = \frac{1}{IR} \cdot F_{wheel} \quad (15)$$

$$k_{spring} = \frac{F_{wheel}}{IR} \cdot \frac{1}{IR \cdot \Delta_{wheel}} \quad (16)$$



$$k_{spring} = \frac{1}{IR^2} \cdot \frac{F_{wheel}}{\Delta_{wheel}} \quad (17)$$



$$IR^2 = \frac{k_{wheel}}{k_{spring}} \quad (18)$$

Because the **Installation Ratio** reduced both the force and displacement of the spring, it must be squared to relate **Wheel Rate** to **Spring Rate**. [2]

2.4.5 ANTI-ROLL BAR (ARB)

When a car corners it rolls. The lateral forces generated in the tires produce a moment about the CG. This moment roll the body of the car which rotates about the RC. The outer spring is compressed, the inner spring is extended. This produces the moment which opposes the moment generated by lateral forces. As suspension springs are normally too soft to limit the roll sufficiently, there has to be some additional device which adds the **roll stiffness** to the chassis but **not bump stiffness** to the wheels. [4]

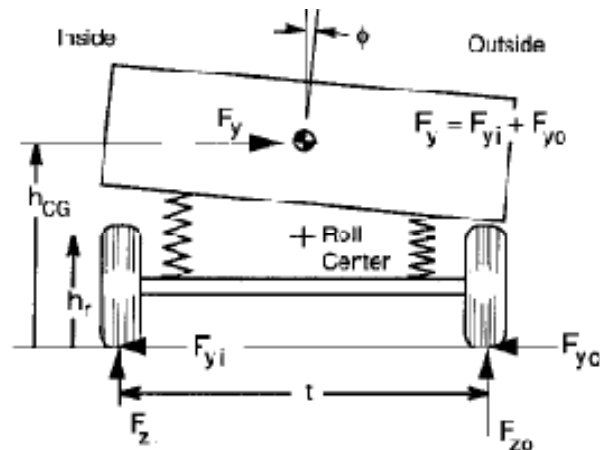


Fig. 40 Force analysis of a simple vehicle in cornering [1]

where:

F_{zo}	[N]	Load on the outside wheel in turn
F_{zi}	[N]	Load on the inside wheel in turn
F_{yo}	[N]	Lateral Force on outside wheel
F_{yi}	[N]	Lateral Force on inside wheel
F_y	[N]	Total lateral force
h_{CG}	[mm]	CG height
ϕ_r	[deg]	Roll angle of the body

These required suspension features are achieved by usage of Anti-roll Bar.

The function of ARB is explained in Fig. 41. The ARB is represented by a torsion bar (Pos.1). As both wheels rise and fall in bump and rebound because of some road obstacles, both ends of ARB (connected to some rigid suspension ling, e.g. lower A-arm, Pos.2) rise and fall together. Since the bar can rotate within the bushings that mount it (Pos.3), the bar has no effect on the wheels. [4]



When the car rolls by contrast, one wheel moves up whilst the other down. This twisting of ARB is resisted by its torsion stiffness thus and so the roll of the car is also resisted.

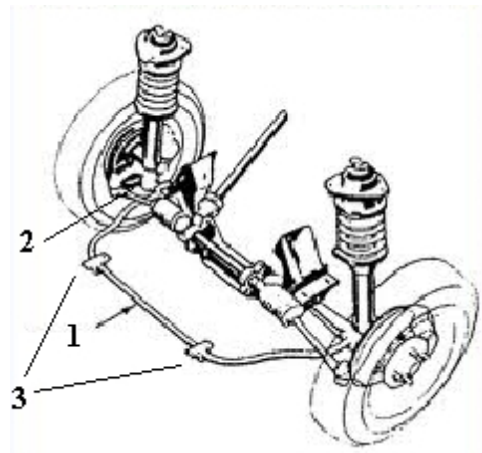


Fig. 41 Antiroll bar [1]

2.4.6 UNISPRING – MONOSHOCK SUSPENSION SYSTEM

As a special combination of rocker operated system with ARB co-operation should be mentioned as a monoshock system.



Fig. 42 Monoshock suspension system [12]

In this configuration (*Fig. 43*) the anti-roll bar is realised by allowing the prism (rocker, Pos.1) to slide in the direction of the arrow shown in Pos.2. Usually the prism slides on a bar (Pos.3) mounted between two supports (Pos.4) and side spring (Pos.5) are placed either side. When both wheels move together (bump, rebound), the rocker rotates about its axis, compressing the spring/ damper unit (Pos.6). When the car is cornering, the prism slides to the side along the bar, compressing the side springs that bias it to the middle position thus providing resistance to roll that is independent to bump. [4]

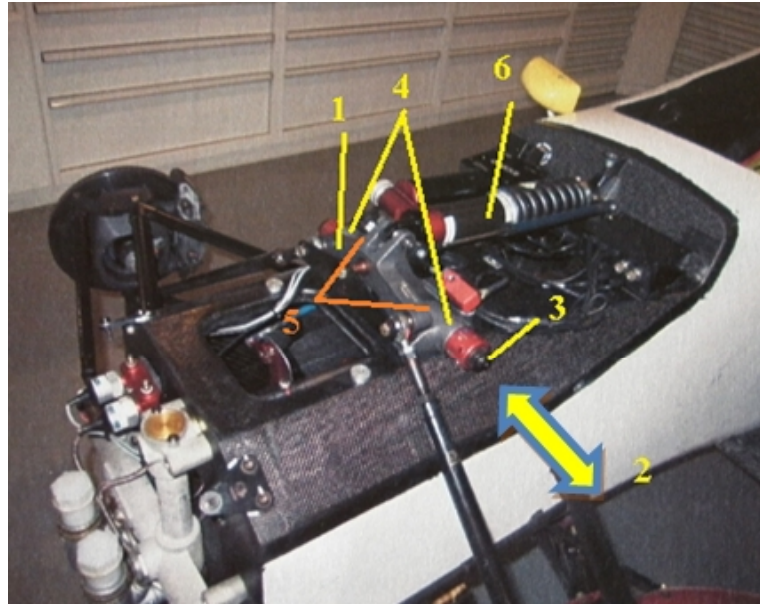


Fig. 43 Function of monoshock suspension system [5]

2.5 DEFINITION OF SUSPENSION GEOMETRICAL CHARACTERISTICS

Although this discussion is of short-long arm suspension systems, many of the concepts are valid for other suspension types. While the practical chapters of this thesis target more at steering than suspension behaviour, this chapter doesn't give as detailed information as the steering theory does.

While the Side view suspension geometry is connected more with dynamics behaviour represented by vehicle load transfer during braking and accelerating, it was decided not to deal with this problematic. The objective there is to determine suspension response to force and torque inputs. Hopefully some another thesis will deal with this topic.



2.5.1 FRONT VIEW SUSPENSION GEOMETRY

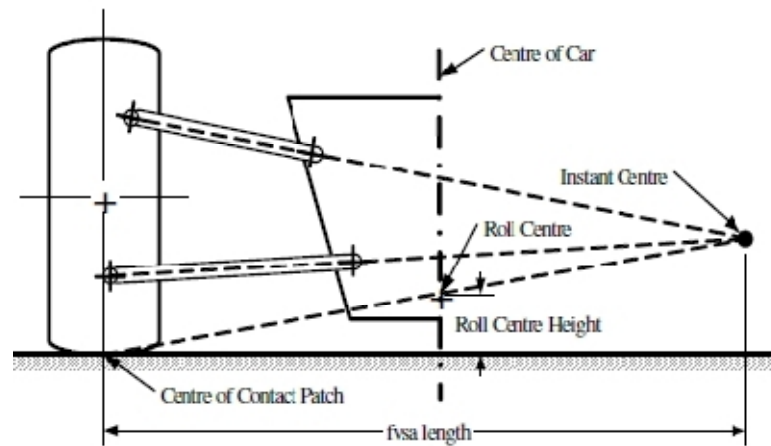


Fig. 44 Front view suspension geometry [2]

INSTANT CENTRE (IC)

Term instant centre is used in describing and determining several common suspension parameters, sometimes it is also called “instantaneous centre”.

Instant centre is the momentary centre which the suspension linkages pivot around. As the suspension moves the instant centre moves due to the changes in the suspension geometry. [7] For small motions of the links (linear range) the Instant Centre remains nearly fixed. In spite of this the normal wheel motions is non-linear, the Instance Centre moves.

Construction:

Instant centre is found by drawing a line which is tangent to arc, around which the upper suspension joint moves, starting in this joint; and by the same meaning another line for the lower joint. The intersection of these lines gives the IC.

ROLL CENTRE (RC)

The roll centre establishes the force coupling point between the sprung and the unsprung masses of the car. When the car corners the centrifugal force acting on the centre of gravity can be translated to the roll centre and down to the tires where the reactive lateral forces are built up. The higher the roll centre is the smaller the rolling moment around the roll centre is. This rolling moment must be restricted by the springs.

Construction:

A line can be drawn from the instant centre to the centre of the tire's contact patch. If done for both sides of the car the point of intersection between the lines is the Roll centre of the sprung mass of the car. The position of the roll centre is determined by the location of the instant centres. High instant centres will lead to a high roll centre and vice versa. [7]



CAMBER

It is the angle between the centre axis of the wheels and the vertical axis of the vehicle.

The camber change rate is a function only of the front view swing arm length, fvsa length. It is intended to eliminate the body roll in turning thus representing the tire to the ground in either unchanged angle or angle with positive character.

Camber Thrust

Camber on a wheel will produce a lateral force known as camber thrust. This force is significantly less than caused by slip angle, nevertheless, camber is additive to the cornering force. Shows a typical camber thrust curve.

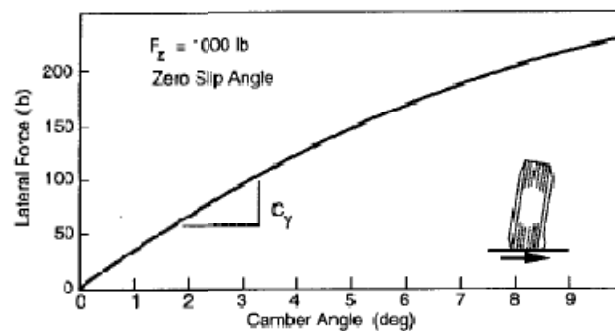


Fig. 45 Lateral force caused by camber of a tire [1]

Positive Camber

The top of the wheel is further out than the bottom. This can be seen in Fig. 46.

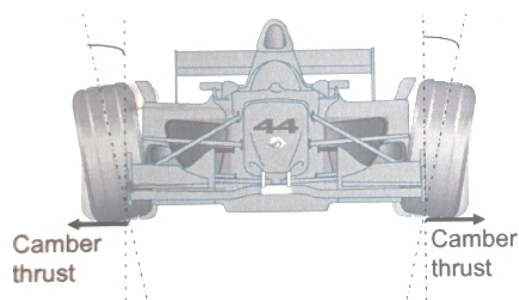


Fig. 46 Positive camber [5]



Negative Camber

The bottom of the wheel is farther out than the top. This can be seen in *Fig. 47*.

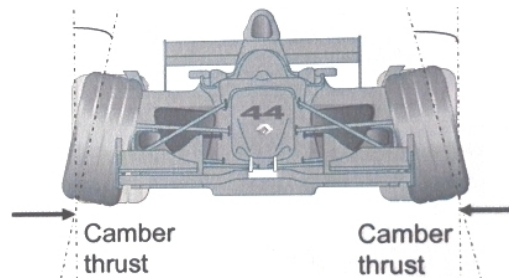


Fig. 47 Negative camber [5]

2.5.2 TOP VIEW SUSPENSION GEOMETRY

WHEEL TOE ANGLE

It is the angle between wheel direction and longitudinal axis of the vehicle. It is function of static geometry adjustment. It is used to overcome handling difficulties in the car.

Some toe angle is desired to create an artificial slip angle and lateral grip, on the other hand minimum static toe is desirable to reduce rolling resistance and unnecessary tyre heating and tyre wear caused by the tires working against each other.

Toe In (Positive)

The front of the wheel is pointing **in** towards the centreline of the vehicle. This can be seen in *Fig. 48*. On the rear tire toe in causes understeer.

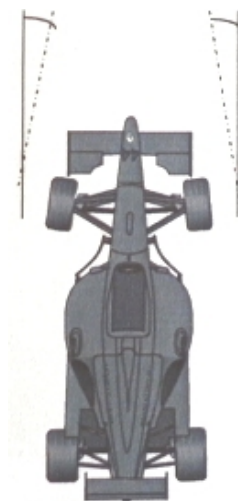


Fig. 48 Toe in [5]



Toe Out (Negative)

The front of the wheel is pointing **away** from the centreline of the vehicle. This can be seen in [Fig. 49](#). Rear toe-out can be used to improve the turn-in vehicle behaviour. Toe out at the front wheels reduces the lateral force and is said to be understeer.

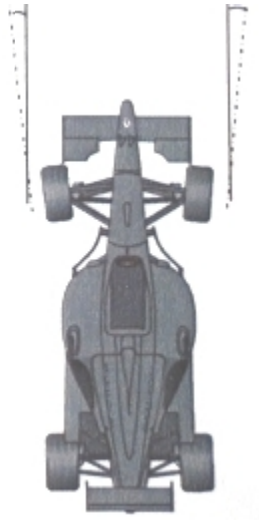


Fig. 49 Toe out [5]



3 STEERING CHARACTERISTICS

In this chapter there will be the main points whose knowledge is necessary to be able to design any well-working steering system.

In suspension field of knowledge there is also some specific common-known technical terminology (as well as in suspension field), which is necessary for being able to communicate in international collective. Some of the expressions became familiar also in foreign languages. Part 3.2 focuses at this terminology.

All the main steering design varieties are mentioned in part no. 3.3 - from the most common used Rack-and-pinion system over Steering Gearbox up to Truck Steering System. Each design description is also accompanied with layout of steering ratio calculation. As this thesis deals about the front axle of a high-performance sports car the main concern is focused on Rack-and-pinion steering system.

Following chapters are considered to be the base of this chapter.

In **part 3.4** here the main steering geometrical characteristics are described, logical ordered by view from front and side of the vehicle.

Part 3.5 is focused at the Ackermann steering geometry.

One has to take in account the fact that steering is always influenced by suspension system - finally the Bump steer problematic is taken apart.

The knowledge of fundamentals and understanding of their advantages and disadvantages are crucial for any steering design.

To fully cover steering design topic there should be also chapters dealing with influence which has the engine torque at steering behaviour, in case of FWD vehicles.

Anyway, as far as this thesis deals with Front Axle of a High-performance Sports Car, clearly RWD, there is no focus at this topic. Furthermore this would cross the stated borders and volume of tasks stated for this work. Hopefully some another thesis will deal with this problematic.

3.1 DEFINITION OF STEERING

In contrast to description in 2.3.2, In spite of rear suspension with one single prescribed path, there is another rotation degree of freedom at front steered axle, but only when demanded from the driver via steering system, which will be topic of this chapter.

3.2 TECHNICAL TERMINOLOGY

3.2.1 SAE TIRE FORCE AND MOMENT AXIS SYSTEM

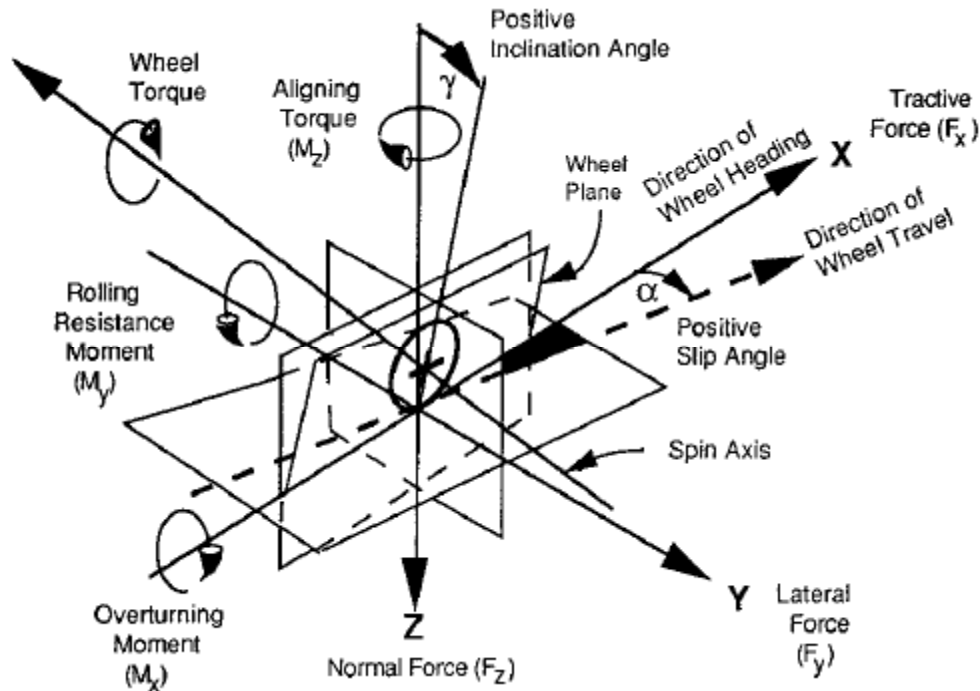


Fig. 50 SAE Tire force and moment axis system [1]

SAE (Society of Automotive Engineers) has selected a convention by which to describe the forces on a tire. The forces are measured at the centre of the tire contact print. The ground reactions on the tire are described by three forces and moments as follows:

<u>symbol</u>	<u>description</u>	<u>symbol</u>	<u>description</u>
F_x	Tractive force	M_x	Overturning torque
F_y	Lateral force	M_y	Rolling resistance moment
F_z	Normal force	M_z	Aligning torque

[1]

As this thesis doesn't deal with influence which has the engine torque at steering behaviour, in case of FWD vehicles, the additional torque from engine power is not mentioned there.

Without any further calculations (which are needed to prove following statement), we can say that the difference between the momentum result from left and right wheel represents the steering wheel torque feedback provided to the driver, graphically shown in [Fig. 51](#), called reverse efficiency. Generally this torques act against the turning motion, thus their effect is understeer.



REVERSE EFFICIENCY

Reverse efficiency refers to the ability of the steering mechanism to pass road inputs back to the driver for feedback. [2]

Some amount of reverse efficiency is always desirable allowing the driver catch the abnormal vehicle behaviour and deal with it. More about this topic can be found in the next part dealing with steering system design varieties.

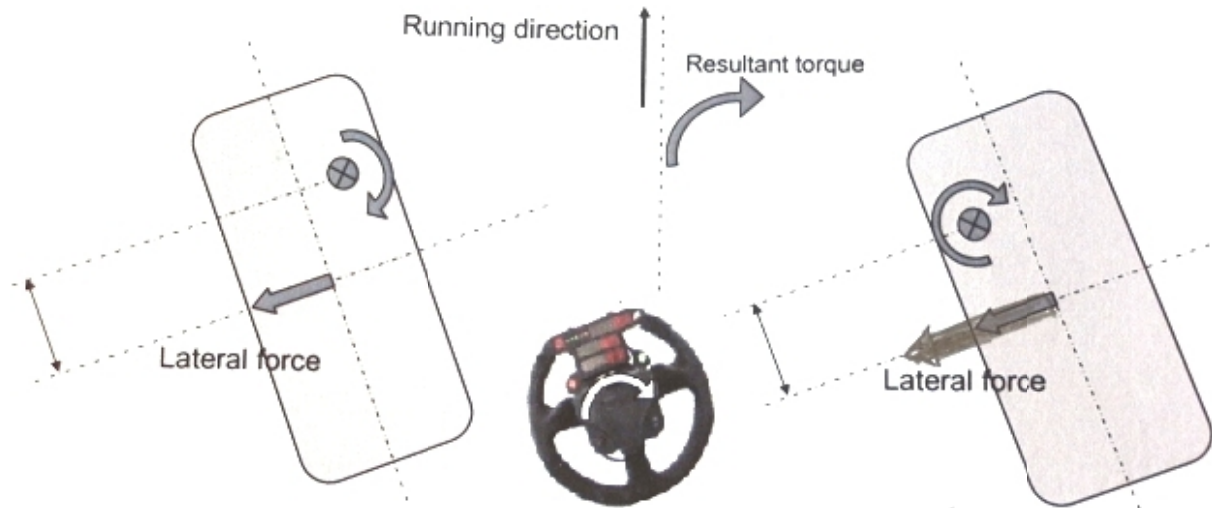


Fig. 51 Reverse efficiency - aligning torque [5]

3.2.2 WHEEL CENTRE LINE

- Vertical line going through the wheel width geometrical centre in the front view (see *Fig. 59*)
- Vertical line going through wheel centre in the side view (see *Fig. 62*)

3.2.3 KINGPIN AXIS

Basically it is practiced by solid pin, which forms an axis about the wheel is steered. Nowadays there is no solid equivalent of this part. Practically, this is an imaginary axis, going through lower and upper ball-joint or lower ball-joint and upper mounting bearing on a strut. This axis is not vertical or centred on the tire contact patch for many reasons. Its inclination is normally out-forward along the way from top to the bottom. By this the **trail** and **scrub radius** are achieved (see 3.4).

Kingpin axis is shown as dashed line in *Fig. 59* and *Fig. 62*.

3.2.4 STEERING RATIO

(SR); [-]

All the steering system designs have their own internal ratio. The **Overall Steering Ratio** of the automobile, then, can be defined in general as the numerical reduction between the rotational input (in degrees) from the pinion or steering wheel and the rotational output about the kingpin axis (in degrees).



Mathematical expression where direct angles values are available:

$$SR = \frac{\Omega}{\delta} \quad (19)$$

where:

Ω [deg] angle of pinion (steering wheel) rotation from instant position

δ [deg] steer angle of front wheel (*Fig. 65*)

Common values of SR for road passenger cars are between 15-20 [1]

Generally, when the power-assisted steering is not used, mainly the steering ratio determines the steering effort that is required for steering manoeuvres.

Layout of steering ratio calculations are described for both Rack-and-pinion (3.3.1) and Steering Gearbox (3.3.2) steering construction in their parts.

Note:

While all the connection links are not usually in one plane and there are not right angles between them, the steering ration becomes non-linear. Furthermore due to Ackermann steering geometry (3.5) there appears another difference between left-right wheels.

The best way how to get the exact steering ratio for any steering wheel angle, left/right wheel, in any time of steering manoeuvre is to use some MBS.

3.2.5 TIRE PROPERTIES

In cornering conditions the tire has to develop lateral force, it will also experience lateral slip.

SLIP ANGLE

(α) , [deg]

- angle between the desired direction of steered tire (direction of heading) and its direction of travel (real direction)

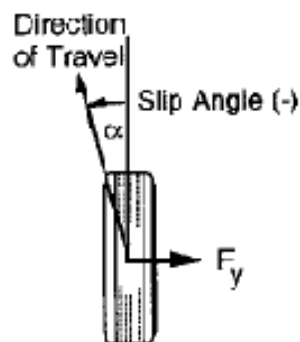


Fig. 52 Slip angle [1]



There is a relation between lateral force F_y and slip angle α , which can be described according to next graph.

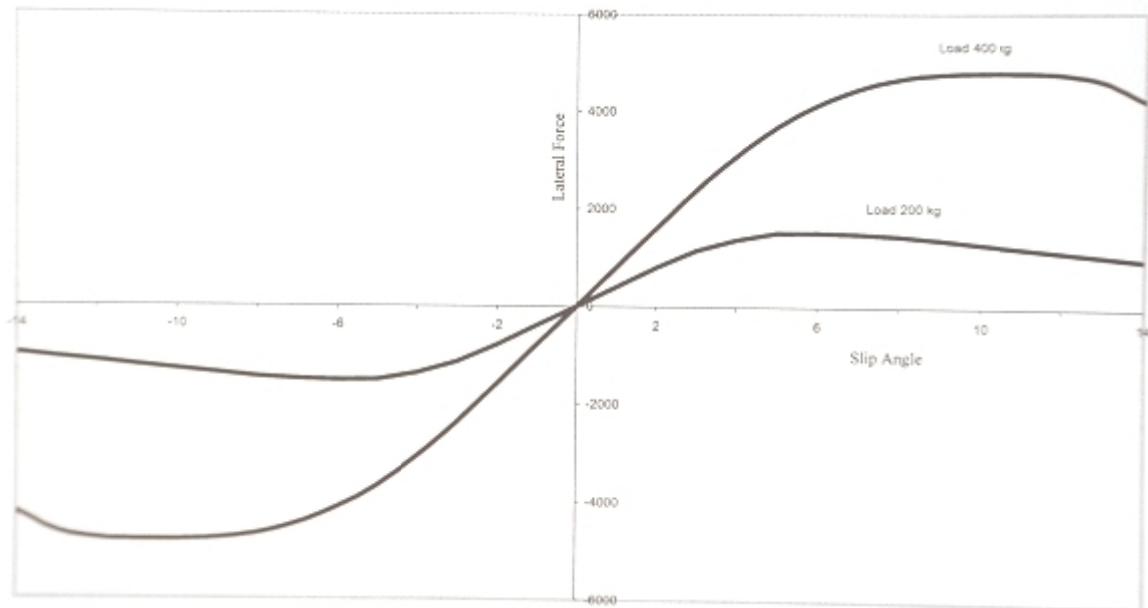


Fig. 53 Lateral force vs. slip angle [4]

CORNERING FORCE

(F_y) , [N]

- lateral force acting at centre of tire print

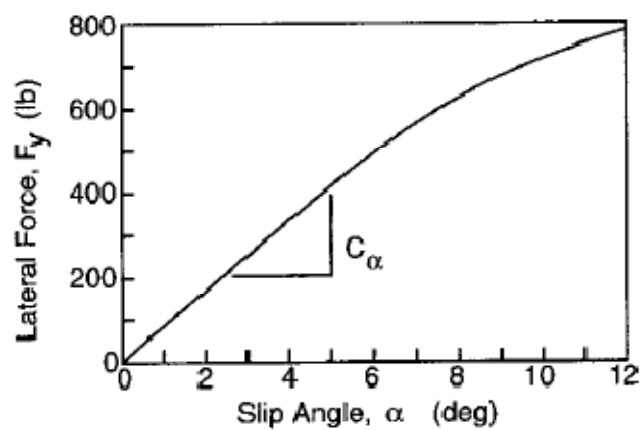


Fig. 54 Cornering force [1]

At low slip angles this force act linear, thus the slope is defined by coefficient: cornering stiffness c_α . [1]

$$F_y = c_\alpha \cdot \alpha \quad (20)$$

**CORNERING STIFFNESS** $(c_{\alpha})[\text{N/deg}]$

Slope of the curve for F_y versus α at $\alpha=0$.

This is property of tire, depending on many variables such: tire size, tire type (radial, bias-ply), width and thread.

3.3 STEERING SYSTEM VARIETIES

In this chapter the main three types of steering system are described. The main idea - to transform the **rotary** motion of steering wheel to **linear** motion of connection linkages (steering tie-rod) and then back to **rotary** (turning the wheel about kingpin axis, by steering arm) - is the same for all of them.

When the tie-rod is located ahead of the wheel centre, it is a **forward-steer configuration**, in case it is placed behind the wheel centre is it **rear-steer configuration**.

Most of modern cars, event the ones in the basic class, are nowadays equipped with power-assisted steering. Anyway this chapter doesn't focus on it, as the fundamentals stay unchanged, while it is only comfort equipment.

There are three main steering system designs:

- Rack-and-pinion
- Steering Gearbox
- Truck Steering System

3.3.1 RACK-AND-PINION

As the name prompts, this construction consists of **rack** (the part which works in translation movement) and **pinion** (the part which works in rotation motion). The lateral translation is relayed by tie-rods to the steering arms, thus turning the wheel about kingpin axis. Initially this construction is represented by fixed gear ratio, constant in all position of components.

This type of steering is characterized by high reverse efficiency. Driver can feel many of tire-road signals.

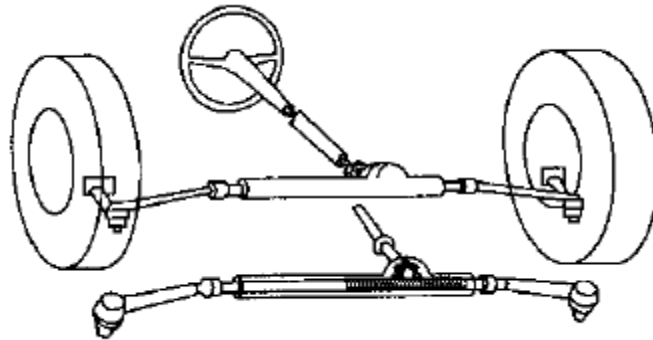


Fig. 56 Rack-and-pinion steering system draft [1]



Fig. 55 Rack-and-pinion Woodward [10]

Drawing of Woodward steering rack can be found in [App. 3. \[9\]](#)

Steering Ratio

Note: the assumptions for further definitions include:

- Tie rod is nearly perpendicular in top and front view, if not a layout is required to determine SR

**C factor [mm/1 rotation] (rack travel number)**

As the Rack-and-pinion directly transforms rotary movement to linear, the “c/factor” of a steering rack became common. The value of c/factor describes the amount the steering rack moves in longitudinal motion according to one full rotation (360°) of pinion.

$$c_factor = \frac{travel}{n_pinion} \quad (21)$$

where

travel	[mm]	total travel of steering rack from instant position according to pinion/steering wheel angle change
n_pinion	[-]	ratio between instant steering wheel rotation angle and one full turn (360°)

$$n_{pinion} = \frac{\Omega}{360^\circ} \quad (22)$$

Often a steering rack is described as a “50-mm rack”; in countries with Imperial System this can be e.g. ”2-inch rack”.

Now the final steering ratio as stated in 3.2.4, (19) can be counted by equation (23):

$$SR = \frac{360^\circ}{\sin^{-1}\left(\frac{c_factor}{s_arm}\right)} \quad (23)$$

where

s_arm	[mm]	steering arm length
-------	------	---------------------

3.3.2 STEERING GEARBOX

Steering Gearbox is nowadays used very rarely at passenger cars and light trucks. In this construction the rotary motion of steering wheel is changed by some gears in the mean of directional and numerical reduction - ratio. This gear can be performed by two cone wheels with different radiuses, or by worm and sector gear. This results again in rotary motion, thus the pitman arm is used to get the linear motion. This is transmitted by a series of relay linkages and tie rods to the steering arm of each wheel, thus turning those wheels about their kingpin axis.



This type of steering system is characterized by low reverse efficiency. In the case of gearbox made out of worn-sector gear wheel, the reverse efficiency is almost zero. Because of reducing driver fatigue, this may be in advantage some cases (heavy trucks, off roads).

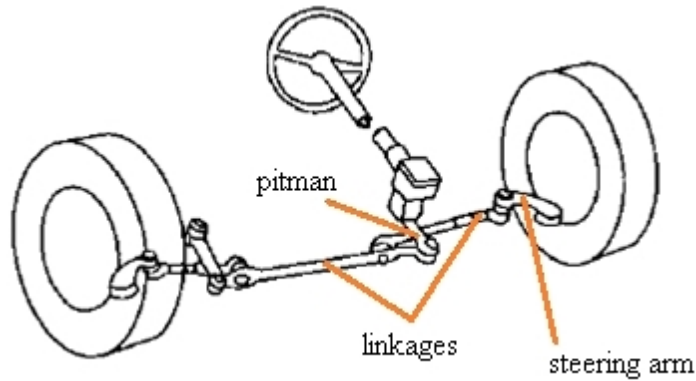


Fig. 57 Steering gearbox [1]

Note: the assumptions for further definitions include:

- Tie rod is nearly perpendicular in top and front view, if not a layout is required to determine SR
- All the linkages are nearly parallel to each other

If the box ratio is unknown, it may be easy to measure the pitman arm motion (with a dial indicator) for 360° of steering wheel station and use this dimension as the c_factor in the Rack-and-pinion system. [2]

If the steering box ratio is known, then the equation (24) can be used to get the SR.

$$SR = BR \cdot \left(\frac{pm_arm}{s_arm} \right) \quad (24)$$

where

BR [-] steering box ratio

pm_arm [mm] pitman arm length

3.3.3 TRUCK STEERING SYSTEM

In general, the Truck Steering System consists of Steering Gearbox, described in previous part, but the linkage layout is different thereafter. Only the left-side wheel is steered directly from the gearbox, the right wheel is steered from the left one via a tie-rod linkage.

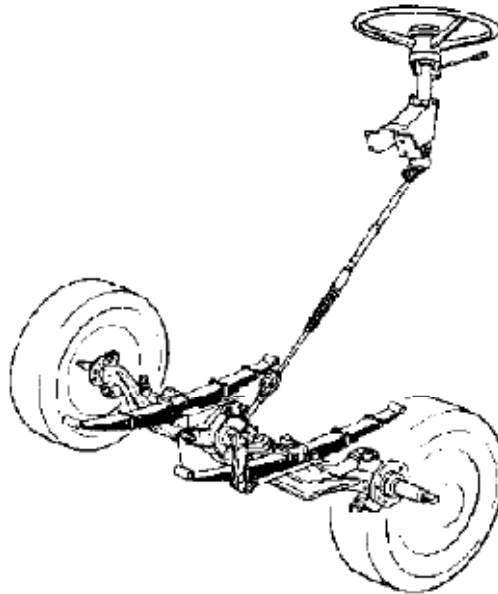


Fig. 58 Truck steering system [1]

3.4 DEFINITION OF STEERING GEOMETRICAL CHARACTERISTICS

Steering geometrical characteristics are common for every suspension and steering system combination. By instance, Double Wishbone suspension system was chosen, in co-operation with Rack-and-pinion steering system. Here, all the following characteristics are caused by position of upper and lower ball-joint.

The specific design of steering system geometry has a well-recognized influence on steering performance measures such as centre feel and returnability. This returnability (self alignment to the straight ahead position) at low speeds is caused mainly by Kingpin Axis Inclination while at high speeds by mainly by Mechanical Trail.



3.4.1 FRONT VIEW STEERING GEOMETRY

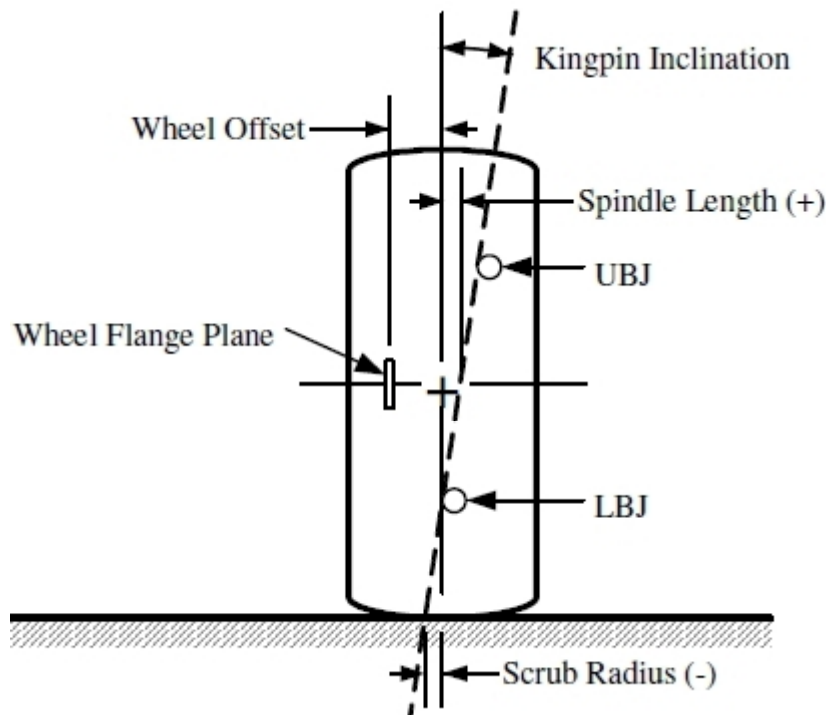


Fig. 59 Front view steering geometry [2]

The main front view geometry characteristics are Kingpin Axis Inclination, Scrub Radius and Spindle Length. Furthermore the Wheel Offset has to also be taken in mind in choosing the final position of upper ball-joint (UBJ) and lower ball-joint (LBJ).

All mentioned are usually compromise between packing and performance requirements.

KINGPIN AXIS INCLINATION

- The angle between the steering axis and the wheel centre line

Normal kingpin axis inclination is toward the centre of the car at the upper end, in front view. Kingpin Axis inclination is (among the others) source of self alignment in the steering system at **low speeds**. Due to this inclination, the car will be raised when left/right steering is applied, with **side equal effect**. Thereafter the wheels are biased towards to straight ahead position because of weight of the car. The more kingpin inclination there is, the larger, effect will be. In case of no caster this will be symmetrical side-to-side.

Disadvantage

The disadvantage can be that this inclination affects the steer camber, bringing unfavourable positive camber to the outside wheel, leaning the top of the wheel outward the car (in case the steering is applied and kingpin axis is inclined in normal direction), see *Fig. 60*. Similar theory for inside wheel is in vice-versa meaning.

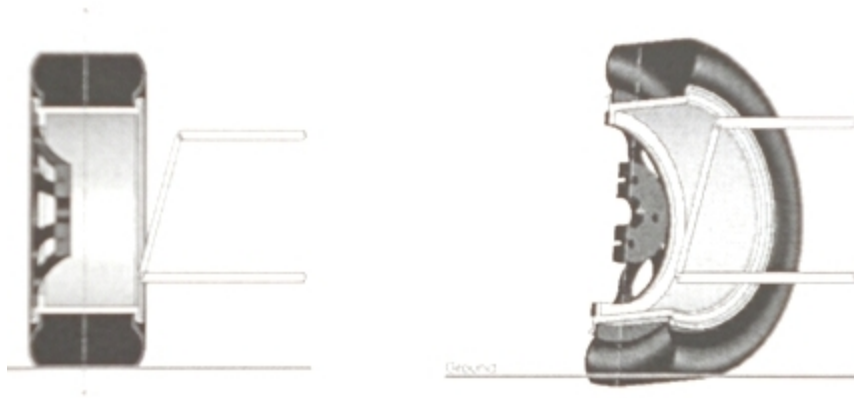


Fig. 60 Kingpin axis inclination disadvantage [4]

The way how to overcome this negative effect is to introduce another inclination in side view
– Caster (3.4.2)

SCRUB RADIUS

- A distance between of the steering axis interception with the ground and the centre line of a wheel, measured along the ground

As the steered wheel must swing around the circle (with scrub radius), the amount of scrub radius should be kept small since it can cause excessive steering forces. However, some positive scrub radius is desirable since it will provide feedback through the steering wheel for the driver.

Positive value

The kingpin axis crosses the road ground inboard of the centre of tire print (see [Fig. 61](#))

Negative value

The kingpin axis crosses the road ground outboard of the centre of tire print (see [Fig. 59](#))

Centre Point Steering

Steering system with zero Scrub Radius is called “centre point steering”.

SPINDLE LENGTH

- Distance from the kingpin axis to the wheel centre plane, measured horizontally at axle height.

This parameter has also task in car rising when the wheels are turned; the longer spindle length the more the car will be raised.

While driving over a bumpy road the rolling radius and thereafter the wheel rotation speed are constantly changing, which gives the longitudinal forces at the wheel centre. [2]

These forces act at the arm of Spindle Length, producing kickback torque to the steering wheel. Zero Spindle Length means no kickback in such a situation.



WHEEL OFFSET

- It is the distance between the wheel centre line and the face of wheel hub to which the wheel is mounted (wheel flange plane)

Wheel offset is a property of wheel rim itself. In rim manufacturers' terminology this is usually called "ET number". The aim is to produce the rims with as large ET number as possible, thus allowing packaging of all components inside the wheel (upright, suspension components, brake callipers etc.)

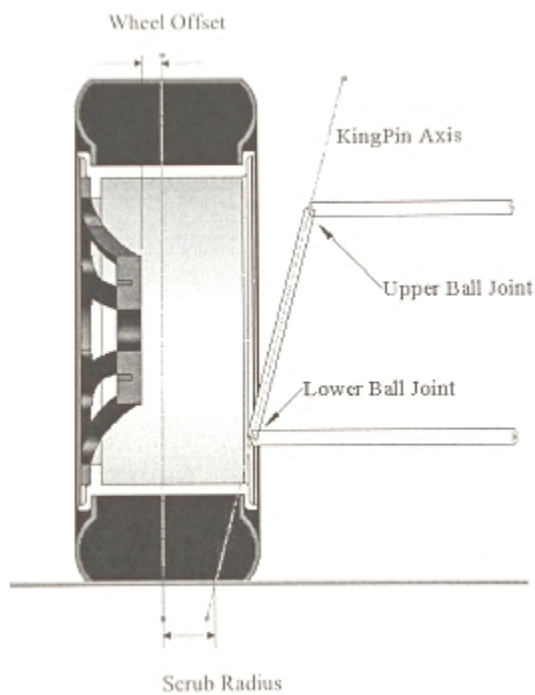


Fig. 61 Wheel offset and scrub radius [4]



3.4.2 SIDE VIEW STEERING GEOMETRY

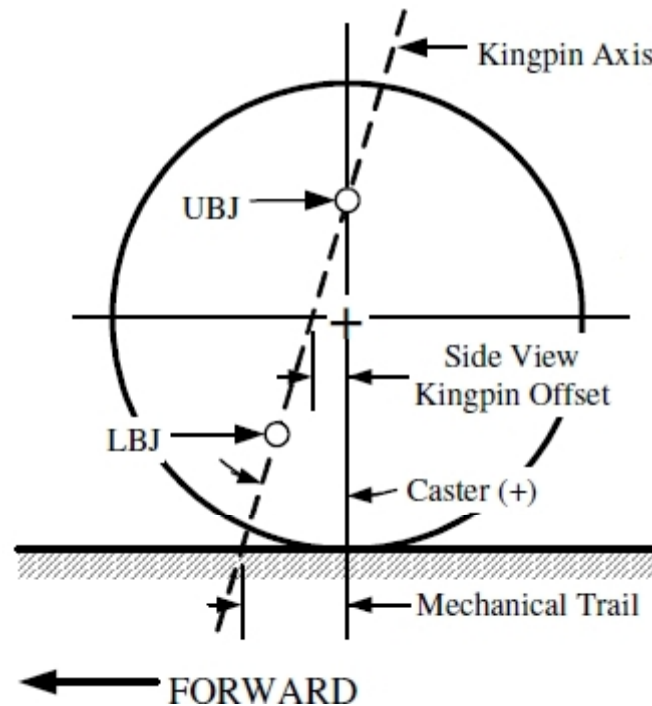


Fig. 62 Side view steering geometry [2]

CASTOR

- The angle between the steering axis and the wheel centre line

Normally is considered positive when the steering axis is tilted towards the rear of the vehicle. When the kingpin axis doesn't pass through the centre of the wheel then there is a side view **Kingpin offset** present.

As stated in 3.4.1, the Castor inclination eliminates unfavourable positive steer camber change caused by Kingpin axis inclination; thus adds favourable steer camber to the outside wheel, leaning the top of the wheel toward the centre of the car. Similar theory for inside wheel is in vice-versa meaning.

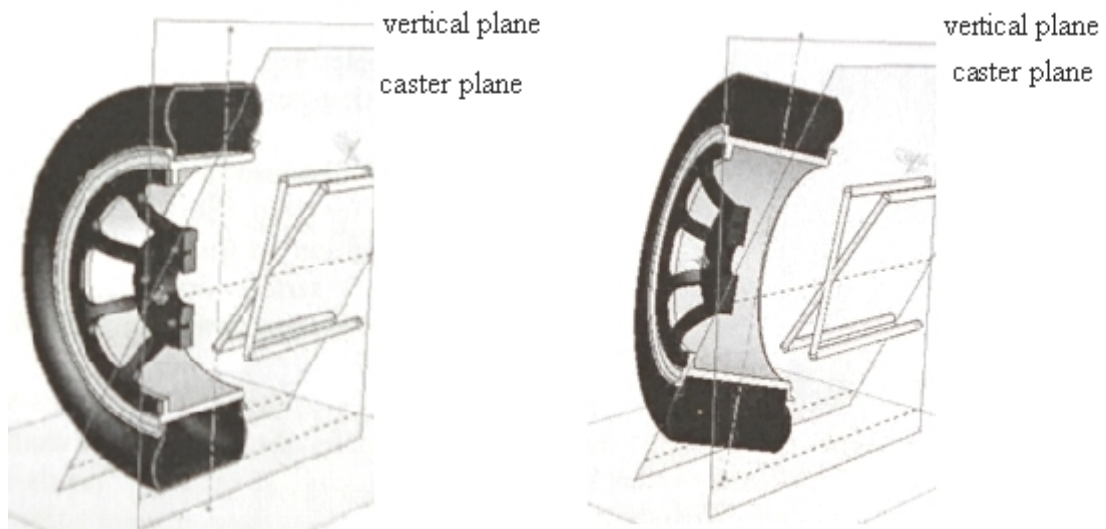


Fig. 63 Wheel castor [4]

Disadvantage

Due to this inclination, the car will be raised/lowered when left/right steering is applied, **with side opposite effect**. This brings a disadvantage as weight shifting. Furthermore it adds some steering instability. This can be seen in the *Fig. 64*. The right circle represents wheel in straight ahead position, while the left ring represents this wheel turned 180° around, lowering the car of some amount of distance, the wheel will find it stable position and will not be urged to turn any further.

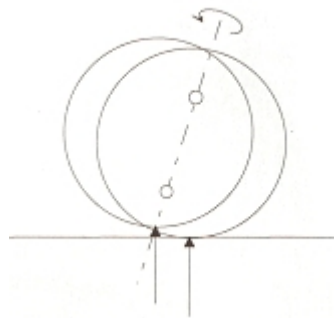


Fig. 64 Steering instability due to castor [4]

Since castor is used to offset the negative effects of Kingpin Axis Inclination, it is normal to find that an amount of castor similar but slightly less than that of Kingpin. [4]

TRAIL

- A distance between of the steering axis interception with the ground and the centre line of a wheel, measured horizontally along the ground



Note:

Sometimes the trail is measured in a direction perpendicular to the steering axis (rather than horizontal) which describes more accurately the lever arm that connects the tire lateral forces to the kingpin. [2]

With normal positive castor the tire print follows behind the steering axis at ground plane.

This is desired for wheel self alignment to the straight ahead position. More trail means that the tire side force has a larger moment arm to act on the kingpin axis, thus providing self-centring moment at **high speeds**. [2]

Thereafter the wheels are biased towards to straight ahead position because of weight of the car. The more kingpin inclination there is, the larger, effect will be. In case of no caster this will be side to side symmetrical.

Disadvantage:

More trail will give high steering force.

3.5 ACKERMANN STEERING GEOMETRY

This part deals with front axle, which is steered about the kingpin axis, with the main aim to steer the inner front wheel more that the outer front wheel. This applies mainly at Low Speed Turning conditions 3.6.1.

While the car is cornering all wheels are travelling along curved paths about their corner centre. When the radius is not too large, then the track of the car plays significant role in considering the radius value and centre position. Thereafter the front wheels have to be steered away from straight-ahead position **in non-parallel way** to each other.

The history of geometry nowadays known as Ackermann goes long to the past. It was firstly used at horse drawn carriages, in order to disturb minimally rich people around while arriving or leaving from the premises on the gravelly roads.

Note: The general presumptions for this part are:

- As Ackermann gives **geometric effect** to the steering, toe angle is just **static adjustment**. It is considered to be zero in straight ahead-position. When there is, actually, any toe angle present it has to be considered in the results.
- The steering tie-rods are parallel to the steering rack, when there is any other angle than 180°, the overall layout has to be considered

The numerical demands stated further refers to the [Fig. 65](#)

(In here the usual definition of corner radius from CG to the corner centre is used.)

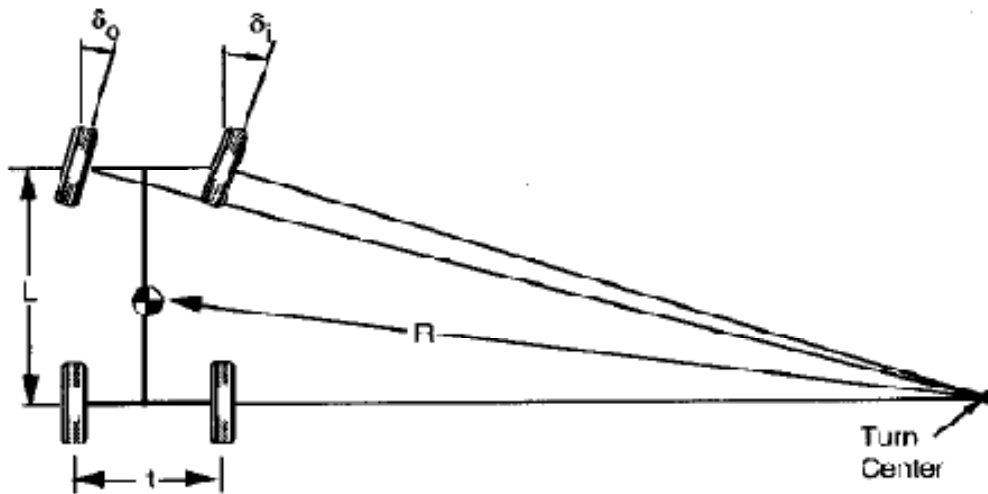


Fig. 65 Ackermann steering geometry [1]

$$\delta_o = \tan^{-1} \frac{L}{(R+t/2)} \quad \Rightarrow \quad (25)$$

for small angles, typical for most turning maneuvers the \tan^{-1} in [rad] is very nearly equal to the angle itself, thereafter:

$$\delta_o = \frac{L}{(R + t/2)} [\text{rad}] \quad (26)$$

$$\delta_o = 57.3 \cdot \frac{L}{(R + t/2)} [\text{deg}] \quad (27)$$

$$\delta_i = \tan^{-1} \frac{L}{(R-t/2)} \quad \Rightarrow \quad (28)$$

$$\delta_i = \frac{L}{(R - t/2)} [\text{rad}] \quad (29)$$

$$\delta_i = 57.3 \cdot \frac{L}{(R - t/2)} [\text{deg}] \quad (30)$$

where

δ_o [deg] steer angle of outer front wheel

δ_i [deg] steer angle of inner front wheel

R [m] radius of the turning circle



3.5.1 POSITIVE ACKERMANN

With positive Ackermann geometry the steering torques tend to increase consistently with steer angle δ , thus providing the driver with a natural feel in the feedback through the steering wheel. [1]

Lines drawn tangentially to front tires' velocity vectors do intersect at the corner centre, which lies on a line through the rear axle.

The Positive Ackermann Geometry is more or less achieved at each road passenger car, according to actual package and layout possibilities.

The disadvantage is that the inner wheel is turned more than necessary to achieve maximum lateral force. Dragging this wheel along a higher slip angles than necessary raises its temperature and slows the car down. [2]

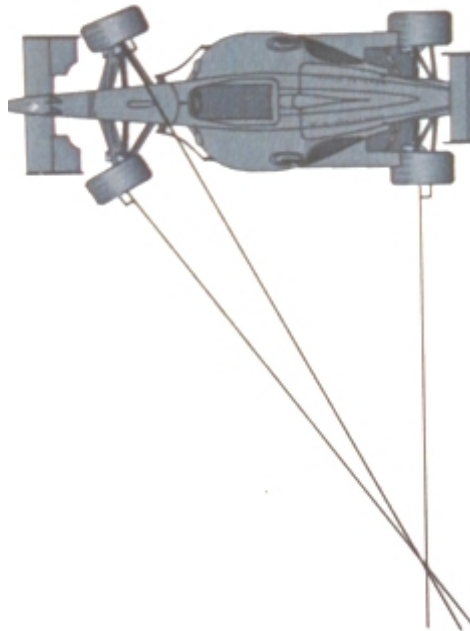


Fig. 66 Positive Ackermann geometry [5]

CREATING POSITIVE ACKERMANN GEOMETRY

The Ackermann steering geometry can be achieved either by progressive steering ratio in the steering system or by geometrical construction. There is some good way how to achieve reasonable approximation of Ackermann geometry shown in the *Fig. 67*.

One- side-construction is represented by a line drawn between the steering axis of front wheel and the vertical axis created in the middle of the rear wheels. The outer steering ball-joint is placed at this line at some distance from the steering axis. This distance represents the steering arm length. The opposite side is just in mirror view. The steering arms layout result to shape of trapezoid with angularity causing the inner wheel steer more than the outer.



The working plane of the construction above is situated horizontally at the same height as the outer steering point.

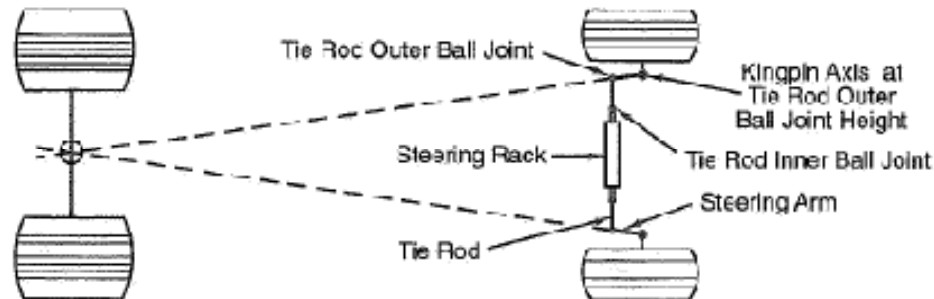


Fig. 67 Positive Ackermann geometry construction [2]

There are two types of general layout:

- Tie-rods placed behind the wheel centre
(This construction provides good package space and wheel clearance from the outer ball-joint and steering arm)
(*Fig. 57*)
- Tie-rods placed ahead the wheel centre
(Less package space)
(*Fig. 56*)

3.5.2 NEGATIVE ACKERMANN

The race-purpose vehicles work most of the time in quite different conditions comparing to road passenger cars. Both slip angles and weight transfer are very much larger, thus the outer wheels have more load on them, thus they are able to generate more lateral force. This can be performed only at higher slip angle (see *Fig. 53*).

Vice-versa, the inner tires have less load, thus require less slip angle to reach the peak of their cornering force. Using a low speed steering geometry on a race car would cause the curve inner tire to be dragged along at much higher slip angles than needed and this would result in raises tire temperature and slowing down the car due to the slip angle induced drag.

That is why sometimes the Reverse Ackermann is also used, providing the outer wheel with higher steer angle.

In this case the moving of a vehicle (e.g. in a paddock) will be force demanding as the wheels will fight to each other for the best surface grip.

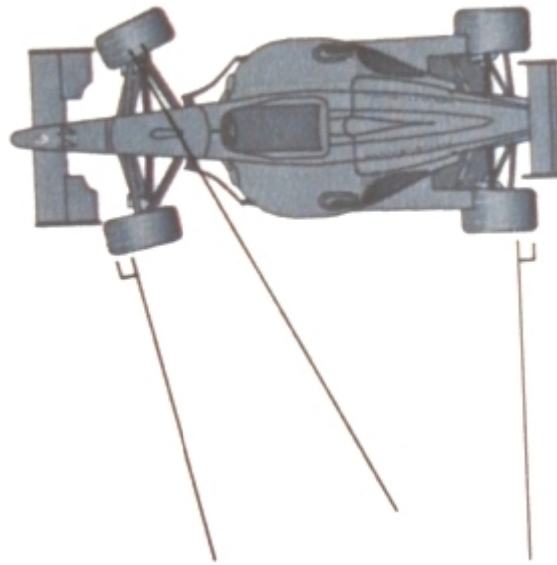


Fig. 68 Negative Ackermann geometry [5]

3.5.3 PARALLEL NON-ACKERMANN STEERING

In this case both wheels are roll tangent to the turning arc of the whole vehicle, they have the same steering angle δ .

The parallel steering brings an undesirable behaviour, when the steering torques grow with steering angle δ initially, but may diminish beyond a certain point, and even become negative – tending to steer more deeply into the turn. [1]

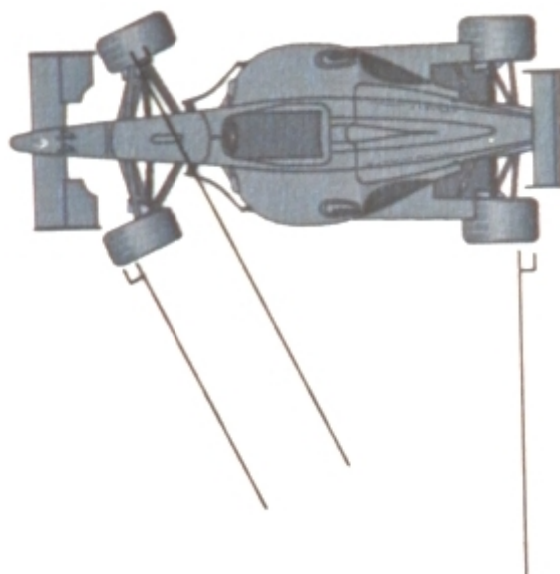


Fig. 69 Parallel Non-Ackermann steering geometry [5]



3.6 CORNERING EQUATIONS

This part will deal with description of vehicle response to steering input from the driver.

Note: the general assumptions for this part include:

- In spite of Ackermann steering geometry in the following part there will be used for purpose of analysis a “bicycle model” of a vehicle. Only one tire is used at front and rear, one Ackermann angle δ is used with a cornering force equivalent to both wheel front and rear.

3.6.1 LOW SPEED TURNING

In Low Speed Turning Theory there is slip considered to be almost zero, the tires are travelling at the same direction as they are pointed; they do not develop any lateral forces. Lines drawn tangentially to tires' velocity vectors intersect at the corner centre. This theory can be applied e.g. parking manoeuvres.

Note: the assumptions for further definitions include:

- Because all tires roll without any slip angle, the centre of cornering must lie at the projection of the rear axle. The usual definition of corner radius (from CG to the corner centre) is approximated as the length from the rear wheel to the corner centre, labelled “R”. Due to the great difference between the turning radius and wheelbase “L” this can be stated as good approximation.

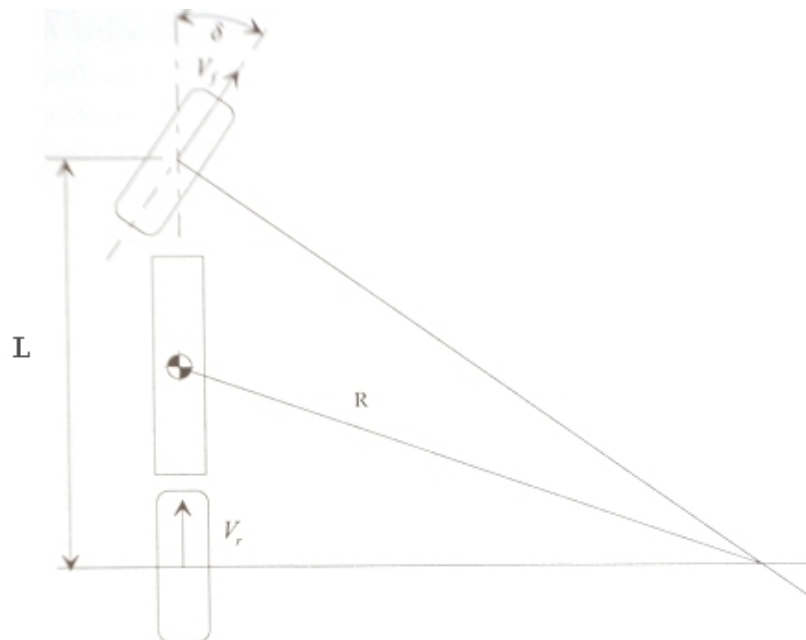


Fig. 70 Low speed turning [4]



$$\delta = 57.3 \cdot \frac{L}{R} \quad (31)$$

Note:

The 57.3 is to get the angle in [deg] instead of [rad].

3.6.2 HIGH SPEED CORNERING

High Speed Cornering Theory describes most of vehicle drive conditions more accurately than Low Speed Turning Theory.

Here the slip angles are playing significant roles at each wheel, the tires are not travelling at the same direction as they are directed; they do develop some lateral forces. Lines drawn tangentially to tires' velocity vectors don't intersect at the corner centre.

Note: the assumptions for further definitions anywhere in this part include:

- The point about which the car is rotating has moved forward significantly. The usual definition of corner radius from CG to the corner centre is used.
- Both front and rear tires are considered to be equal in material, wear, radius and width, The cornering stiffness c_{af} a c_{ar} are equal \hat{a} c_α

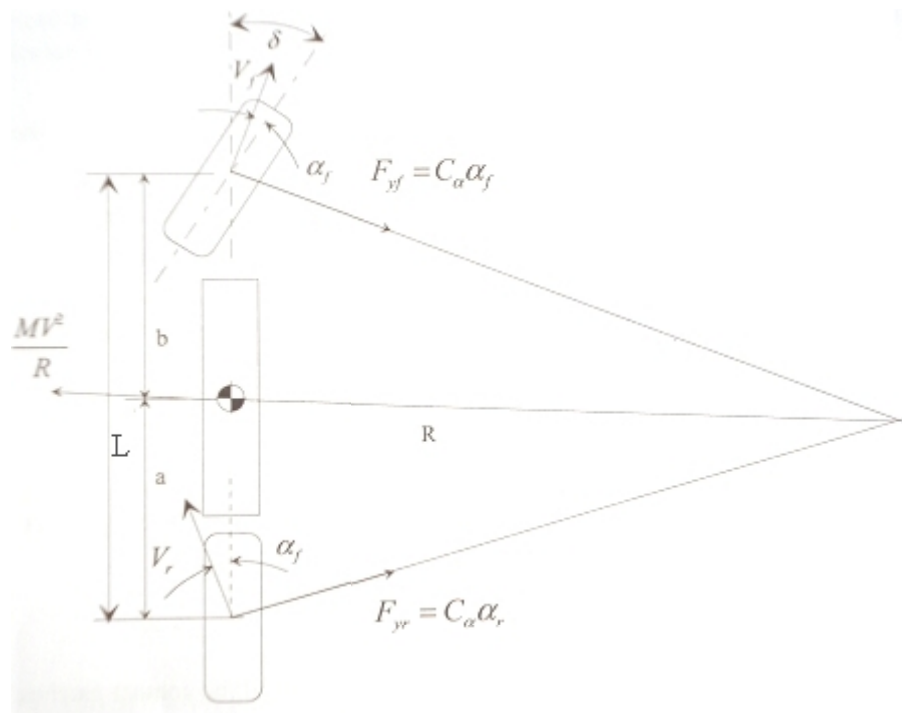


Fig. 71 High speed cornering [4]

The sum of forces in the lateral direction from the tires must equal the mass times the centripetal acceleration:



$$F_{yf} + F_{yr} = \frac{M \cdot V^2}{R} \quad (32)$$

→ comparing with (20) we get:

$$c_{\alpha} \cdot \alpha_f + c_{\alpha} \cdot \alpha_r = \frac{M \cdot V^2}{R} \quad (33)$$

For vehicle to be in momentum equilibrium about rear axis, the moments from front lateral forces and CG centripetal acceleration force have to be equal:

$$c_{\alpha} \cdot \alpha_f \cdot (b + a) = \frac{M \cdot V^2}{R} \cdot a \quad (34)$$

$$c_{\alpha} \cdot \alpha_f \cdot (b + a) \cdot \frac{1}{a} = \frac{M \cdot V^2}{R} \quad (35)$$

→ comparing with (33) we get:

$$c_{\alpha} \cdot \alpha_f + c_{\alpha} \cdot \alpha_r = c_{\alpha} \cdot \alpha_f \cdot (b + a) \cdot \frac{1}{a} \quad (36)$$

$$\frac{\alpha_f + \alpha_r}{\alpha_f} = \frac{(b+a)}{a} \quad (37)$$

$$\frac{\alpha_r}{\alpha_f} = \frac{a}{b} \quad (38)$$

where:

F_{yf}	[N]	lateral cornering force at the front axle
F_{yr}	[N]	lateral cornering force at the rear axle
M	[kg]	mass of the vehicle
V	[m/s]	forward velocity of whole vehicle
α_f	[deg]	slip angle at front axle
α_r	[deg]	slip angle at rear axle
a	[m]	distance between rear axle and CG
b	[m]	distance between front axle and CG

[1]

VEHICLE BEHAVIOUR IN CORNER

While getting the final equation to be able to consider the vehicle behaviour in corner the equation (31) can be used as starting point. Furthermore the tire slip properties have to be added, which is obvious from [Fig. 72](#).

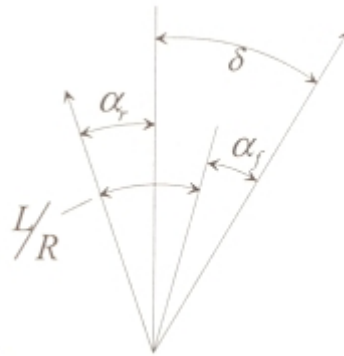


Fig. 72 High speed cornering detail [4]

$$\delta = 57.3 \frac{L}{R} + \alpha_f - \alpha_r \quad (39)$$

There are three basic types of vehicle behaviour in corners:

- Neutral steer
- Oversteer
- Understeer

NEUTRAL STEER

The CG is directly in the middle of tire contact patches.

$$a=b \quad \Rightarrow \quad \alpha_f = \alpha_r$$

Equation is reduced to:

$$\delta = 57.3 \cdot \frac{L}{R}$$

The fundamental Ackermann equation applies.

OVERSTEER

In this case the CG is closer to the rear axis:

$$b > a \quad \Rightarrow \quad \alpha_r > \alpha_f$$

then, $\alpha_f - \alpha_r$ is **negative** number, which delivers smaller turning radius than the driver demanded. The certain radius of corner is less than in the neutral steering case.

The steer angle has to be decreased as the speed is increased to keep desired turning radius.



UNDERSTEER

In this case the CG is closer to the front axis:

$$a > b \Rightarrow \alpha_f > \alpha_r$$

then $\alpha_f - \alpha_r$ is **positive** number, which delivers larger turning radius than the driver demanded. The certain radius of corner is more than in the neutral steering case.

The steer angle has to be increase as the speed is increased to keep desired turning radius.

The car is understeered, when it delivers larger turning radius than the driver demanded. The certain radius of corner is less than in the neutral steering case (- driver gets the steering he asked for).

3.7 RIDE STEER (BUMP STEER)

Ride and Roll Steer (known as “steering geometry errors”) are a function of the suspension geometry and the steering system geometry [2]

Note:

- For further explanation, Double Wishbone suspension system was chosen, in co-operation with Rack-and-pinion steering system
- As Camber and Toe Angle are static adjusted values, they are considered to be zero at the beginning of each simulation. Whether there is any non-zero value in the beginning, this has to be taken into account to determine the final value in any suspension position.

Every car has to be steered by driver input rather than by suspension movement. It is very serious problem if a vertical travel of the front wheels (bump, rebound) also steers them. This is called **Ride Steer**.

Sophisticated Bump Steer Geometry gives the vehicle desired direction stability while driving at high speeds even on roads with not perfectly smooth surface.

The aim is to let the steering tie-rod finish in the same IC (2.5) as the suspension geometry in the front view. Thereafter the outer steering tie-rod ball-joint will follow an arc with the same centre as outer wishbone ball-joint has. This is determined by the kinematic behaviour. Otherwise steer will occur with ride because the steering and suspension linkages are moving about different centres. [2]

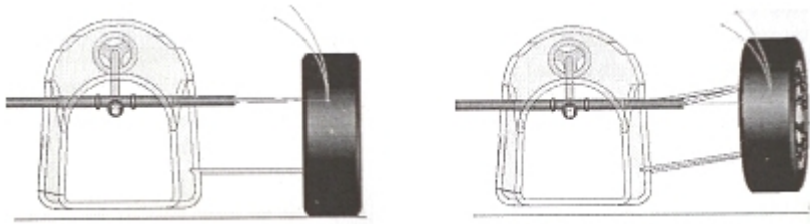


Fig. 73 Bump steer [4]

The easiest way how to refrain the suspension and steering system from Ride Steer is to place steering rack and steering tie-rods in the same plane (from the front view) as one of the wishbone, perpendicularly to the centre line of the car. Theoretically this solution will give zero bump steers with inner and outer ball-joints directly in line forward/backward with appropriate wishbone ball-joint. This solution is also desired for aerodynamics drag.

This cannot be usually performed due to package space and general vehicle layout. Anyway, there are some ways how to achieve sufficiently accurate Ride Steer geometry even with steering rack placed in different vertical height to the wishbone.

One of the solutions is described by **Hartmann's Construction of Bobilier Line**. Please have a look at the [App. 4](#), where a work manual how to perform Hartmann's Construction of Bobilier Line is written. This construction can be used for steering tie rod at the front wheels, tie-rod at the rear wheels and half driveshaft as well.

The result is shown in [Fig. 74](#).

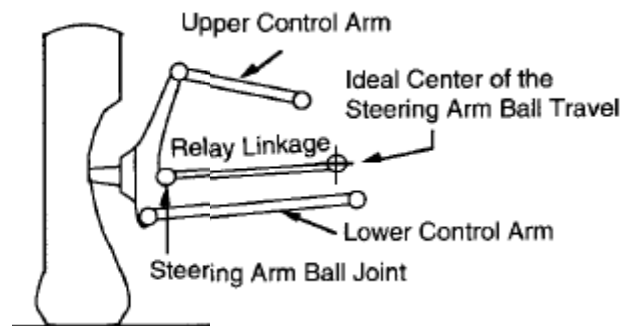


Fig. 74 Hartmann's construction of Bobilier line – ideal geometry [1]

The best way how to check the truth of Ride Steer geometrical construction is to use some of MBS software.

3.7.1 GEOMETRY ERROR

Sometimes the position of steering rack is stated according to overall vehicle construction or due to other circumstances and cannot be changed. Also in this case the achievement of sufficiently accurate Ride Steer is possible, but with some geometry error present. It should be noted, that some of these geometry error are used by intention.



TOE CHANGE

When the outer steering point is constructed according to previous advices, but, then, the inner steering point is moved laterally (away from ideal inner centre), the toe change caused by this geometry error occurs. (*Fig. 75*)

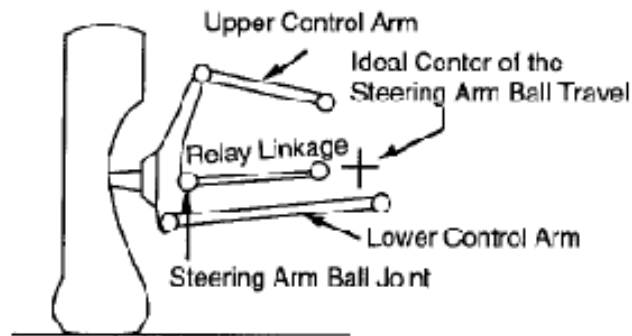


Fig. 75 Steering geometry error causing toe change [1]

This produces toe in/toe out (according to lateral mean of displacement of inner steering point **and** steering rack location – ahead or rearwards to kingpin axis) both in bump and rebound. Thereafter this error will be experienced also in body roll behaviour.

ROLL STEER

Roll steer can be considered a special type of Ride steer. While Ride Steer is caused by bumps in the road and road obstacles negotiation, Roll Steer is caused by lateral load transfer in corners. Anyway the theory stated above applies for both of them.

When the outer steering point is constructed according to previous advices, but, then, the inner steering point is moved vertically (away from ideal inner centre), the roll steer error occurs. (*Fig. 76*)

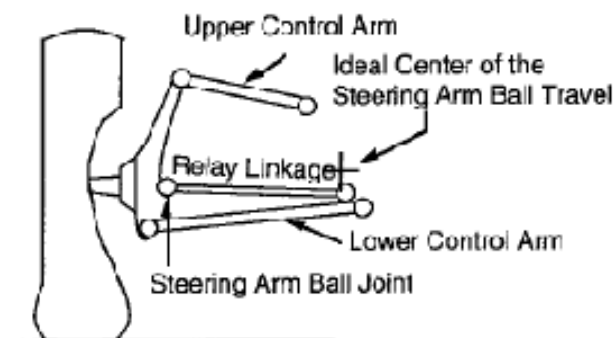


Fig. 76 Steering geometry error causing steering [1]

This produces toe in/toe out (according to vertical mean of displacement of inner steering point **and** steering rack location – ahead or rearwards to kingpin axis) in bump and vice versa in rebound.



In spite of this different error will be experienced in body roll behaviour. Here the body rolls, thus each side of suspension is travelling in opposite way, thereafter both wheels will steer to left/right side, adding understeer/oversteer effect to the vehicle's directional response (according to relays layout).

Sometimes this may be used intentionally, to alter handling behaviour. [1]



4 REAL STEERING CLEVIS

In a.d.Tramontana, while the progress never stops, the necessity of front suspension design change appeared. In the time when the author of this thesis came to the company, the new design was already done and prepared to become a reality. The last thing, which wasn't done, was dealing with all steering geometry questions.

As the designer of this new front suspension wasn't already in the company, we can only quest what were the priorities and design milestones.

Anyway, probable reasons new front suspension was introduced are stated further on:

- Different values of Camber, Kingpin Axis Inclination, Scrub Radius
- Camber can be easily changed by adjustable upper ball-joint
- Different values of Caster, Trail
- Better material and calculation allowed making the wishbones with more compact size with less weight, thus less unsprung mass and faster response to road obstacles.
- Wheelbase became 50 mm shorter comparing to previous design, thus allowing better behaviour in corner rather than at straights. In the future also the rear suspension will be redesigned in the same meaning.

All changes of wishbone design go hand in hand with new design of upright:

- Better material and calculation allowed making the upright with more compact size with less weight, thus less unsprung mass.
- The steering bracket is now a separate piece, which can be easily changed to another, to get desired steering behaviour, described in 3.4. By instance, Reverse Ackermann can be achieved, to push the performance from public road usage to race circuit performance. The design of another type of bracket should be further work according to e.g. customer needs and vehicle intended purpose.

4.1 PREFACE

While this vehicle is supposed to be used mainly on public roads without racing aims, the task for this case was to make as Positive Ackermann Geometry as possible.

As it is hard, or even impossible, to get perfectly both Ackermann and also Bump Steer, the priority was set and the main task was to create geometry with Bump Steer as close to zero as possible.

In this chapter, there is mention the whole process to achieve these, including the results being tested in MB Software simulation. Finally the real steering clevis, which fulfils all the results, was machined and assembled to the car. This is mentioned in the last part of this chapter.



4.1.1 WORK PROCESS LAYOUT

Here is a general layout of work process, which was followed both in part 4.2 and 4.3.

1. State the initial geometry, which is done and cannot be change.
2. State the position of steering rack.
3. CAD Software: Assembly together all the necessary parts, where the car is placed “on the wheels” – steady state of drive, allowing the suspension travelling up and down of desired amount.
4. CAD Software: Create geometry according to theory from previous chapters, working with real 3D parts
5. CAD Software: Get the coordinates of the points necessary to be able to run MBS simulation
6. MB Software: Use the points from CAD to create the MBS Simulation subsystems and thereafter assembly
7. MB Software: Run the desired simulation with prescribed bump/rebound wheel travel.
8. MB Software: Work with the results from the simulation in the post-processor window, draw desired relations in a plot.
9. MB Software: Final adjustment of outer steering point coordinate, which can be adjusted.
10. Make decision that the result is sufficient.
11. Create the 3D part representing steering clevis, which places the outer steering point according to decision from the previous step. Design it according to be able to attach it to the upright.
12. Create 2D drawing of this steering clevis, send to manufacturer and let it produce.
13. Mount the real 3D clevis at the front suspension.
14. Make the first feeling test in workshop, moving the car on polished workshop ground, and thereafter during ride on the road/race circuit

4.1.2 SOFTWARE DESCRIPTION

CAD SOFTWARE

Catia V5 R19 was used as CAD Software. This represents very comprehensive tool equipped with many specialized working environments. Many of top companies in motorsport and mass production (not only from automotive field) use this tool.

Among the others, these environments were used:

- Mechanical design
 - Part Design
 - Assembly Design
 - Drafting
- Shape
 - Generative Shape Design
- Digital Mock up
 - DMU Kinematics



MBS

Adams/Car MD Adams R3 was used as MB Software. Adams/Car, subprogram of the whole package MD ADAMS R3, is simulation software for mechanical systems, especially vehicles. The main advantage is that it is equipped with many pre-prepared subsystems, which can create the whole car. There is no need to waste time to create geometry each time; you just use the appropriate template of subsystem. The subsystems interact with each other via communicators.

All simulations can be visualized, written to files or viewed as graphs with the included post-processor tool.

Among the others, these subsystems were used:

- Front Suspension, pushrod operated
- Steering
- Front Wheel

4.1.3 DEFINITION OF MAIN POINTS

The new front suspension design is shown in *Fig. 77* and *Fig. 78*.



Fig. 77 Front left suspension 1 [9]

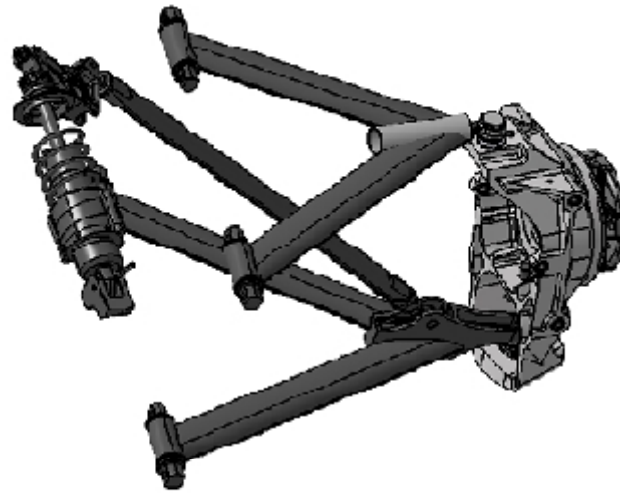


Fig. 78 Front left suspension 2 [9]

STEERING RACK POSITION

The steering rack is Woodward Steering Rack, USA manufacturer with European department settled in The Netherlands. They offer great range of steering racks, with or without power steering; with left hand, right hand and centre positioned pinion. Please have a look at the [App. 3](#) where you can find original drawing of this product.

The complication in the beginning was that the steering rack position was fixed in the chassis and couldn't be change due to other layout (steering column, driver leg space etc.) Second minor complication was rack length, thus this can be in case of need changed with some spacer/special part.

Because of this fixed position the easiest way how to refrain the from Ride Steer (by placing the steering rack and steering tie-rods in the same plane from the front view as one of the wishbone) couldn't be performed. Anyway, there are some ways how to achieve sufficiently accurate Ride Steer geometry even in the case that the steering rack is placed in different vertical height to the wishbone.

One of the solutions was described by **Hartmann's Construction of Bobilier Line**; please refer to 3.7 and [App. 4](#).

If the steering rack wasn't fixed, the **Hartmann's Construction of Bobilier Line** could start with the outer steering point (in step no.9 in the construction manual), which could be defined by previous performed Ackermann geometry. Thus this is not possible with fixed steering rack; some assumption in Ackermann will have to be done.



Steering rack specifications:

- turns lock-to-lock: 2
- total rack travel lock-to-lock: 100 mm
- c_factor: 50mm
- rack length: 720 mm
- custom adjusted power steering

In the following figure you can see the new front suspension including the steering rack.

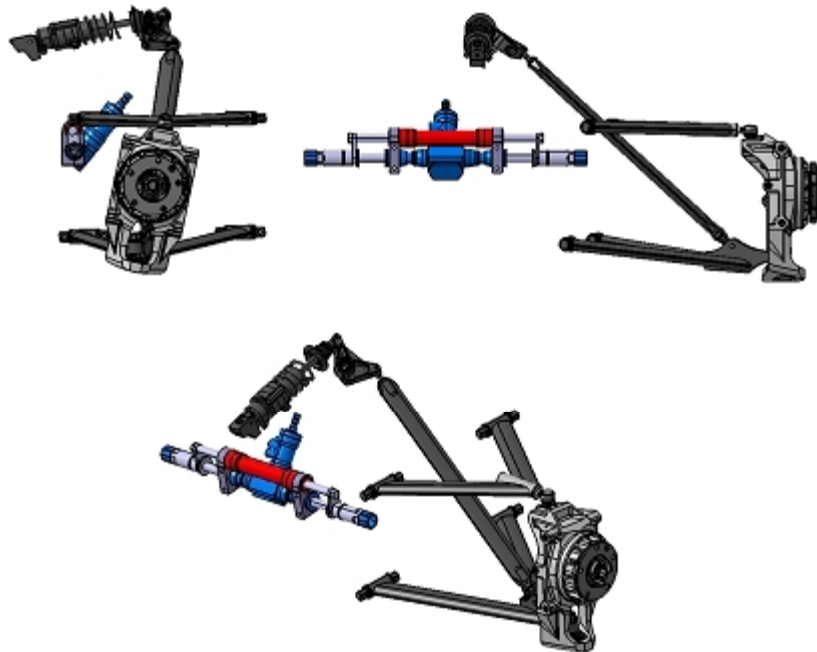


Fig. 79 Front left suspension with steering rack [9]

TURNING CIRCLE

The turning cycle was set to 12 metres.

The equation (31) allows us to determine the desired Ackermann steer angle with maximally turned wheels:

$$\delta = 57.3 \cdot \frac{L}{R}$$

$$(\delta) = 57.3 \cdot \frac{3.05}{12}$$

$$\underline{\delta = 14.5 \text{ deg}}$$



As the c_factor here is equal to full rack travel from zero to one side lock, corresponding with 360° of steering wheel rotation ($\Omega = 360^\circ$); and steer angle was defined in the previous step, next equation to achieve steering arm length can be written:

$$\sin \delta = \frac{c_factor}{s_arm} \quad (40)$$

$$s_arm = \frac{c_factor}{\sin \delta}$$

$$(s_arm) = \frac{50}{\sin 14.5}$$

$$\underline{s_arm = 200mm}$$

STEERING RATIO

The equation (19) allows us to determine the overall steering ratio:

$$SR = \frac{\Omega}{\delta}$$

$$(SR) = \frac{360}{14.5}$$

$$\underline{SR = 24.8}$$

4.2 DESIGN ACCORDING TO BUMP STEER

As the car is supposed to drive at high speeds also on roads with not perfectly smooth surface, the great attention was paid to the Bump Steer Geometry (3.7), and then at Ackermann Geometry, where some assumption will have to be done.

4.2.1 CAD SOFTWARE

The easiest way how to avoid the suspension and steering system from Ride Steer (by placing steering rack and steering tie-rods in the same plane (from the front view) as one of the wishbone, perpendicularly to the centre line of the car) is obviously not met (because of fixed steering rack, according to *Fig. 79*). Anyway, **Hartmann's Construction of Bobilier Line** will achieve some good results, which will be used with MBS simulation thereafter to prove them.

As far both wishbones are inclined in all three views, the construction will be performed in front view plane with projection of all the necessary lines and points. Otherwise the lines would never meet. As the wishbones are inclined in longitudinal plane, some assumption to get inner points has to be done. A point to be projected for getting the lower inner point (step no.1 in manual) was chosen point **1** in *Fig. 80*. This point represents the intersection of plane inclined of caster angle, going through lower outer ball-joint, upper outer ball-joint and wheel



centre; and line, which connects front inner and rear inner bushing of lower wishbone. In similar way the point no.2 is created.

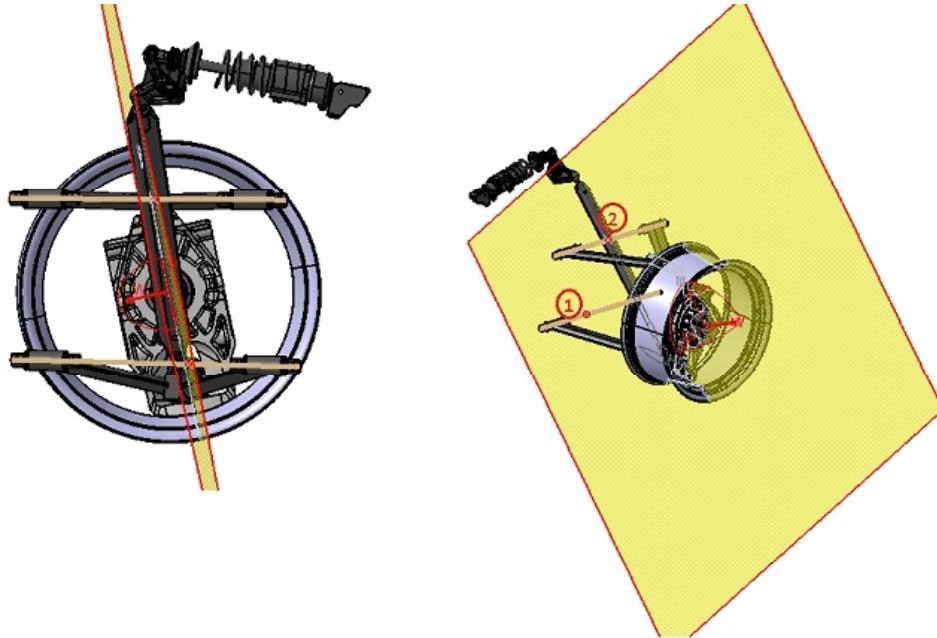


Fig. 80 Bump steer geometry CAD preparation

Now the construction according to manual can continue as following. As the pushrod and rocker deals with suspension tasks and not kinematics, they are not displayed anymore.

1. Draw a line from inner lower wishbone to inner upper wishbone
2. Draw a line from outer lower wishbone to outer upper wishbone
 - o Find the intersection of line (1) and line (2)

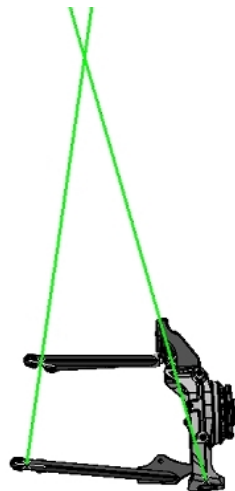


Fig. 81 Hartmann's construction of Bobilier line, step 1.+ 2.



3. Draw the line from inner to outer upper wishbone in order to find the IC
4. Draw the line from inner to outer lower wishbone in order to intersect with line (3) to find IC

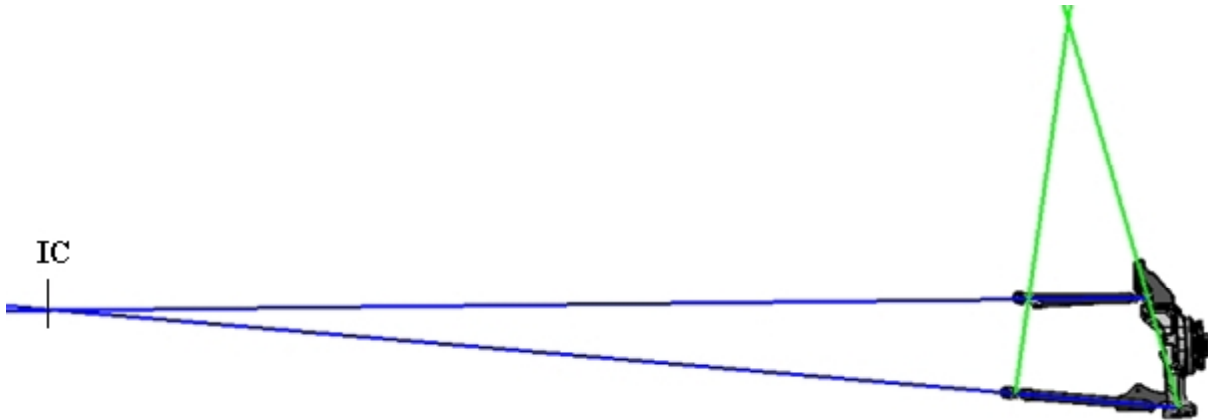


Fig. 82 Hartmann's construction of Bobilier line, step 3.+ 4.

5. Create the line from IC to the intersection of line (1) and line (2)
 - This creates the Bobilier line

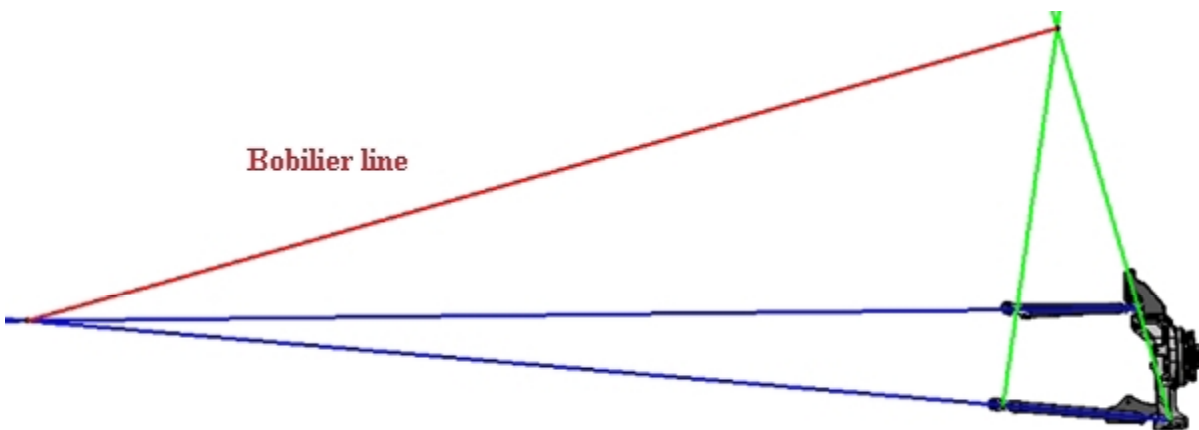


Fig. 83 Hartmann's construction of Bobilier line, step 5.



6. Draw the bisecting line of upper and lower wishbone
 - The angle of this bisecting line should be same as the angle to upper and lower wishbone

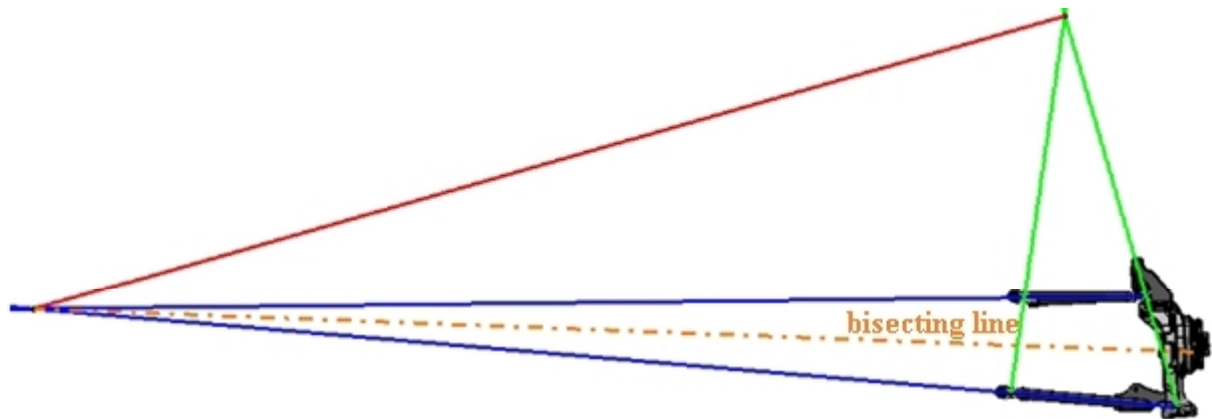


Fig. 84 Hartmann's construction of Bobilier line, step 6.

7. Find the angle between Bobilier line (5) and the bisecting line (6)
8. Draw the symmetrical Bobilier line (5) with angle of (7)
 - This creates symmetrical Bobilier line

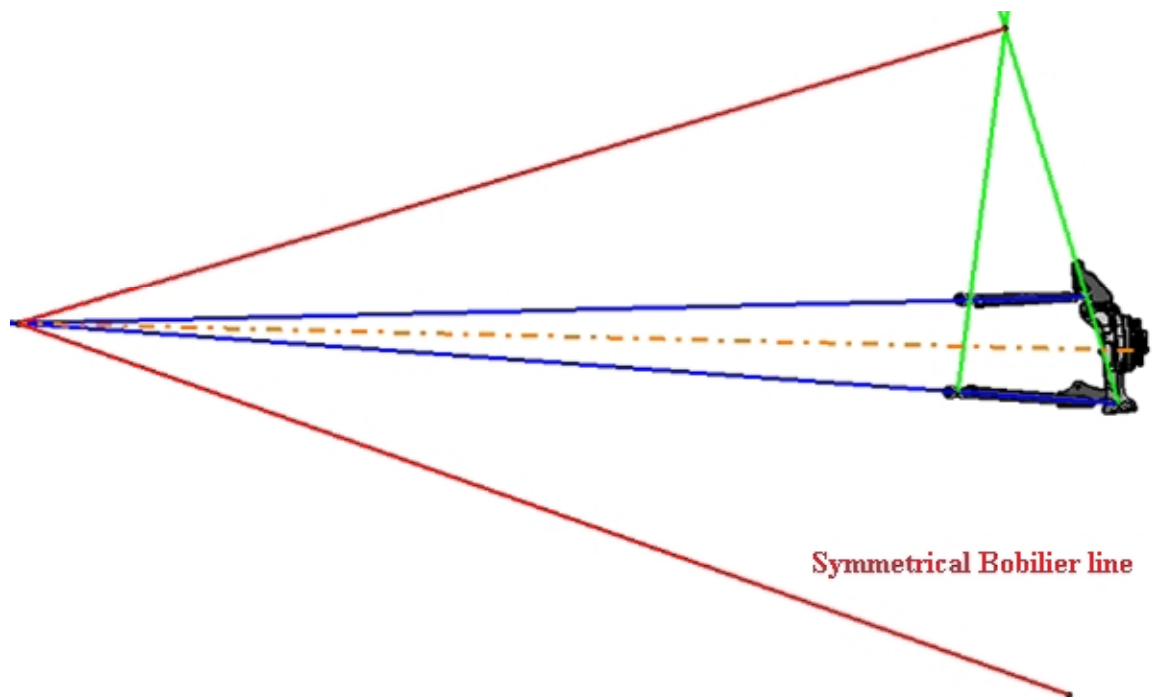


Fig. 85 Hartmann's construction of Bobilier line, step 7.+ 8.



9. Define the inner/outer point for the tie rod/transmission axle (any points you want to define. In this case it will be inner steering point, the aim is to find the outer steering point)
10. Draw a line from the defined point in (9) to IC (“steering line”)

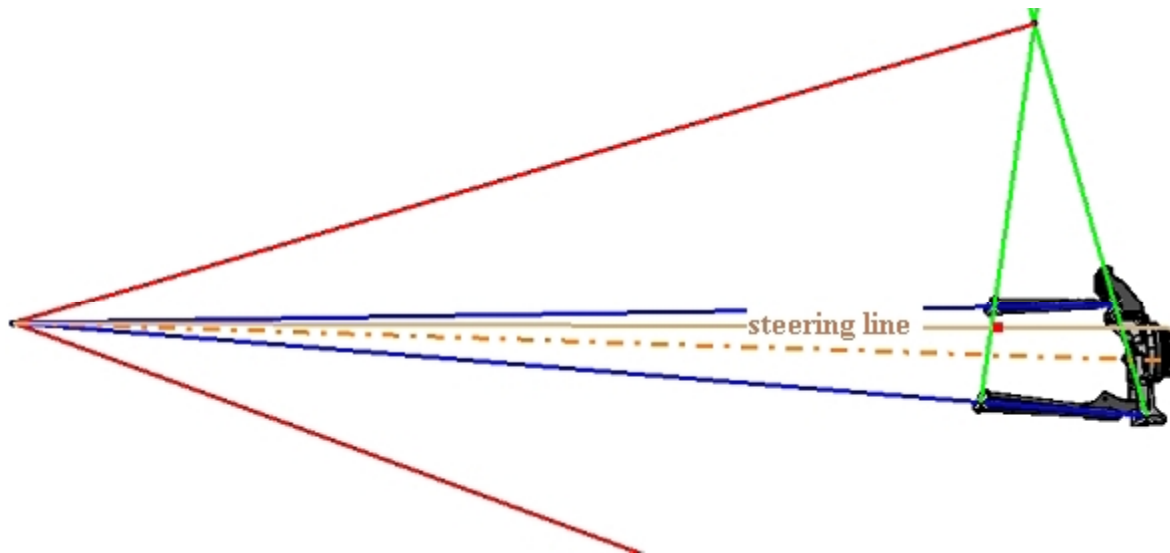


Fig. 86 Hartmann's construction of Bobilier line, step 9.+ 10.

11. Find second bisecting line between the line (10) and line from lower wishbone to IC (4)

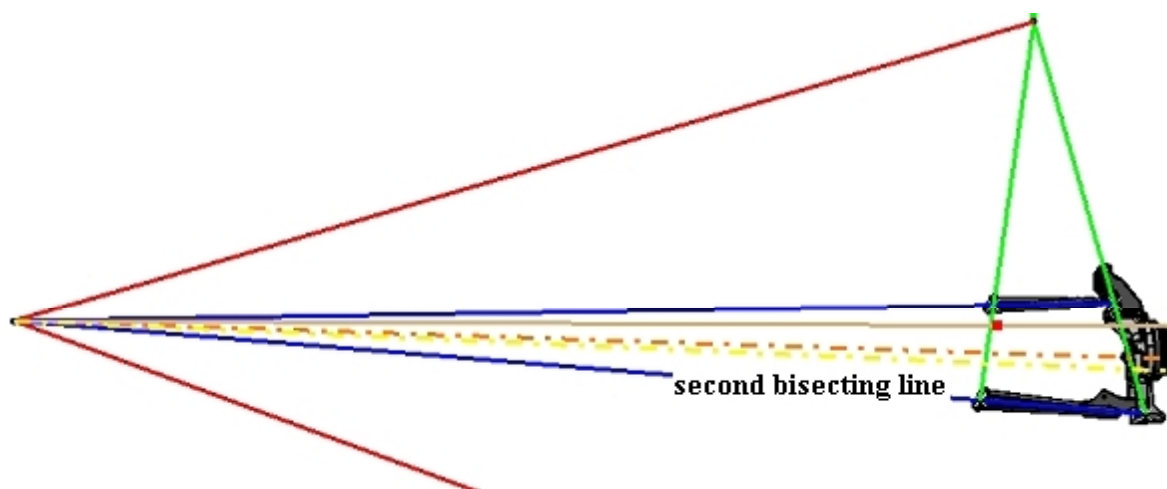


Fig. 87 Hartmann's construction of Bobilier line, step 11.



12. Find the angle between bisecting line (11) and symmetrical Bobilier line (8)
13. Draw the line from IC with angle of (12) respect to the bisecting line (11) ("new Bobilier line")

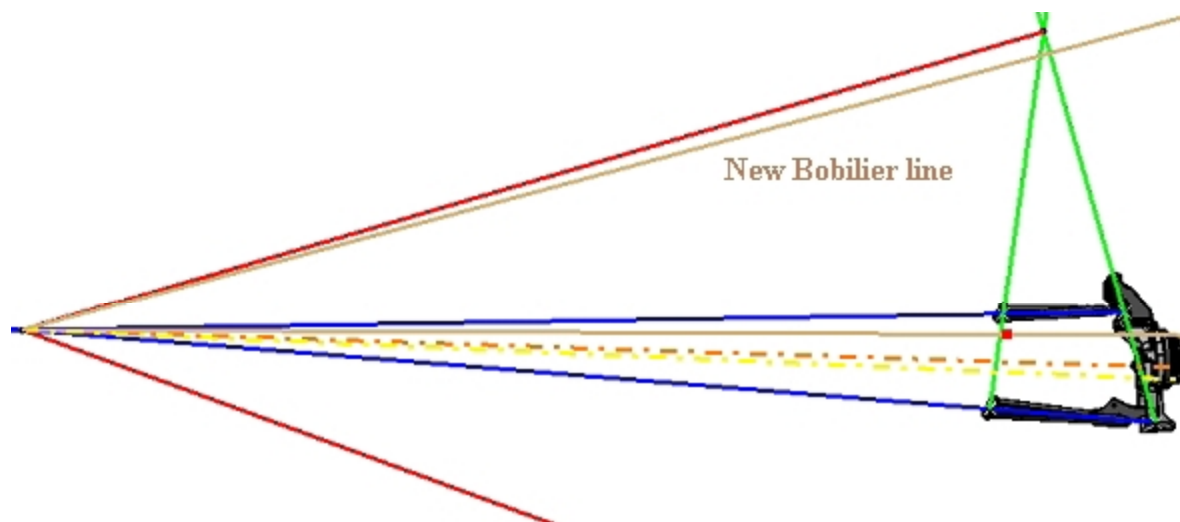


Fig. 88 Hartmann's construction of Bobilier line, step 12.+ 13.

14. Draw a line from LBJ (from lower wishbone) to defined point (9) to find the intersection point between line (13) and (14)

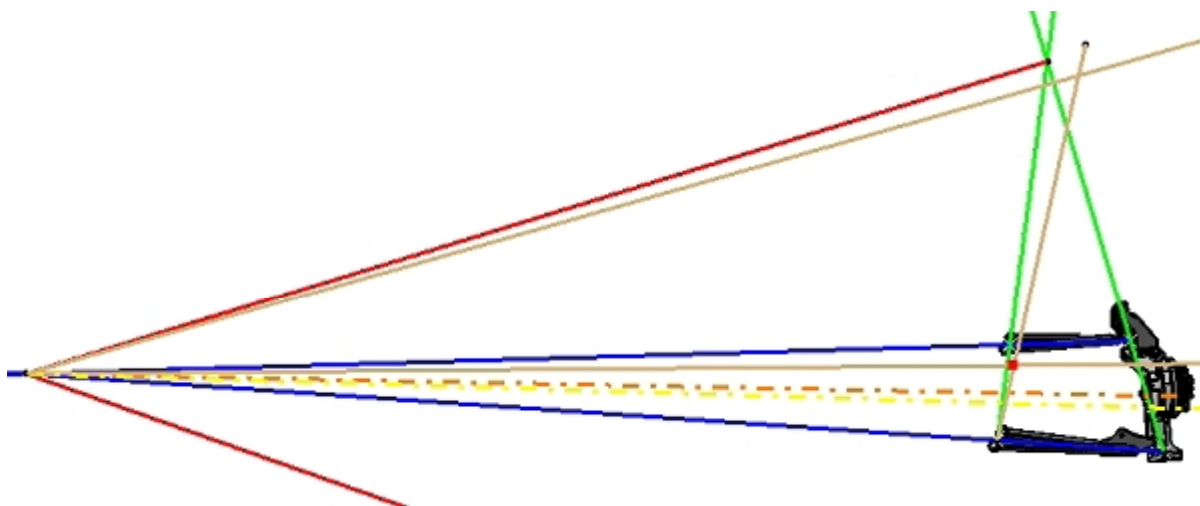


Fig. 89 Hartmann's construction of Bobilier line, step 14.



15. Draw a line from the intersection found from (14) to the outer suspension points for lower wish bone.
 - this will find the end point for the tie rod/transmission axle as this is intersection of line (10) and line (15)

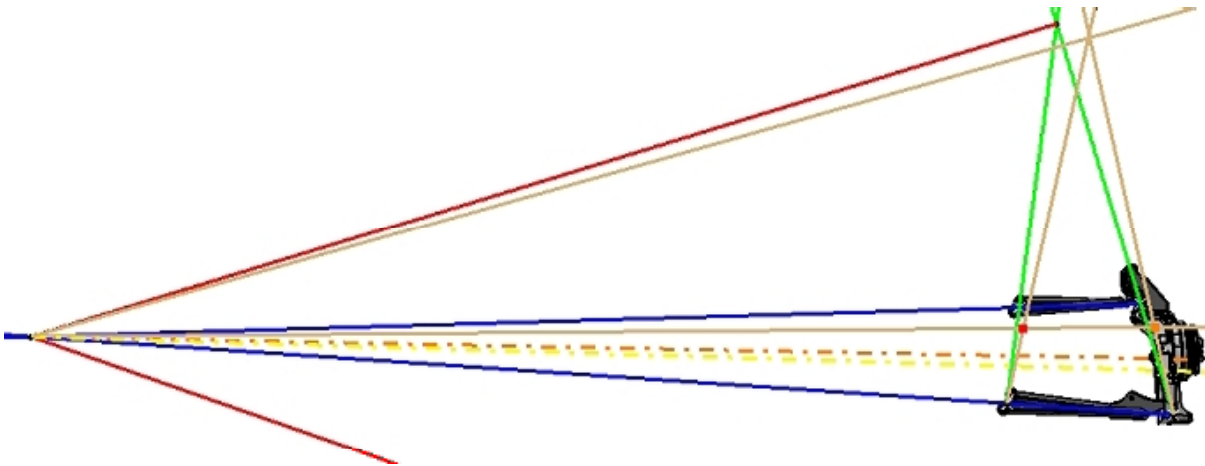


Fig. 90 Hartmann's construction of Bobilier line, step 15.

4.3 DESIGN ACCORDING TO ACKERMANN

As a.d.Tramontana is homologated for public-road use and is intended to be used more on these roads than at race circuit, it was decided to make the Ackermann as true as possible, not e.g. negative (3.5) as this could be desired at true race-track car.

Anyway, as stated before in the beginning of this chapter, the steering geometry can be change according to instant demands and different steering clevis can be manufactured and mounted.

In the following construction the theory was applied to practise.

The simplest way of providing a reasonable approximation to Ackerman geometry is to arrange for a line between the steering linkage (steering tie-rod) outer ball joint and the kingpin axis (at the height of the steering linkage outer ball-joint) to pass through a point in the centre of the rear wheels. [4]

The Wheelbase is 3050mm and as the length of steering arm was used the value of 200 mm calculated in previous part.



4.3.1 CAD SOFTWARE

At the beginning the height of horizontal working plane was set to pass through the steering rack axis. The height of this plane matters, as there is some Kingpin Axis inclination and Caster angle. The purple circle represents the steering arm length of 200mm, the blue line starts at the point in the centre of the rear wheels, passing through the Kingpin Axis.

By this construction Positive Ackermann is achieved.

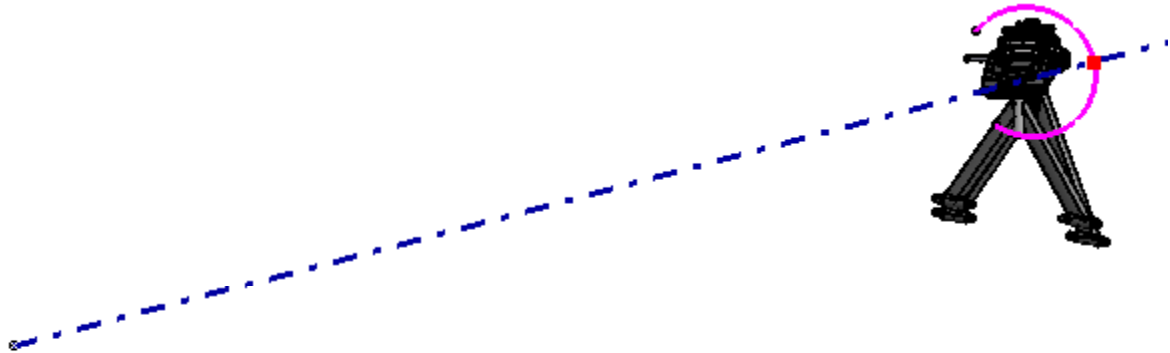


Fig. 91 Design according to Ackermann steering geometry

As said before, if there is no demand from Bump Steer, we can achieve Positive Ackermann and desired steering arm length. While the front view position of this point doesn't correspond with theoretical position got from Bump Steer Geometry, next assumptions has to be done. Furthermore the steering arm length 200mm cannot be suited inside the rim.

4.4 OUTER STEERING POINT CONCLUSION

While in part 4.2 all points and lines are projections into front view plane, this plane can be parallel moved. This action was thereafter performed to get close to Ackermann line, while keeping the steering arm length in acceptable borders, which resulted in $s_{arm} = 165$ mm.

The outer steering point coordinates were used in MBS, to prove the sufficiency of result and/or to finite adjustment.

4.4.1 MBS

MODEL PREPARATION

The simulation model was assembled out of three subsystems: Front Suspension (pushrod operated), Steering and Front Wheel. The final look of a model can be seen in [Fig. 92](#). For hardpoints adjustment the *Hardpoint modification Table* was used. Symmetric function was activated to get both sides of front suspension at once.

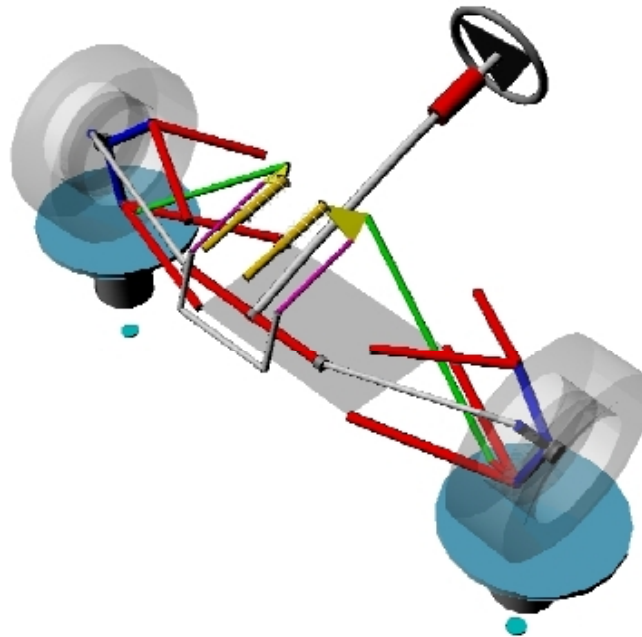


Fig. 92 MBS model

Bump Steer Simulation

Suspension Analysis: Parallel Wheel Travel was used to get the results for Bump Steer, as it gives desired relations.

The movement input was performed by vertical travel relative to wheel centre.

This was decided, according to some calculations and knowledge of ride behaviour borders, to be set as following: 25mm of rebound and 50 mm of bump.

POST PROCESSOR

After the simulation process is finished the Animation postprocessor can be run. Thus this gives a general overview of movement, this can be used just to check the truth of parameters (e.g. travel distance). As Bump Steer error should move around decimal value of degree, this is not sufficient for further decision. Thus the Postprocessing Window has to be used. Here you can let the software draw in a graph relations between desired values; in many combinations.

For evaluating Bump Steer kinematics simulation the relation between wheel travel and toe angle was chosen. This represents exactly, how much are the wheels steered by bump/rebound movement.

The results of this plot are shown in [Fig. 93](#).

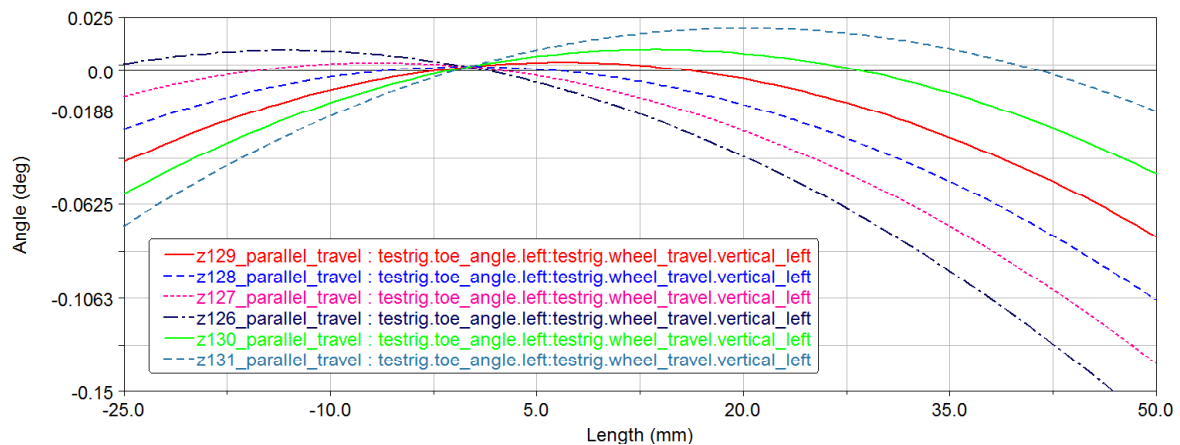


Fig. 93 Plot: Toe angle [deg] vs. Wheel travel [mm]

The first iteration of results is described by dashed blue line, $z = 128$ mm

This is represented directly by the suspension points from geometry layout and outer steering point got from 4.2.

In the next step the “z” coordinate of outer steering point was changed in *Hardpoint modification Table* in preparation part MBS process. The increments were decided to be 1mm as more precise value cannot be followed in real suspension geometry. The simulation was run again each time and the results were added to the same graph.

The convergence of each step was considered, allowing us to go the good way e.g. “z = 127 mm” and “z = 126 mm” examples aim to more negative values in bump movement. The “z” coordinate has to be raised thereafter. From some value it is noticeable that the result curves are aiming to the more negative values in rebound movement. Thus this value range is sufficient and the best behaviour can be chosen.

The sum of absolute maximum value and absolute minimum value of each curve was chosen as criteria for evaluation. In the following list only the two best curves are calculated:

Green solid curve: “z = 130 mm”:

Red solid curve: “z = 129 mm”:

$$|-0.0580 \text{ deg}| + |0.0100 \text{ deg}| = \underline{0.068 \text{ deg}} \quad |-0.0790 \text{ deg}| + |0.00750 \text{ deg}| = \underline{0.0865 \text{ deg}}$$

This allow us to make a decision and state the outer steering point to have “z” coordinate equal to 130 mm, “x” and “y” coordinates stay the same with no changes.



ACKERMANN GEOMETRY SIMULATION

Suspension Analysis: Steering Simulation was used to get the results for Ackermann Geometry, as it gives desired relations. The movement input was performed by steering wheel rotation, which was set to 360° one side from zero (straight-ahead) position, in meaning of time duration. The results in opposite meaning of turning can be described by inverse value for each wheel.

POST PROCESSOR

For evaluating Ackermann Steer Geometry simulation the relation between left wheel toe angle and time duration (representing full turn of steering wheel) was chosen. The same was performed for the right wheel; plot was made in the same graph to see easily the difference between the wheels. This represents exactly, how much each wheel is steered according to steering wheel position and also it allows comparing both wheel steer angle.

Note:

While having in mind there is zero toe angle in the beginning, this gives directly the steer angle. While positive/negative meaning of toe angle is taking in account in Adams simulation, the meaning of one wheel toe angle has to be to inversed (by adding “-1” to the appropriate equation).

The results of this plot are shown in *Fig. 94*.

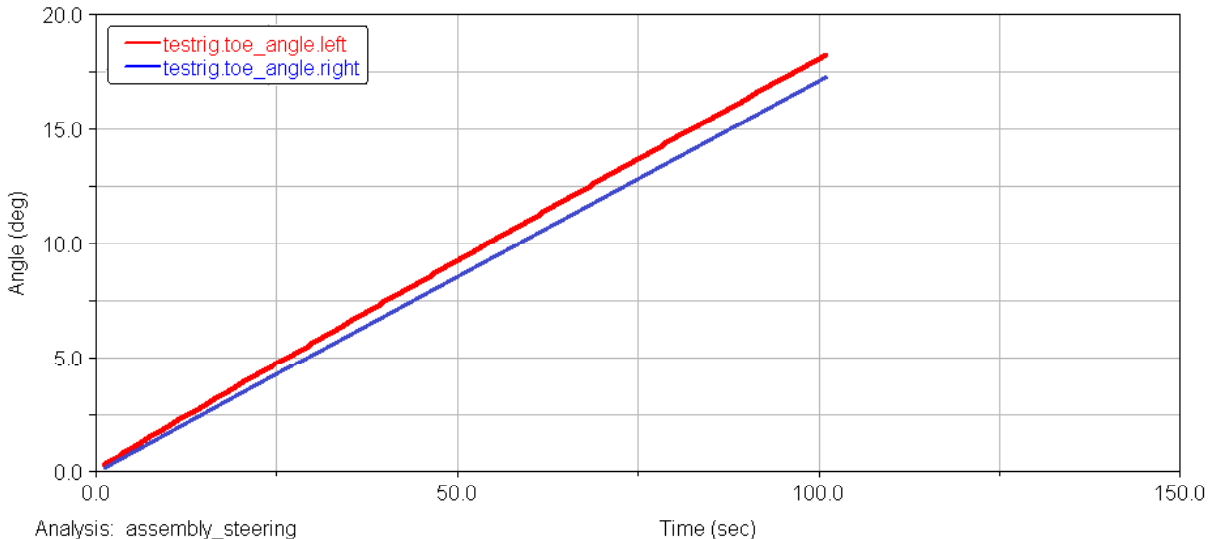


Fig. 94 Plot: Toe angle vs. time representing 360° turn of steering wheel



4.4.2 RESULT VS. STARTING POINT

Steering angle:

$$\sin \delta = \frac{c_factor}{s_arm}$$

$$\delta = \sin^{-1}\left(\frac{c_factor}{s_arm}\right)$$

$$(\delta) = \sin^{-1}\left(\frac{50}{165}\right)$$

$$\underline{\delta = 17.6 \text{ deg}}$$

Turning radius

$$\delta = 57.3 \cdot \frac{L}{R}$$

$$R = 57.3 \cdot \frac{L}{\delta}$$

$$(R) = 57.3 \cdot \frac{3.05}{17.6}$$

$$\underline{R = 9.9 \text{ m}}$$

Steer angle of outer wheel (theory, according to (27)):

$$\delta_o = 57.3 \cdot \frac{L}{(R + t/2)}$$

$$(\delta_o) = 57.3 \cdot \frac{3.05}{(9.9 + 1.9/2)}$$

$$\underline{\delta_o = 16.1 \text{ deg}}$$

Steer angle of inner wheel (theory, according to (30)):

$$\delta_o = 57.3 \cdot \frac{L}{(R - t/2)}$$

$$(\delta_o) = 57.3 \cdot \frac{3.05}{(9.9 - 1.9/2)}$$

$$\underline{\delta_o = 19.5 \text{ deg}}$$

Steering ratio

$$SR = \frac{\Omega}{\delta}$$



$$(SR) = \frac{360}{17.6}$$

$$\underline{SR = 20.4}$$

4.4.3 CONCLUSION:

Even that the steering rack had fixed position, some good results were achieved.

Sophisticated Bump Steer geometry was proven by MBS simulation with results, which are comparable with race cars. Furthermore real life tests, performed at Alcarrás circuit, Spain, proved this design. The straight at this circuit is not perfectly smooth, but, in spite of this there were mainly positive reactions from the test driver, Francesc Gutierrez.

The behaviour of steering is according Ackermann rules – inner wheel turns more than the outer. Anyway, the steering angles are not exactly according to theoretical calculations.

- Outer wheel: 17.2 deg in reality vs. 16.1 deg in theory
- Inner wheel: 18.3 deg in reality vs. 19.5 deg in theory

Anyway, sufficiency of Ackermann was tested in workshop, moving the car on polished workshop ground. There was no serious slack between tires and ground, and if any, it was barely hear able.

Finally it has to be stated that some vehicle performance parameters were changed comparing to primarily defined requirements; mainly Steering Ratio and turning circle radius.

4.4.4 STEERING CLEVIS DESIGN

In the following Figure there is Cad model of steering clevis.

Refer to [App. 5](#) drawing of this part.

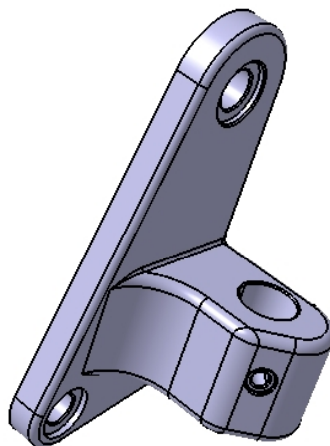


Fig. 95 Real steering clevis CAD model



5 WISHBONES' ASSEMBLY

Another task connected to new front suspension was dealing with the manufacturing process (5.1) and thereafter the way how to connect them to the chassis (5.2).

5.1 WISHBONES' MANUFACTURING

As it might seem that this is just manual work, also some engineering work has to be performed in advance to make it easier to the workers and to achieve as nice units as possible with exact geometrical layout. The functionality has to be assured in any case.

5.1.1 WORK PROCESS LAYOUT

Work process starts with CAD preparation; some way how to transfer the shape of wishbone beams from computer to the real part has to be found out. Thereafter some assembly tool – jig has to be manufactured before the final assembly can be performed.

CAD PREPARATION

From *Fig. 96* and *Fig. 97* it is obvious, that each of the wishbones is in general created out of five pieces:

- two inner parts
- one outer piece with appropriate shape
- two connection beam with cross-section shape of water drop

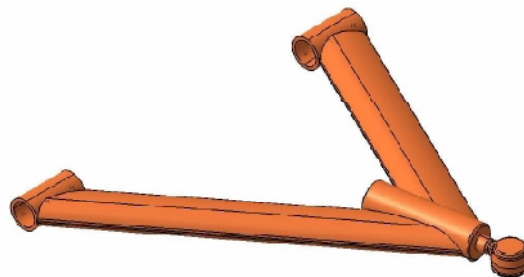


Fig. 96 Upper front wishbone CAD model [9]

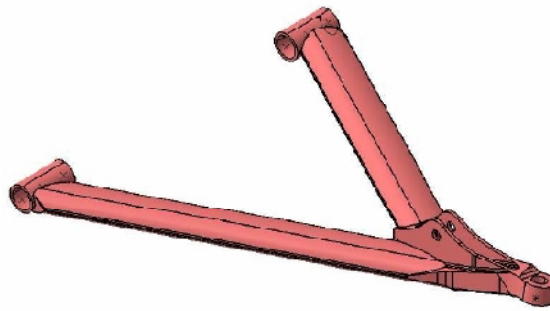


Fig. 97 Lower front wishbone CAD model [9]

As far the two inner and one outer piece are manufactured at either turning or CNC machine, these won't be described in this chapter anymore. But, actually, they will be used in the final assembly work process in this part below. Because of their difficult shape (mainly the outer piece) it would be almost impossible to use try-fault method to get the appropriate shape of the two beams, some way to achieve this has to be introduced.

Catia V5 R19 environment "Shape – Generative Shape Design" was used to achieve the desired shape at the real beam. The function "unfold" was used to get the 3D beam shape onto 2D plane (*Fig. 98*), which could be thereafter printed in scale 1:1 (*Fig. 99*). This concept was repeated for both beams of lower wishbone and upper wishbone as well. The next side is represented by mirror view of the results.

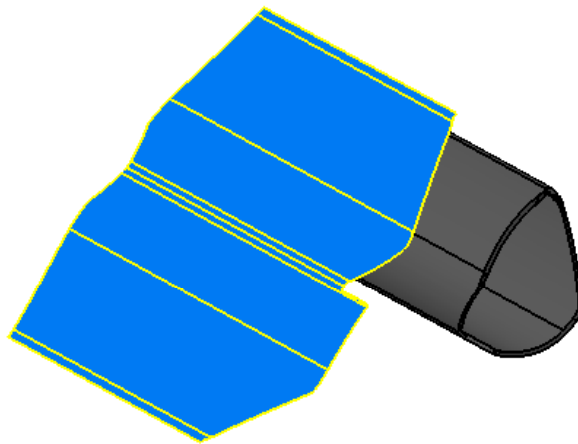


Fig. 98 Unfolded beam shape

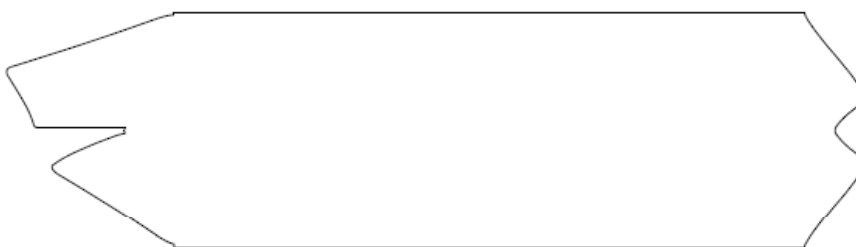


Fig. 99 Unfolded shape to be printed in scale 1:1



REAL PART PREPARATION

This printed shape is cut precisely by scissors. Thereafter it is supposed to be folded back to the real beam, acting as template of the exact shape.

This action can be understood also as: “Transferring the shape from the planar paper to the non-planar 3D surface of the beam” and can be seen in *Fig. 100*.

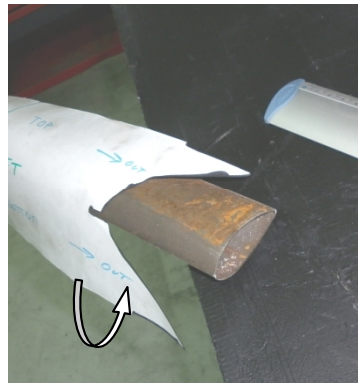


Fig. 100 Transferring beam shape from 2D to 3D

This shape can be copied to the real beam using a marker pen (*Fig. 101*). From now on the beam can be cut by e.g. angular grinder. Final shape adjustment can be done by air grinder tool.



Fig. 101 Beam shape copy using a marker pen

ASSEMBLY TOOLS

As all the suspension geometrical and steering characteristics depend on suspension points coordinates, the final assembly of all five components can't be done just by direct measuring during the manufacturing process and/or holding the part by hand, which is not sufficiently precise. Moreover the influence of welding process has to be considered.

A tool which fulfils all described presumptions can be called “Wishbones Jig”.

This tool consists of one main plane, to which all the brackets are attached by bolts to fulfilling geometrical demands. For each type of wishbone there are different brackets, moreover their position varies according to type and side of each wishbone. In spite of this some great effort was done to find some common bracket position, aiming to push the price down and make the assembly easier.



In App. 6 there is an example of real "Front suspension Jig assembly" created for workshop purposes. In first two pages there is the main plate assembly manual common for all four wishbones. In the next two pages there is assembly manual for one of the wishbones, lower left wishbone was chosen as an example.

The welding can start when all previous processes are successfully finished (*Fig. 102*).

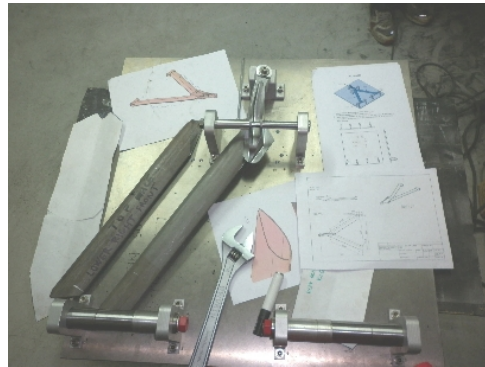


Fig. 102 Wishbone's assembly

5.2 WISHBONE'S BUSHINGS

Wishbones' bushings represent the joint connection between chassis and moving suspension wishbones. They are characterized by 1 DOF. In this case one can be described as a rigid metal beam with some plastic sealing around, inserted in the inner part of wishbone.

5.2.1 OLD BUSHINGS' DESIGN

The old design of bushing consisted of one piece of metal beam, inserted into the inner part of wishbone from one side, locked by circlip at the other end. The plastic sealing had too much hardness. This design appeared to be insufficient due to many reasons; mainly it was hard to achieve desired clearance allowing rotary movement caused by geometry and manufacturing tolerance (especially of the plastic part). In case there was bigger clearance than needed, a couple of very thin metal washers had to be inserted, in vice-versa it was hard to achieve the clearance. Furthermore the material of sealing was too hard for this purpose.

5.2.2 NEW IMPROVED DESIGN

The new improved design consists of five pieces: male part with thread, female part with thread, two types of sealing and an O-ring. In this design the sealing pieces are inserted into the inner part of wishbone firstly, then the female part is pushed from one side and locked from another side with male part by mean of screwing movement. The fine-thread M16x1 allows to adjust the clearance in 0.5° steps. The O-ring refrain this threaded connection from dust and water. The CAD model is shown in *Fig. 103*.

The assembly with lower wishbone is shown in *Fig. 104*.

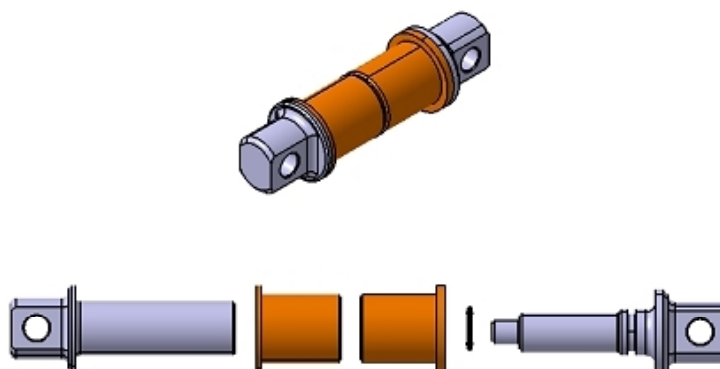


Fig. 103 Bushing

As far the carbon fibre monocoque is considered to be fully rigid, there is need to use some soft material in the bushings, acting as silent block. Thus the sealing parts are made from Wullkolan plastic, whose material properties can be seen in [App. 7](#) (in Spanish language) [9].

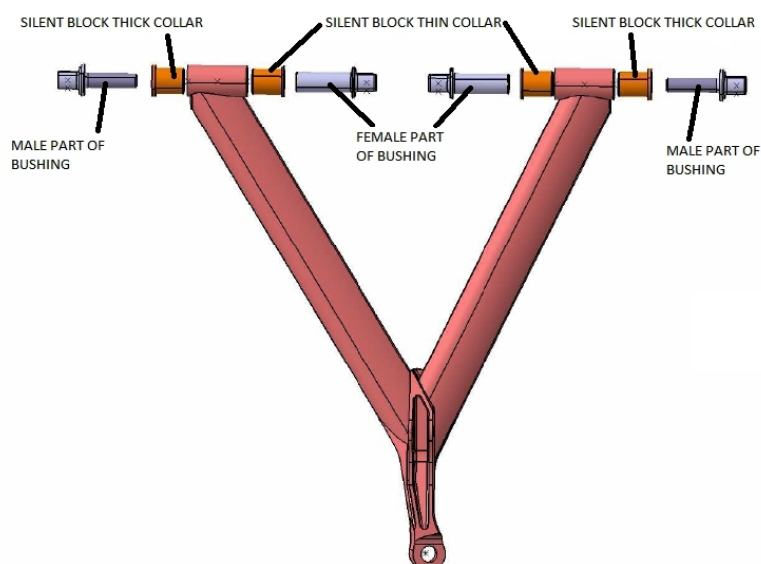


Fig. 104 Bushings mounting

Refer to [App. 8](#) to check the bushings' drawings.

5.2.3 CONCLUSION

The bushings, according to design described above, were manufactured, mounted and tested. The functionality was proven and thus this design will be used at the next cars.

Refer to [App. 9](#) to see the photo of a real part.



6 SWEPT VOLUME

As new front suspension is used, the need to know the overall area it can move has arose.

The enquiry from the designing company was clear – they needed to know the volume or area of any travel of front wheels which would be possible (full bump/rebound travel with wheels steered straight ahead, locked-left and locked-right). This will be used e.g. for new design of front part, which is planned in the near future.

Catia V5 R19 environment “Digital Mockup – DMU Kinematics” was used to satisfy this demand. In this environment it is possible to assembly and make a self-moving the suspension unit, thus simulating real behaviour. Furthermore there is an option “Swept Volume” which saves the result into cad format.

6.1 WORK PROCESS LAYOUT

For simplifying reasons the kinematic simulation can be run just for one side and the results mirrored thereafter.

6.1.1 SIMULATION ASSEMBLY

FIXED PARTS ASSEMBLY

Fixed constraint takes all 6 DOF.

The assembly starts with chassis, which is fixed in the coordinate system. Then all bushings are placed in their position by appropriate constraints. To avoid any misunderstanding in “Assembly Constraints Conversation” process and refrain from error messages, the bushings constrains should be deleted thereafter and without moving fixed to the position.

MOVING PARTS ASSEMBLY

1. Upper wishbone

The assembly continues with upper wishbone. Because wishbone bushings are characterized by 1DOF, following constraints were used:

<u>Type of constraint</u>	<u>No.</u>	<u>DOF taken</u>	<u>Between components</u>
Coincidence between axis	1x	4 DOF - 2 translation - 2 rotary	This aligns axes of one bushing and one inner wishbone part (as the bushing axes are aligned, it doesn't matter which one will be picked)
Contact Constraint between planes	1x	1 DOF - translation	Between appropriate faces at bushing and inner wishbone part



- è There remains 1 rotary DOF for each wishbone, thus they can only rotate about the bushings

2. Lower wishbone

Exactly the same as in step no.1 applies also for lower wishbone.

3. Upright

Next, the upright assembly including the fixed rim and fixed wheel can be added

<u>Type of constraint</u>	<u>No.</u>	<u>DOF taken</u>	<u>Between components</u>
Coincidence between points	2x	2 DOF - translation	Between upper wishbone outer ball-joint housing centre and upright upper ball-joint centre Between lower wishbone outer ball-joint centre and upright lower ball-joint housing centre

The point coincidence constraint corresponds exactly with the real movement of ball-joint. These constraints will connect the upright to the wishbone in the way they all will move together during bump/rebound simulation; the rotary position of all three planes can be change because of front view and side view kingpin axis geometry.

4. Steering tie-rod

The last piece to be assembled is steering tie-rod. This will keep the wheels in unchanged directional position during bump/rebound movement.

<u>Type of constraint</u>	<u>No.</u>	<u>DOF taken</u>	<u>Between components</u>
Coincidence between points	2x	3 DOF - translation	Between tie-rod inner ball joint centre and steering rack outer ball-joint housing centre. Between tie-rod outer ball-joint housing centre and steering clevis ball-joint centre.

These constraints will keep the wheels in unchanged directional position during bump/rebound movement.

There will three different position of steering rack (rack in centre position and full rack travel to the left and right), which will steer the wheel in their maximal steer angle δ .

6.1.2 DMU KINEMATICS SIMULATION

After running DMU Kinematics environment, firstly the Assembly Constraint Conversion process has to be done. This transforms the assembly constraints into simulation joints. Sometimes the auto conversion doesn't work properly and it needs to be performed manually.

In the assembly like this, where the steering tie-rod is represented by simplified rod with point at its axis at each face, another joint need to be added manually to restrict rotary movement of this rod. This comes true with "Universal Joint" connection. Otherwise the software will not allow the simulation to be run due to 2 DOF present.

All the other tasks were performed without any difficulty. The final layout of assembly and joints before running the simulation is shown in *Fig. 105* and *Fig. 106*.

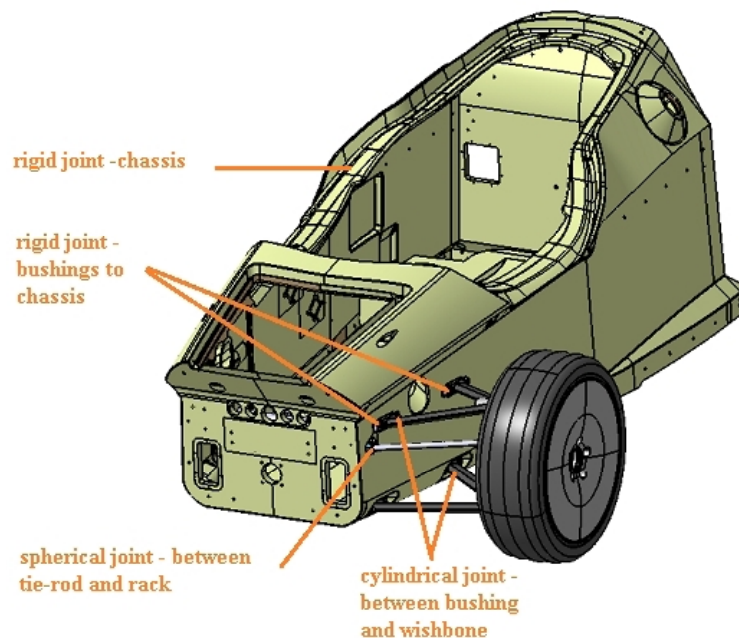


Fig. 105 DMU Kinematics simulation assembly – left-front view

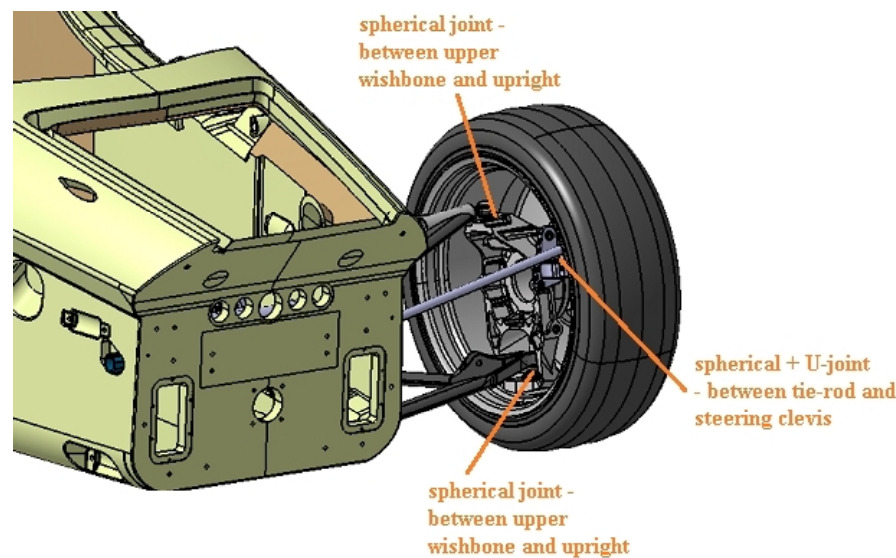


Fig. 106 DMU Kinematics simulation Assembly – right-front view

The last 1 DOF is represented by movement command necessary to make the assembly moving. The angle command was chosen and applied at one of the cylindrical joints between bushing and wishbone. The top and bottom values were discovered before from another 3D assembly.

Now the simulation can be run and Swept Volume created. Because of three different position of steering rack due to its travel, altogether three simulations has to be performed to get the overall Swept Volume.

6.2 CONCLUSION

All simulations were performed successfully. The pictures of swept volumes taken from three planes with wheels directed straight ahead, lock-left and lock-right can be seen in [App. 10](#). The total swept volume is also shown there, with very clear visibility of Kingpin Axis in side view. This represents a set of points common for every steer angle.

In spite these pictures give some good idea of total wheel travel, the 3D file is necessary to deal with this problematic any further.



CONCLUSION

This thesis covers all main kinematic characteristic of suspension and steering design, whose knowledge is unexceptionable fundamental to be able to build competitive vehicle.

This theory was thereafter applied at front axle of high-power sport car. The main concern was focused at steering clevis design and manufacturing. This clevis satisfies demands for Bump Steer; and also Ackermann Steering Geometry in acceptable borders.

Moreover some practical examples of daily tasks in small-series vehicle production supplement the overall dealing with front axle. These are represented by wishbones' manufacturing and assembling together; their connection to chassis by mean of new bushing's design and the total wheel travel area.

During the work many sources of foreign literature were used as well as CAD and MBS computer software.

The author would like to say that he enjoyed some fun while writing this master's thesis, mainly because it was dealing with real thing in real life experience. Both this experience and writing the theory helped to organise his thoughts and knowledge about the topic of Suspension and Steering Geometry Characteristics.

The author would also like to state that in the real-life production process there is not everything and not always done after exact computer modelling and verifying, due to either lack of time (not in confrontation with neither quality nor accuracy). The praxis and experience take place in day-to-day tasks.

The author would like to state that he is not an expert yet neither in overall vehicle technical disciplines nor in suspension and steering theory which was analyzed above. To become an expert it takes many years of experience and learning.



BIBLIOGRAPHY REFERENCES

- [1] GILLESPIE, T. *Fundamentals of Vehicle Dynamics*. Society of Automotive Engineers, Inc., First edition, Warrendale, PA, USA, 1992. 519 p. ISBN 1 1-56091-199-9.
- [2] MILLIKEN, W., MILLIKEN, D. *Race car vehicle dynamics*. Society of Automotive Engineers, Inc., First edition, Warrendale, PA, USA, 1995. 890 p. ISBN 1-56091-526-9.
- [3] CORSINI, D. *Racing Words S.A.R.L.* Corlet Imprimeur S.A., Condé su Noireau, France, 2006. 1021p. ISBN 2-9511426-4-1.

(There are no references to this book but it has been used quite often to use technical terminology in good way.)

- [4] BALKWILL, J. *Advanced Chassis Engineering*. Motorsport Engineering MSc. Level Module, Oxford Brookes University [199-?]. 392 p.
- [5] LECOMTE, Michael. *Motorsport terminology*. MSc. Level Module, Le Mans University [200-?], 115p.
- [6] HRUDIK, J. *Tramontana Technical Description*. Tramontana internal technical and marketing documents, Second Edition, Palau de Santa Eulàlia, España, 2011. 12 p.
- [7] THEANDER, Adam. *Design of a Suspension for a Formula Student Race Car*. Stockholm Royal Institute of Technology, Sweden 2004..74p. TRITA-AVE-2004-26 ISSN 1651-7660.
- [8] VLK, F. *Dynamika motorových vozidel*. Prof. Ing. František Vlk, DrSc., nakladatelství a vydavatelství, Druhé vydání, Brno, 2003. 464 s. ISBN 80-239-0024-2.

(There are no references to this book but it has also been used in the previous times for gathering some valuable knowledge.)

- [9] A.d.Tramontana internal server data.
- [10] URL <<http://www.woodwardsteering.com>>
- [11] URL <<http://www.wikipedia.com>>
- [12] URL <www.constructorsf1.com>
- [13] MSC Software, Adams/Car MD Adams R3 subsystem library.

Furthermore the CAD software **CATIA V5 R19** and MBS **Adams/Car MD Adams R3** have been very useful. Besides that Microsoft Office pack has been very useful as well



LIST OF SYMBOLS

Symbol	Unit	Description
2D	-	Two Dimensions
2WD	-	Two Wheel Drive
3D	-	Three Dimensions
4WD	-	Four Wheel Drive (All Wheel Drive)
a	[m]	Distance between rear axle and CG
ARB	-	Anti-roll Bar
b	[m]	Distance between front axle and CG
BR	[-]	Steering Box Ratio
C_factor	[mm/1 rot]	Rack Travel Number
CG	-	Centre Of Gravity
CNC	-	Computer Numerical Control
c_{α}	[N/deg]	Cornering Stiffness
DOF	-	Degree of Freedom
ET number	mm	Wheel Offset
FR	[-]	Force Ratio
F_{spring}	[N]	Force applied at the spring, acting directly along spring axis
fvsa	[m]	Front View Swing Arm Length
FWD	-	Front Wheel Drive
F_{wheel}	[N]	Vertical force applied to the wheel
F_x	[N]	Tractive Force
F_y	[N]	Total lateral force
F_y	[N]	Lateral Force
F_y	[N]	Cornering Force
F_{yf}	[N]	Lateral cornering force at the front axle
F_{yi}	[N]	Lateral Force on inside wheel
F_{yo}	[N]	Lateral Force on outside wheel
F_{yr}	[N]	Lateral cornering force at the rear axle
F_z	[N]	Normal Force
F_{zi}	[N]	Load on the inside wheel in turn
F_{zo}	[N]	Load on the outside wheel in turn
g	[m/s ²]	Gravity Force Acceleration, standard gravity: 1g=9.80665m/s ²
h_{CG}	[mm]	CG height
IC	-	Instant Centre
IR	[-]	Installation Ratio – Linear/non-linear
IR^2	[-]	Wheel Rate to Spring Rate Ratio
k_{spring}	[N/mm]	Spring Rate
k_{wheel}	[N/mm]	Wheel Rate
L	[m]	Wheelbase
LBJ	-	Lower Ball-joint
M	[kg]	Mass of the vehicle
M_x	[Nm]	Overturning Torque
M_y	[Nm]	Rolling Resistance Moment
M_z	[Nm]	Aligning Torque



n_{pinion}	[-]	Ratio between instant steering wheel rotation angle and one full turn (360°)
pm_{arm}	[mm]	Pitman Arm Length
R	[m]	Radius of the turning circle
R_1	[mm]	Length between rocker axis and first pivot
R_2	[mm]	Length between rocker axis and second pivot
RC	-	Roll Centre
RWD	-	Rear Wheel Drive
s_{arm}	[mm]	Steering Arm Length
SAE	-	Society of Automotive Engineers
SLA	-	Short-long Arm (~Wishbone)
SR	[-]	Steering Ratio
$svsa$	[m]	Side View Swing Arm Length
$travel$	[mm]	Total travel of steering rack from instant position according to pinion/steering wheel angle change
UBJ	-	Upper Ball-joint
V	[m/s]	Forward velocity of whole vehicle
α	[deg]	Slip Angle
α_f	[deg]	Slip angle at front axle
α_r	[deg]	Slip angle at rear axle
β	[deg]	Rocker specific angle
δ	[deg]	Steer angle of front wheel
δ_i	[deg]	Steer angle of inner front wheel
δ_o	[deg]	Steer angle of outer front wheel
Δ_{spring}	[mm]	Displacement of the spring (measured axially along the centreline)
$\Delta_{\text{springdamper}}$	[mm]	Horizontal displacement of spring/damper unit
Δ_{upright}	[mm]	Vertical pushrod displacement
Δ_{wheel}	[mm]	Displacement of the wheel (measured relative to the chassis)
ΔX	[mm]	Vertical displacement of one rocker side
ΔX	[mm]	Spring/damper displacement change
ΔY	[mm]	Horizontal displacement of other rocker side
ΔY	[mm]	Upright displacement change
η	[deg]	Angular change of pushrod relative to vertical axis
θ	[deg]	Rocker axis angular change
ϕ	[deg]	Angular change of spring/damper unit relative to horizontal axis
ϕ_r	[deg]	Roll angle of the body
Ω	[deg]	Angle of pinion (steering wheel) rotation from instant position



LIST OF FIGURES

Fig. 1 A.d.Tramontana [9]	19
Fig. 2 A.d.Tramontana 2 [9]	20
Fig. 3 Sprung/Unsprung mass general layout	22
Fig. 4 SAE vehicle axis system [2]	23
Fig. 5 Wheel base [5]	23
Fig. 6 Track width [5]	24
Fig. 7 Centre of Gravity - side view [5]	24
Fig. 8 Parallel and roll motion of Solid axle suspension [2]	26
Fig. 9 Hotchkiss Solid axle suspension [1]	27
Fig. 10 De Dion axle suspension, with coil springs [12]	28
Fig. 11 Twist beam axle suspension Audi A2 [11]	28
Fig. 12 Panhard bar lateral restriction [2]	29
Fig. 13 Watt's linkage lateral restriction [2]	29
Fig. 14 Cam follower-in-track lateral restriction [2]	29
Fig. 15 Swing axle suspension – 3 plane view geometry [2]	30
Fig. 16 Swing axle suspension - roll behaviour [1]	31
Fig. 17 Pure-trailing arm suspension – 3 plane view geometry [2]	31
Fig. 18 Pure trailing arm suspension – Chevrolet Corvette rear axle [1]	32
Fig. 19 Pure-trailing arm suspension – VW Beetle front axle [1]	33
Fig. 20 Semi-trailing arm suspension – 3 plane view geometry [2]	33
Fig. 21 VW Transporter suspension [11]	34
Fig. 22 Semi-trailing axle – rear axle [1]	34
Fig. 23 A-Arm general layout [2]	35
Fig. 24 Tie rod link at rear suspension connected a) to the chassis; b) to the wishbone [2]	35
Fig. 25 McPherson strut general layout [2]	36
Fig. 26 McPherson suspension [13]	37
Fig. 27 McPherson suspension – rear axle Tri link configuration at Mazda 323F, 1996	38
Fig. 28 McPherson suspension – rear axle Tri link configuration [2]	38
Fig. 29 Multilink suspension [13]	39
Fig. 30 Coil spring [11]	40
Fig. 31 Leaf spring [11]	40
Fig. 32 Suspension damper with two-way adjustment [12]	40
Fig. 33 Push-rod actuated suspension [5]	42
Fig. 34 Pull-rod actuated suspension [5]	42
Fig. 35 Wheel and spring rate [4]	44
Fig. 36 Non-linear Installation Ratio [4]	45
Fig. 37 Non-linear Installation Ratio graph [2]	46
Fig. 38 Non-linear Installation ratio – calculations [4]	46
Fig. 39 Non-linear Installation Ratio suspension construction [5]	49
Fig. 40 Force analysis of a simple vehicle in cornering [1]	50
Fig. 41 Antiroll bar [1]	51
Fig. 42 Monoshock suspension system [12]	51
Fig. 43 Function of monoshock suspension system [5]	52
Fig. 44 Front view suspension geometry [2]	53
Fig. 45 Lateral force caused by camber of a tire [1]	54
Fig. 46 Positive camber [5]	54
Fig. 47 Negative camber [5]	55



Fig. 48 Toe in [5]	55
Fig. 49 Toe out [5]	56
Fig. 50 SAE Tire force and moment axis system [1]	58
Fig. 51 Reverse efficiency - aligning torque [5]	59
Fig. 52 Slip angle [1]	60
Fig. 53 Lateral force vs. slip angle [4]	61
Fig. 54 Cornering force [1]	61
Fig. 55 Rack-and-pinion Woodward [10]	63
Fig. 56 Rack-and-pinion steering system draft [1]	63
Fig. 57 Steering gearbox [1]	65
Fig. 58 Truck steering system [1]	66
Fig. 59 Front view steering geometry [2]	67
Fig. 60 Kingpin axis inclination disadvantage [4]	68
Fig. 61 Wheel offset and scrub radius [4]	69
Fig. 62 Side view steering geometry [2]	70
Fig. 63 Wheel castor [4]	71
Fig. 64 Steering instability due to castor [4]	71
Fig. 65 Ackermann steering geometry [1]	73
Fig. 66 Positive Ackermann geometry [5]	74
Fig. 67 Positive Ackermann geometry construction [2]	75
Fig. 68 Negative Ackermann geometry [5]	76
Fig. 69 Parallel Non-Ackermann steering geometry [5]	76
Fig. 70 Low speed turning [4]	77
Fig. 71 High speed cornering [4]	78
Fig. 72 High speed cornering detail [4]	80
Fig. 73 Bump steer [4]	82
Fig. 74 Hartmann's construction of Bobilier line – ideal geometry [1]	82
Fig. 75 Steering geometry error causing toe change [1]	83
Fig. 76 Steering geometry error causing steering [1]	83
Fig. 77 Front left suspension 1 [9]	87
Fig. 78 Front left suspension 2 [9]	88
Fig. 79 Front left suspension with steering rack [9]	89
Fig. 80 Bump steer geometry CAD preparation	91
Fig. 81 Hartmann's construction of Bobilier line, step 1.+ 2.	91
Fig. 82 Hartmann's construction of Bobilier line, step 3.+ 4.	92
Fig. 83 Hartmann's construction of Bobilier line, step 5.	92
Fig. 84 Hartmann's construction of Bobilier line, step 6.	93
Fig. 85 Hartmann's construction of Bobilier line, step 7.+ 8.	93
Fig. 86 Hartmann's construction of Bobilier line, step 9.+ 10.	94
Fig. 87 Hartmann's construction of Bobilier line, step 11.	94
Fig. 88 Hartmann's construction of Bobilier line, step 12.+ 13.	95
Fig. 89 Hartmann's construction of Bobilier line, step 14.	95
Fig. 90 Hartmann's construction of Bobilier line, step 15.	96
Fig. 91 Design according to Ackermann steering geometry	97
Fig. 92 MBS model	98
Fig. 93 Plot: Toe angle [deg] vs. Wheel travel [mm]	99
Fig. 94 Plot: Toe angle vs. time representing 360° turn of steering wheel	100
Fig. 95 Real steering clevis CAD model	102
Fig. 96 Upper front wishbone CAD model [9]	103



Fig. 97 Lower front wishbone CAD model [9].....	104
Fig. 98 Unfolded beam shape	104
Fig. 99 Unfolded shape to be printed in scale 1:1	104
Fig. 100 Transferring beam shape from 2D to 3D	105
Fig. 101 Beam shape copy using a marker pen.....	105
Fig. 102 Wishbone's assembly	106
Fig. 103 Bushing	107
Fig. 104 Bushings mounting	107
Fig. 105 DMU Kinematics simulation assembly – left-front view	110
Fig. 106 DMU Kinematics simulation Assembly – right-front view	111



LIST OF APPENDIXES

App. 1	A.D. TRAMONTANA TECHNICAL SPECIFICATIONS	I
App. 2	A.D. TRAMONTANA PHOTO	III
App. 3	WOODWARD STEERING RACK DRAWING	V
App. 4	HARTMANN'S CONSTRUCTION OF BOBILIER LINE	VI
App. 5	REAL STEERING CLEVIS DRAWING	VII
App. 6	FRONT SUSPENSION JIG ASSEMBLY	VIII
App. 7	WULKOLLAN MATERIAL PROPERTIES (ES)	XII
App. 8	BUSHINGS DRAWING	XIII
App. 9	BUSHINGS PHOTO	XVII
App. 10	SWEPT VOLUME	XVIII



TRAMONTANA TECHNICAL SPECIFICATIONS

GENERAL

- F-1-inspired carbon-fiber monocoque with multi-tube subframe in the rear.
- 4 independent wheels, each with double wishbone suspension design, pushrod operated. Front and rear anti-roll bar.
- Engine and transmission layout along the central axis.
- Electro-hydraulic ride height adjustment.
- Bespoke carbon fiber bodywork.
- Two seats in a row.
- Upward rising hinge door system - unique at the market.
- Fully detachable glass copula.

PROPULSION

Engine – 5.5-litre V12 60°

Layout:

- 12 cylinders in V at 60°, twin turbo superchargers, each with intercooler
- 3 valves per cylinder
- 2xSOHC (Single Overhead Camshaft)
- Twin Spark Ignition per Cylinder
- SFI Fuel Injection (Sequential Fuel Injection)



Type	V12 – 60° , Biturbo
Layout	Mid-engine, Longitudinal Alignment, Rear Wheel Drive
Total Displacement	5,513 cm ³
Supercharging	Twin Turbochargers, 1.3 Bar Boost Pressure
Maximum Power	720 bhp /529kW/ at 5,750 rpm
Specific Output	130 bhp/litre
Maximum Torque	920 Nm from 4,000 rpm
Compression Ratio	9:1
Fuel	Unleaded 98 Octanes

Optimized Air Intake

Transmission & Clutch - Bespoke Sequential 6-Speed Manual

- Manual Sequential or Bespoke Electronic Paddle Shift (optional)
- Auto-lock Differential
- Double Clutch Ø 240 mm
- 4-level Traction Control

DIMENSIONS

Total Length	4,900 mm
Total Width	2,080 mm
Total Height	1,220-1,275 mm
Ground Clearance	85-135 mm
(Electronically adjustable ride height)	
Wheelbase	3,050 mm
Wheel Track Front	1,900 mm
Wheel Track Rear	1,810 mm
Front Overhang	997 mm
Rear Overhang	780 mm
Approach Angle	6°
Departure Angle	12°

WEIGHT

Dry Weight	from 1,050 kg
Weight-To-Power Ratio	1.7 kg/bhp
Weight Distribution	45 / 55 %
Weight Distribution	Front Axle / Rear Axle
Weight Distribution	Left Side / Right Side
Fuel Capacity	50 / 50 % 100 litres



PERFORMANCE	
Maximum Speed	> 300 km/h /186 mph/
0-100 km/h / 0-62 mph / Acceleration	< 3.7 s
Lateral g-force	1.35 g
Longitudinal g-force	
Braking	1.4 g
Accelerating	0.8 g

BRAKES	
Front	Carbon-Ceramics Ventilated Disos Ø 380x34 mm /Ø14.96x1.34 in./ 6-piston AP Racing Caliper
Rear	Carbon-Ceramics Ventilated Disos Ø 380x34 mm /Ø14.96x1.34 in./ 6-piston AP Racing Caliper
	<ul style="list-style-type: none">• Light Weight and Long Wear• Advanced ABS• Master Cylinder Ø23 mm /0.9 in./, Vacuum Booster Ø 254 mm /10 in./• Two Independent H Circuits

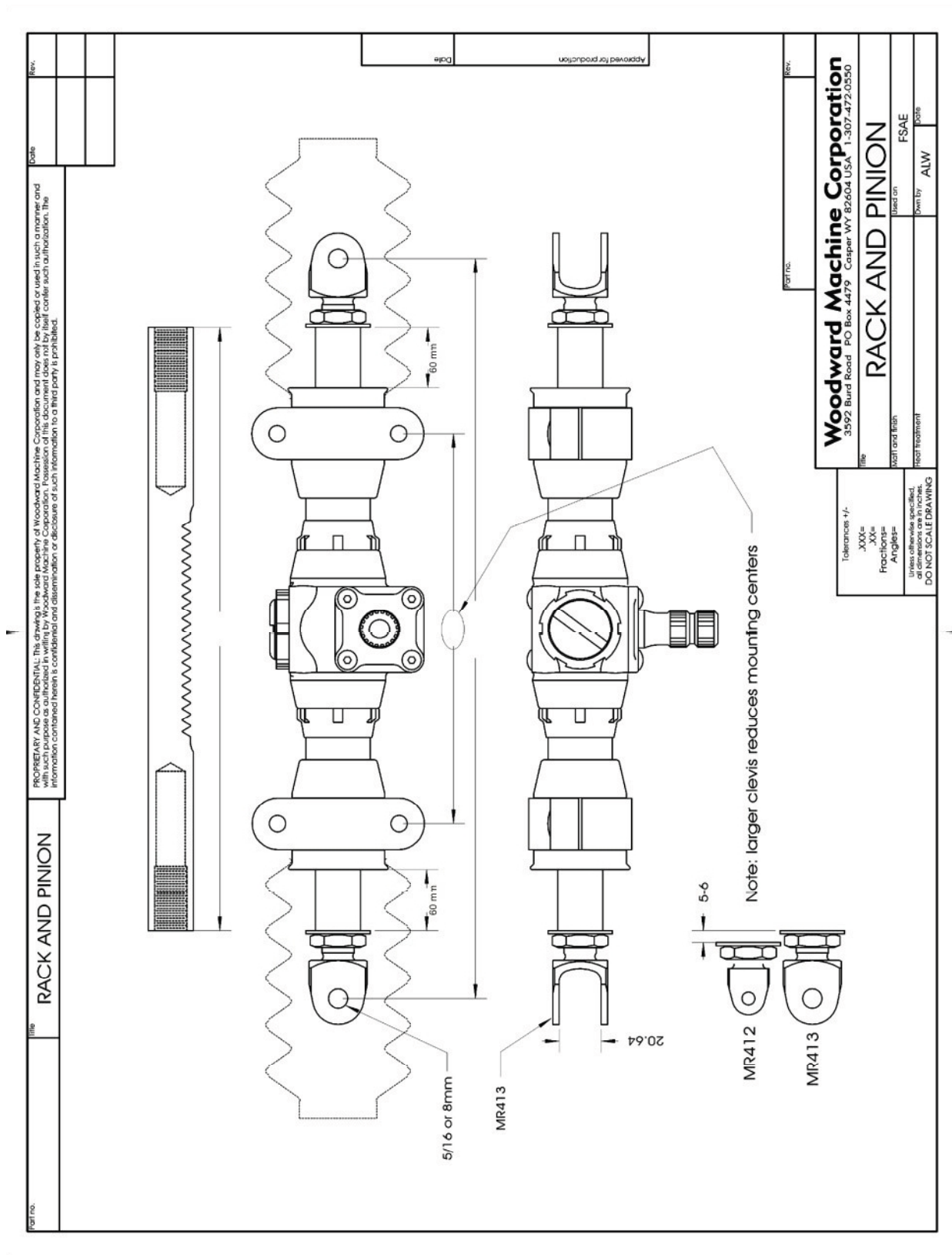
WHEELS & TIRES	
Front	8.5x Ø 20" Aluminum Monobloc Forged Wheel Carbon Ring / Magnesium Core (optional)
Tires	245/40 ZR20 (99Y) Specification: High Load (775 kg /1,709 lbs) The Highest Speed Rating
Rear	12x Ø 20" Aluminum Monobloc Forged Wheel Carbon Ring / Magnesium Core (optional)
Tires	335/30 ZR20 (104Y) Specification: High Load (900 kg /1,984lbs) The Highest Speed Rating

STEERING	
	Rack and Pinion, Hydraulic Power Assisted
	2.0 Turns Lock to Lock
	Fully Adjustable Steering Column
	Steering Wheel Quick Release
	12 m /3.66 ft./ Turning Radius

SAFETY	
	1 Rigid Central Zone (passengers' protection)
	8 Deformable Side Zones (impact energy absorption)
	High Resistance Main Rollover Hoop
	FIA Safety Regulations Fulfilled





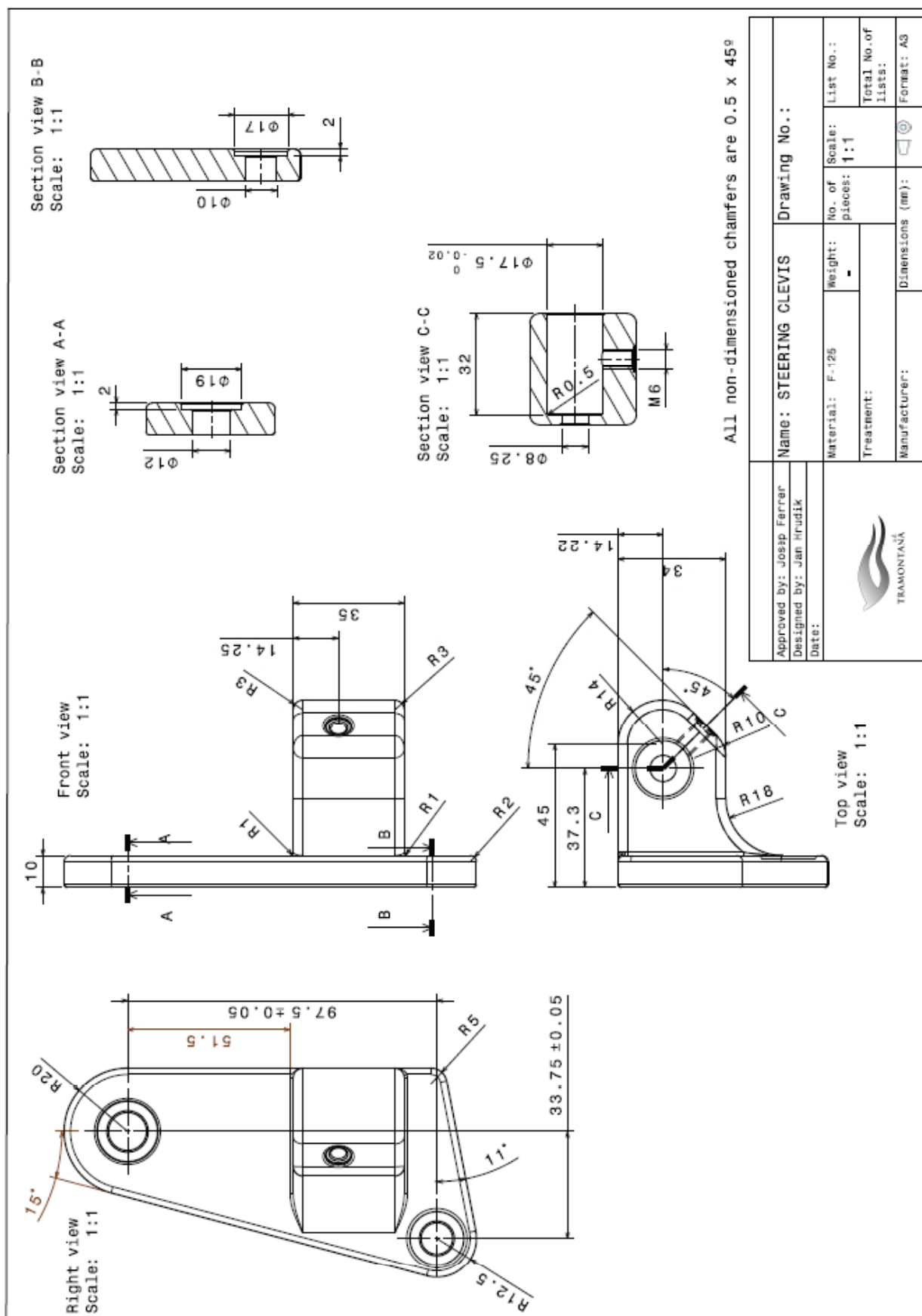




Hartmann's Construction of Bobilier Line (tie rod, transmission axle):

Front View:

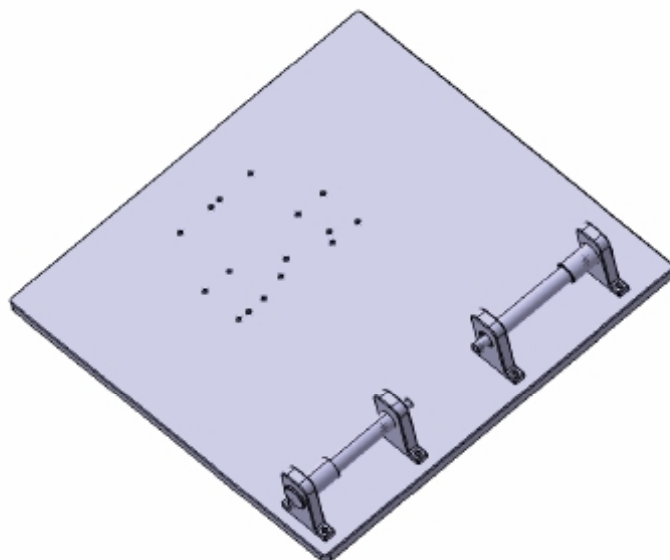
1. Draw a line from inner lower wishbone to inner upper wishbone
 2. Draw a line from outer lower wishbone to outer upper wishbone
 - Find the intersection of line (1) and line (2)
 3. Draw the line from inner to outer upper wishbone in order to find the IC
 4. Draw the line from inner to outer lower wishbone in order to intersect with line (3) to find IC
 5. Create the line from IC to the intersection of line (1) and line (2)
 - This creates the Bobilier line
 6. Draw the bisecting line of upper and lower wishbone
 - The angle of this bisecting line should be same as the angle to upper and lower wishbone
 7. Find the angle between Bobilier line (5) and the bisecting line (6)
 8. Draw the symmetrical Bobilier line (5) with angle of (7)
 - This creates symmetrical Bobilier line
 9. Define the inner/outer point for the tie rod/transmission axle (any points you want to define)
 10. Draw a line from the defined point in (9) to IC ("steering line")
 11. Find second bisecting line between the line (10) and line from lower wishbone to IC (4)
 12. Find the angle between bisecting line (11) and symmetrical Bobilier line (8)
 13. Draw the line from IC with angle of (12) respect to the bisecting line (11) ("new Bobilier line")
 14. Draw a line from LBJ (from lower wishbone) to defined point (9) to find the intersection point between line (13) and (14)
 15. Draw a line from the intersection found from (14) to the outer suspension points for lower wish bone.
- this will find the end point for the tie rod/transmission axle as this is intersection of line (10) and line (15)





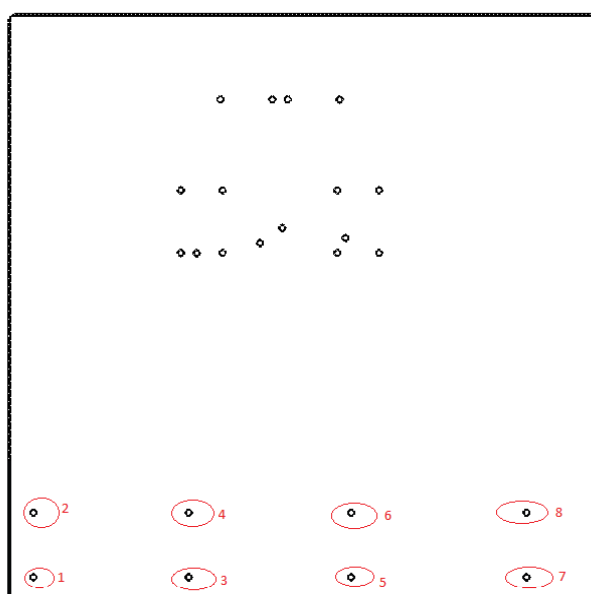
FRONT SUSPENSION JIG ASSEMBLY

MAIN PLATE



FOLLOWING WILL BE THE SAME FOR ALL FRONT WISHBONES (left lca, left uca, right lca and right uca). FOR ASSEMBLY TO THE MAIN PLATE - USE BOLTS M8 WITH APPROPRIATE LENGTH. FOR FIXING THE AXLES USE NUTS WITH APPROPRIATE SIZE.. BOLTS AND NUTS ARE NOT DISPLAYED IN ANY PICTURE. THE SIDE OF ALL HOLDERS (EXCEPT **G11-LCA JIG OUTER**) AND SPACERS DOESN'T MATTER AS THEY ARE SYMMETRIC. THE SIDE OF ALL THE AXLES DOES MATTER.

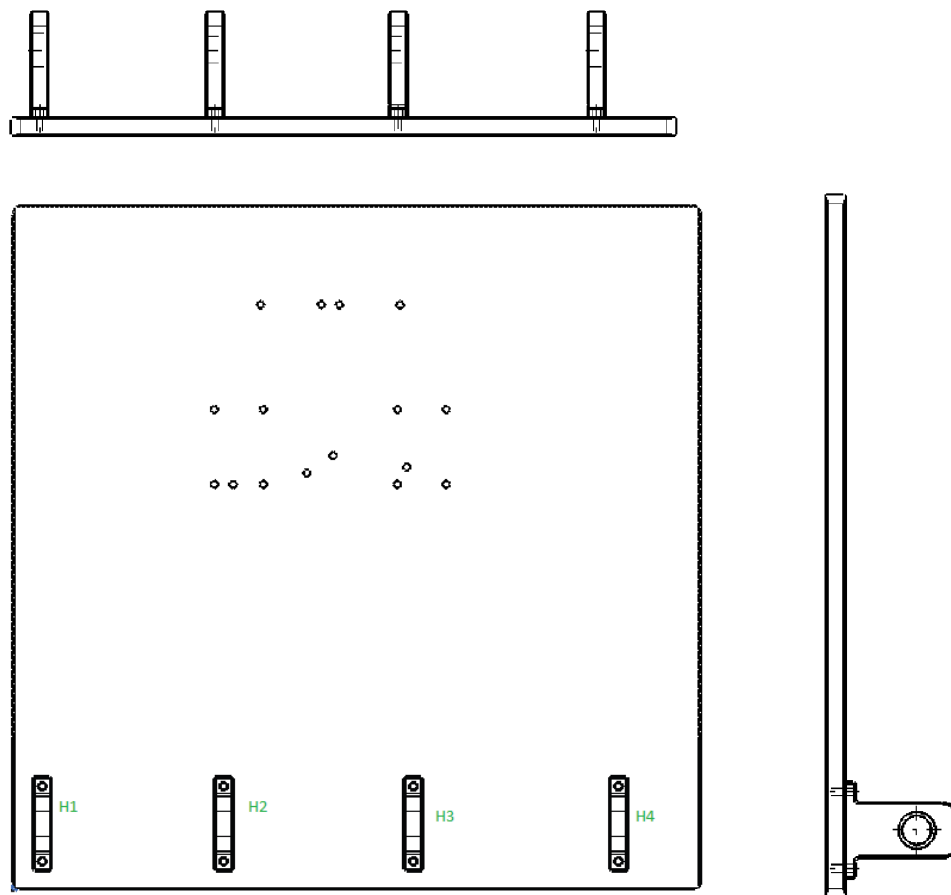
1. PLACE THE ALUMINIUM MAIN PLATE AS YOU CAN SEE IN THE PICTURE:
2. USE ALL OF 8 HOLES IN RED CIRCLE (POSITION 1 UNTIL 8)





3. MOUNT 2 PIECES OF **G11-CA JIG OUTER** TO THE HOLES 1, 2 AND 7, 8.
4. MOUNT 2 PIECES OF **G11-CA JIG INNER** TO THE HOLES 3,4 AND 5,6

YOU SHOULD GET ASSEMBLY LIKE THIS:

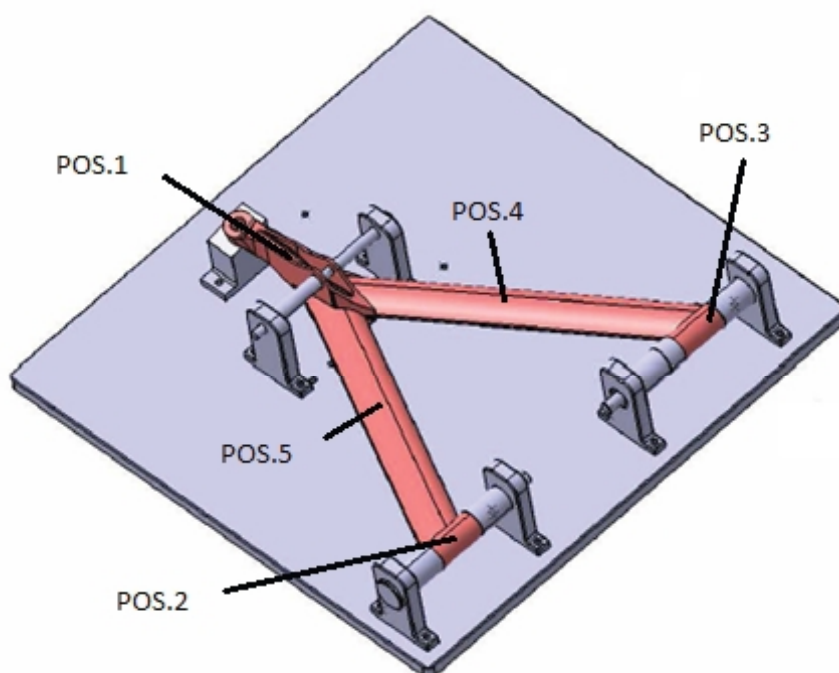


H1 - HOLDER No.1

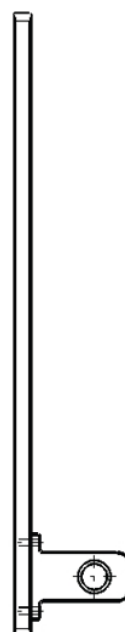
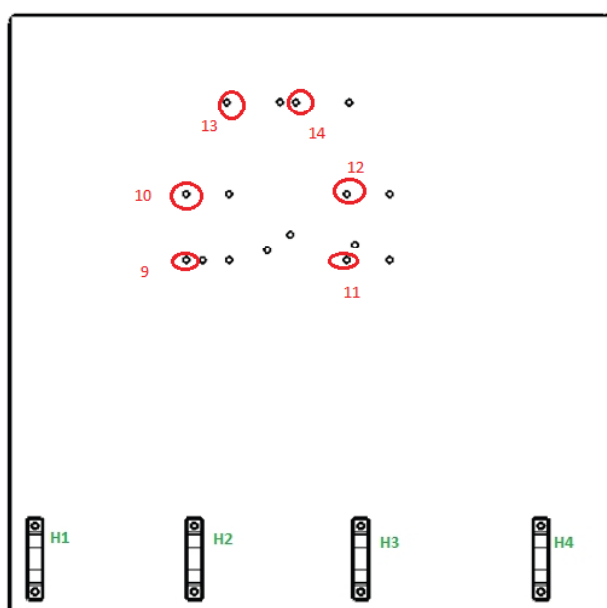
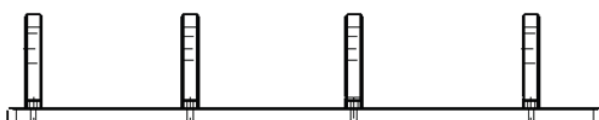
H2 – HOLDER No.2

H3 – HOLDER No.3

H4 – HOLDER No.4

LCA LEFT

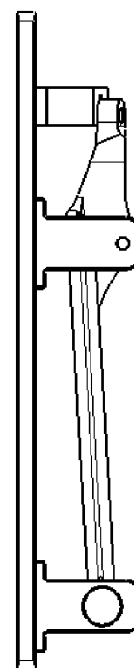
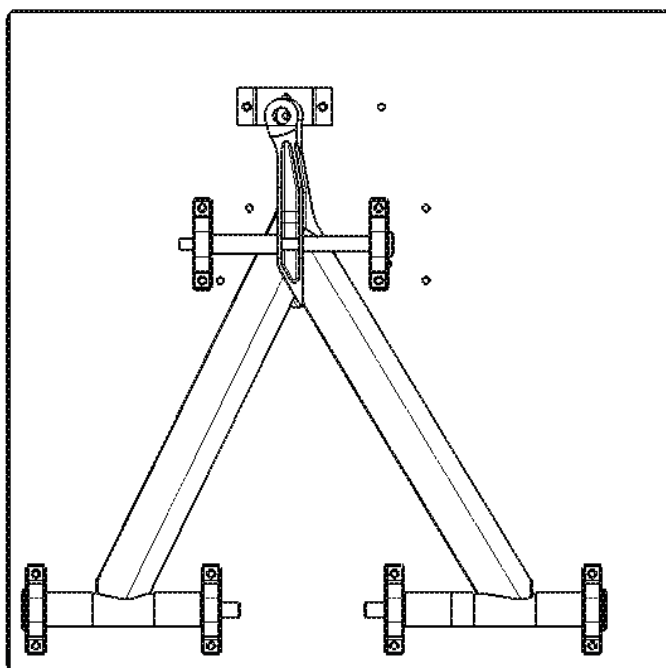
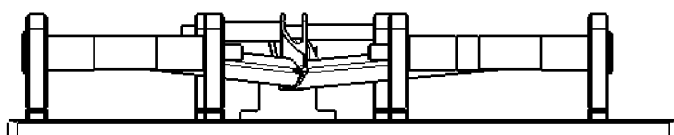
1. MOUNT **G11-LCA JIG PUSH SMALL** TO THE HOLES **9, 10**.
2. MOUNT **G11-LCA JIG PUSH BIG** TO THE HOLES **11, 12**.
3. MOUNT **G11-LCA JIG OUTER** TO THE HOLES **13, 14**. THE SIDE DOES MATTER – PLACE IT THE WAY THAT THE INCLINATION OF THE UPPER PLANE GOES FROM RIGHT UP TO THE LEFT BOTTOM.





4. PLACE THE OUTER PIECE OF LOWER LEFT WISHBONE (POS.1) TO THE POSITION LIKE IN THE PICTURE. FIX IT WITH BOLT AND APPROPRIATE WASHER TO THE **G11-LCA JIG OUTER**.
5. INSERT **G11-LCA JIG AXLE PUSH** TO THE **G11-LCA JIG PUSH BIG**; LET IT GO THROUGHT TWO EYES IN THE PIECE OF POS.1 , THEN INSERT **G11-LCA JIG SPACER PUSH** AND FINISH THROUGH **G11-LCA JIG PUSH SMALL**.
6. FIX THE AXLE WITH APPROPRIATE NUT AND WASHER.
7. INSERT FROM THE LEFT SIDE **G11-CA JIG AXLE SHORT** TO THE **HOLDER H1**; LET IT GO THROUGHT THE INNER PIECE OF LOWER LEFT WISHBONE (PREPARED PIECE OF TUBE, POS.2), THEN INSERT **G11-CA JIG SPACER LONG** AND FINISH THROUGH **HOLDER H2**.
8. FIX THE AXLE WITH APPROPRIATE NUT AND WASHER.
9. INSERT FROM THE RIGHT SIDE **G11-CA JIG AXLE LONG** TO THE **HOLDER H4**; LET IT GO THROUGHT THE INNER PIECE OF LOWER LEFT WISHBONE (PREPARED PIECE OF TUBE, POS.3), THEN INSERT **G11-CA JIG SPACER SMALL AND G11-CA JIG SPACER LONG** AND FINISH THROUGH **HOLDER H3**.
10. FIX THE AXLE WITH APPROPRIATE NUT AND WASHER.
11. PLACE IN THE RIGHT POSITION BOTH PREPARED ARM PIECES (POS.4 AND POS.5).

YOU SHOULD GET ASSEMBLY LIKE THIS:



12. THE WELDING CAN START



2011-03-24 11:26

manxa industrial

704100480 >>

P 1/1



CARACTERÍSTICAS TÉCNICAS

POLIURETANO			
Propiedades	Método de ensayo	Unidades	Valores
Dureza	DIN - 53505	Shore A	90 ± 3
Peso específico	DIN - 53479	g/cm³	1,23
Resistencia a la tracción	DIN - 53504	MPa	62,5
Módulo al 100%	DIN - 53504	MPa	6,7
Módulo al 300%	DIN - 53504	MPa	14,8
Alargamiento a la ruptura	DIN - 53504	%	640
Pérdida por abrasión	DIN - 55514	mm³	< 25
Resistencia al desgaste	DIN - 55515	Km / m	125,5
Temperatura de servicio	—	°C	- 20 + 80
Deformación remanente a la Compresión (22 h/70°C)	DIN - 5217	%	27

MANXA INDUSTRIAL
AGUSTI CM, S.L.

TELE VENDES 902 455050

TELE 972 274527 FAX 972 259600

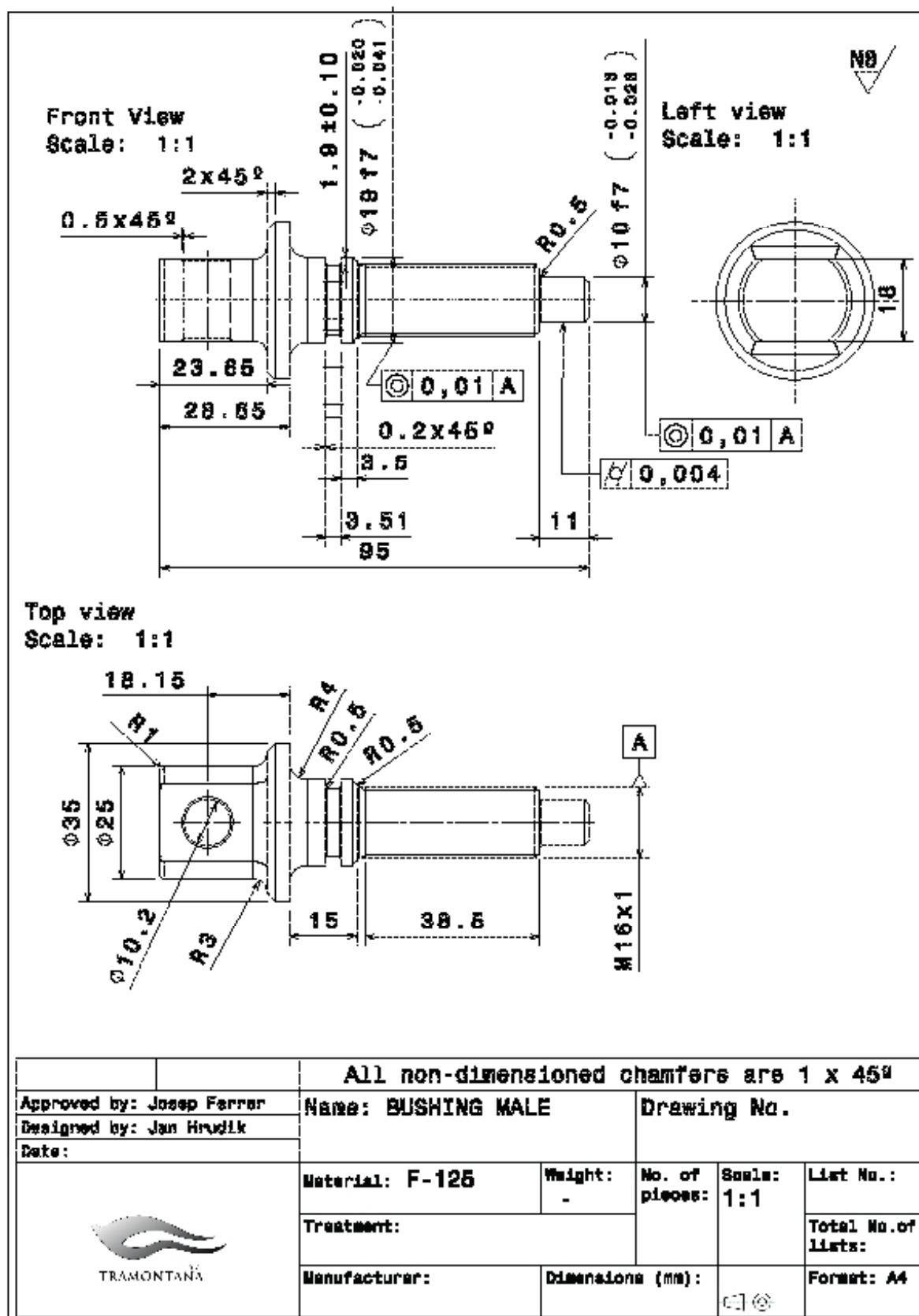
e-mail: industrial@manxa.es

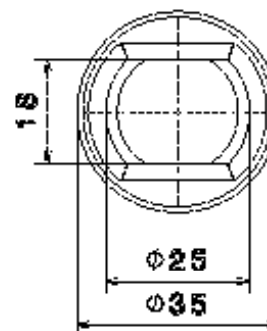
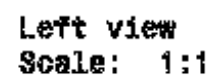
Ctra. Les Trinc, 85

17800 - OLOT - Girona

C/ CARACAS, 11 08030 - BARCELONA TEL.0034 93 346 82 12 FAX 0034 93 311 30 60

Email: lork@lorkindustrias.com


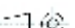




Section view A-A
Scale: 1:1

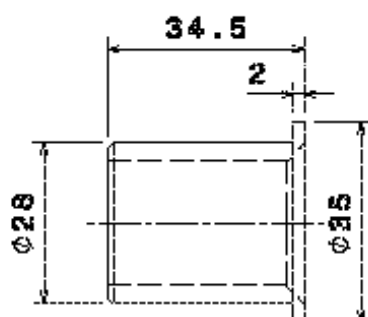
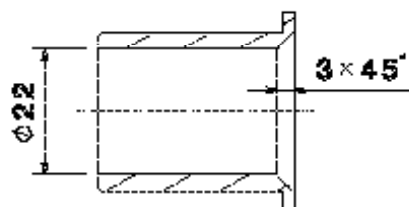
Dimensions and Tolerances:

- Overall length: 55
- Distance from end to start of thread: 53
- Thread length: 14.5
- Thread specification: M16x1
- Thread tolerance: 0.01 B
- Central bore diameter: $\phi 10.2$
- Central bore tolerance: 0.022 (+0.022/0)
- Flange diameter: $\phi 19H8 (+0.033/0)$
- Flange tolerance: 0.004
- Flange surface finish: 0.01 B
- Material: B
- Surface finish: 1x45²

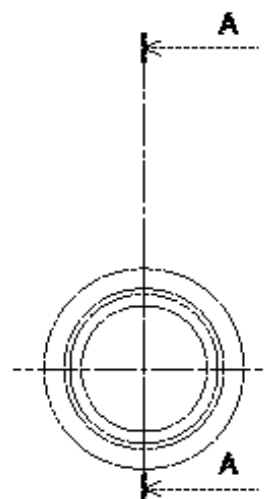
		All non-dimensioned chamfers are 0.5 x 45°				
Approved by: Josep Ferrer		Name: BUSHING FEMALE		Drawing No.:		
Designed by: Jan Hrudik						
Date:		Material: F-125		Weight: -	No. of pieces:	Scale: 1:1
		Treatment:				Total No. of lists:
		Manufacturer:			Dimensions (mm):	Format: A4


 NS

Section view A-A
Scale: 1:1




Front view
Scale: 1:1



Left view
Scale: 1:1

All non-dimensioned chamfers are 1 x 45°

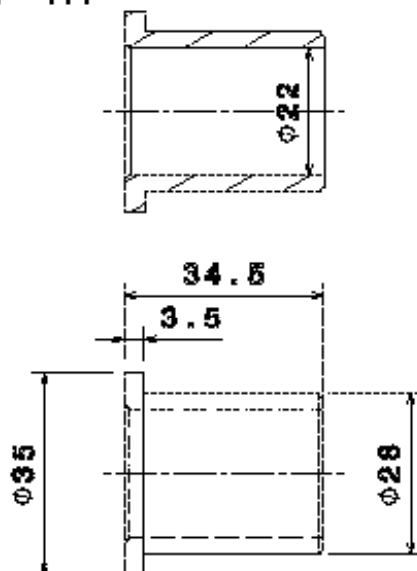
Approved by: Josep Ferrer		Name: SILENTBLOCK INNER		Drawing No.:		
Designed by: Jan Hrudik						
Date:						
 TRAMONTANA		Material: WUKOLLAN	Weight: -	No. of pieces:	Scale: 1:1	List No.:
		Treatment:				Total No. of lists:
		Manufacturer:		Dimensions (mm):		Format: A4



NB ✓

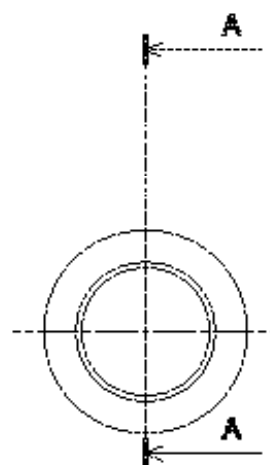
Section view A-A

Scale: 1:1





Front view

Scale: 1:1

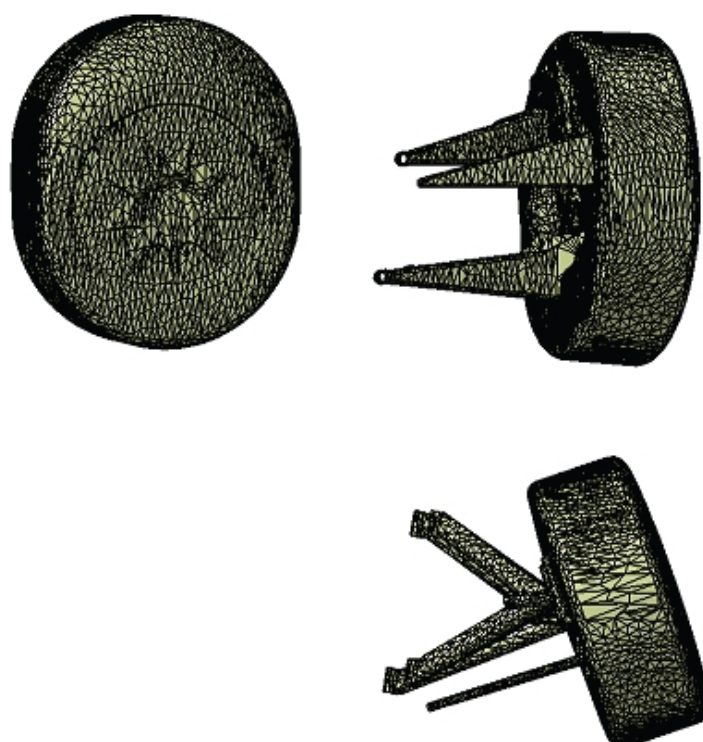


Left view

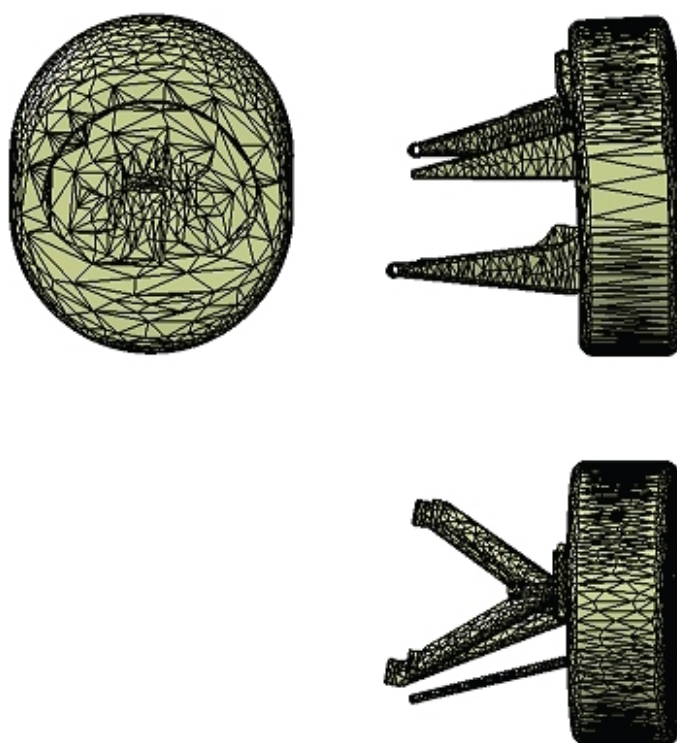
Scale: 1:1

		All non-dimensioned chamfers are 1 x 45°					
Approved by: Josep Ferrar		Name: SILENTBLOCK OUTER		Drawing No.:			
Designed by: Jan Hrudik							
Date:		Material: WUKOLLAN		Weight: -	No. of pieces:	Scale: 1:1	List No.:
		Treatment:					Total No. of lists:
		Manufacturer:		Dimensions (mm):			Format: A4

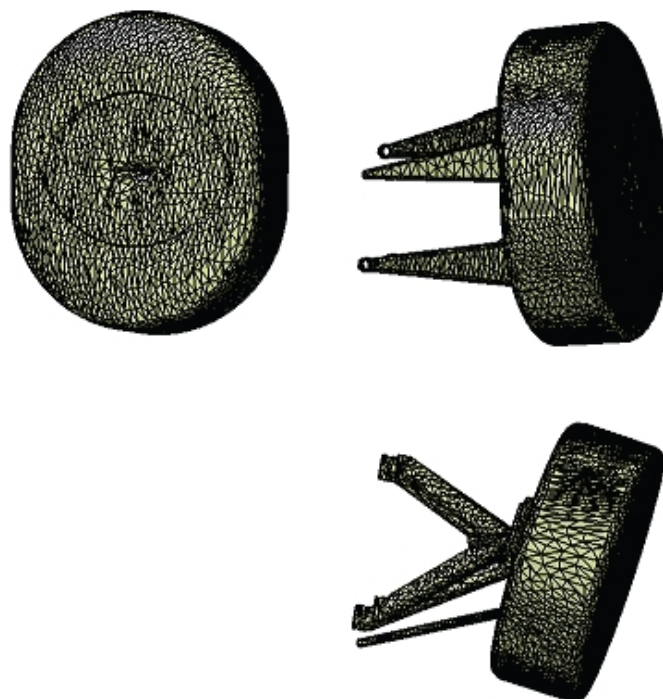




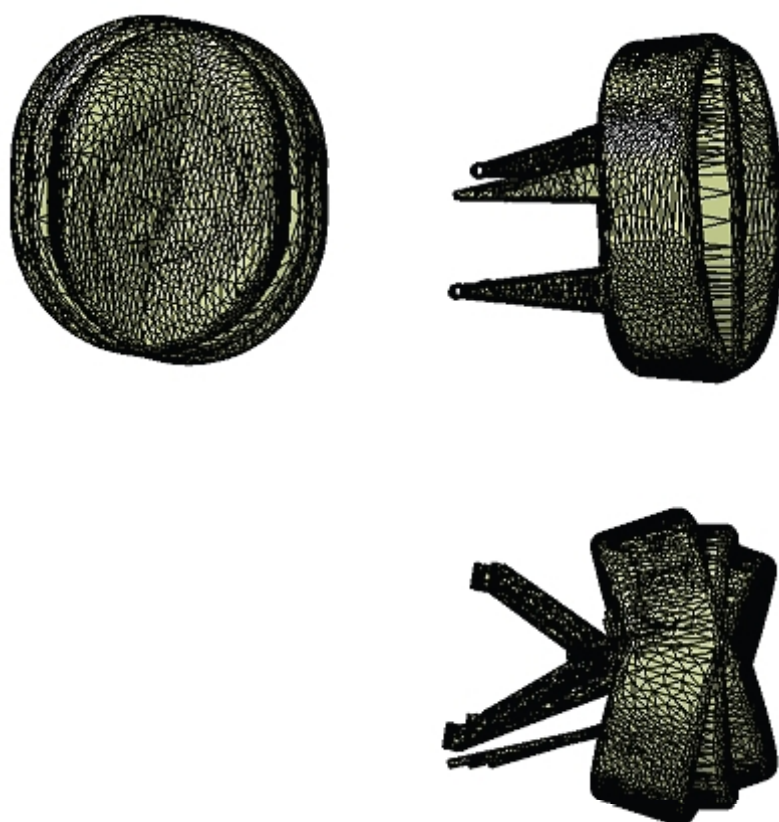
App. 10a Swept Volume left turn



App. 10b Swept Volume straight direction



App. 10c Swept Volume right turn



App. 10d Swept Volume together

